Spring 2024

Biochar for Heavy Metal Removal in Water: Opportunities, Challenges, and Sustainable Solutions

Pushpita Kumkum
Old Dominion University, pushpitakumkum04@gmail.com

BIOCHAR FOR HEAVY METAL REMOVAL IN WATER:

OPPORTUNITIES, CHALLENGES, AND SUSTAINABLE SOLUTIONS

by Pushpita Kumkum
B.S. December 2009, Bangladesh University of Engineering & Technology
M.S. May 2013, University of Akron

A Dissertation Submitted to the Faculty of
Old Dominion University in Partial Fulfillment of the
Requirements for the Degree of

DOCTOR OF PHILOSOPHY

CIVIL & ENVIRONMENTAL ENGINEERING

OLD DOMINION UNIVERSITY
May 2024

Approved by:

Sandeep Kumar (Director)

Mujde Erten-Unal (Member)

James W. Lee (Member)

ABSTRACT

BIOCHAR FOR HEAVY METAL REMOVAL IN WATER: OPPORTUNITIES, CHALLENGES, AND SUSTAINABLE SOLUTIONS

Pushpita Kumkum
Old Dominion University, 2024
Director: Dr. Sandeep Kumar

The presence of heavy metals in drinking water is a significant concern due to the harmful impacts it can have on human health. Biochar has emerged as a low-cost alternative to activated carbon for lead (Pb) adsorption due to its porous structure and high surface-to-volume ratio. The last 10 years of studies have been reviewed to investigate the biochar production, activation methods, kinetic, adsorption isotherms, mechanism, regeneration, and adsorption capacities to guide future researchers and practitioners in using biochar to remove Pb from water. However, several challenges hinder the actual application of biochar as an adsorbent. These challenges include variability in adsorption capacity, potential desorption or leaching of Pb from the biochar back into the solution, and lack of studies on scalability issues for its application as an adsorbent.

To address the lack of column studies in the field of heavy metal removal using biochar as an adsorbent, a fixed-bed adsorption study was conducted to remove Pb(II) from water. The study evaluated the impact of initial Pb(II) concentration, mass of adsorbent, and flow rate on the adsorption potential. The Adams-Bohart model, Thomas model, and Yoon-Nelson model were used to analyze the adsorption data. The breakthrough data obtained from this study can be applied in the design of a point-of-use filter that can effectively remove Pb(II) from drinking water.

The use of biochar as an adsorbent for metals like chromium in combination with microalgae

cultivation for treating tannery wastewater was also investigated. The study tested two types of biochar - pinewood biochar (PB) and a commercial biochar (CB)- as a pretreatment step before cultivating microalgae. Results showed that the application of both types of biochar led to a significant increase in growth rates (61% and 126% for PB and CB, respectively) compared to cultivation in raw wastewaters. The study also found that the biochar production process and its physiochemical characteristics strongly influenced Cr(III) adsorption performances.

This research aims to provide a comprehensive resource on the opportunities and engineering challenges associated with using biochar for heavy metal removal from water.

This thesis is dedicated to my brother Ashique Rahman who is one of the smartest people I know, who had so much potential, who could have achieved so many things, had life not been unfair to him.

"Perseverance is the act of continuing to move forward, even when you want to give up."
- Rachel Scott.

ACKNOWLEDGMENTS

Many people have contributed to the successful completion of this dissertation. I would like to express my sincere appreciation and gratitude to my advisor Dr. Sandeep Kumar for his guidance, advice, and support. Most importantly, I am grateful for his inspiration. I still remember one incident when I told him that I was very nervous about speaking in public. He instantly said, "If it's so then I will send you even more for presenting in different places, in front of different audiences." I think that is a key feature of a true mentor; they get us out of our comfort zone so that we can overcome the barrier, utilize our full potential, gain confidence, and achieve anything we want. I am truly grateful to Dr. Kumar for always being that mentor. I would like to express my sincere gratitude to Dr. Unal and Dr. Lee for their guidance and support. I would like to express special thanks to Dr. Lee's former PhD student, Oumar for his immense help in sample characterization and analyses. I am thankful to the Department of Civil and Environmental Engineering, Dr. Ishibashi, and Dr. Wang for relying on me with the teaching assistantship opportunity that provided me some experience of a rewarding job like teaching. Thanks to the current and former members of the Biomass Research Laboratory Ali, Chen, Alex, Jake, Kameron, Ashani, Anuj, George, Mason and Martino who helped me along the way with their friendship, help, advise, and discussions; I am glad that we are still connected. Thanks to the University of Padova, Italy group for the collaborative research. I have learned about the whole publication process during that time which helped me immensely for the publication of my other manuscripts.

My sincere gratitude to my parents for always being there for me, for instilling in me the importance of hard work and discipline since I was a kid, these two qualities are the ones which I believe can take people anywhere they want to be. My heartfelt gratitude to my husband for

believing in me. If it weren't for him, I would have never known my strengths, have never felt confident, have never known what I can accomplish. Thanks to my kids for their existence, a smile, or a hug from them can take away all the exhaustion after a hectic day; I feel recharged anytime I look at their faces. I would like to extend my heartfelt appreciation to everyone who has played a role in supporting me throughout my dissertation journey. Your valuable assistance, encouragement, motivation, and acts of kindness have made a significant impact on my progress and success. Thank you for being a part of this journey with me.

NOMENCLATURE

Pb	Lead
GAC	Granular Activated Carbon
FTIR	Fourier-Transform Infrared Spectroscopy
BET	Brunauer-Emmett-Teller Surface Area Analyzer
H/C	Hydrogen-Carbon Molar Ratio, (No Units)
O/C	Oxygen-Carbon Molar Ratio, (No Units)
Z	Bed Depth, cm
C/C_0	Effluent-Influent Metal Concentration
q_{eq}	Equilibrium Uptake of Metal Per Unit Mass of Adsorbent, mg/g
q_{max}	Maximum Metal Adsorption, mg
Q	Flow Rate, mL/min
K_{AB}	*Adams-Bohart Rate Constant,*
L/mg/min) K_{TH}	Thomas Rate Constant,
mL/mg/min	
K_{YN}	Yoon-Nelson Rate Constant, min^{-1}
π	50% Adsorbate Breakthrough Time, min
M	Total Dry Weight of Biochar,
mg Cr	Chromium

TABLE OF CONTENTS

CHAPTER 1

INTRODUCTION

Lead (Pb) is a neurotoxic heavy metal naturally occurring in Earth's crust and also can be easily mined and refined [1]. It is a soft, malleable material with high density, durability and resistance to corrosion which makes it a compound known for its diverse use in different application. The use of lead has a long history, dating back to the Roman era, where it was extensively mined in Spain and Britain. The Romans utilized lead for a variety of purposes, including water pipes, dishes, cosmetics, coffins, and as a means of debasing their silver coinage. Lead was believed to enhance the taste of wine and food due to its sweet notes. The metal enhanced one-fifth of the 450 recipes in the Roman Apician Cookbook [2]. Although the mining of lead declined in the Dark Ages (early medieval period), its use resurfaced in Medieval times. During this period, lead was employed in new applications such as bullets, printing type, and pottery glazes [1,3,4]. Lead remained in widespread use until the 20th century, with various applications such as in gasoline, lead- acid batteries, paint, radiation shielding, and as a stabilizer in the polyvinyl plastic industry [5]. This prolific metal played a significant role in the technological advancements of the American colonies and the American Republic [6]. The correlation between exposure to Pb and the adverse health effect is not something recently known. Around 250 BC, the Greek philosopher Nikander of Colophon documented cases of colic and anemia caused by lead poisoning [7]. Although the link between gout and lead poisoning was not yet known between 450-380 BC, the Greek physician Hippocrates associated gout with the consumption of certain foods and wine. However, during the Roman period, it became apparent that the prevalence of gout among the wealthy was due to their high intake of lead [7]. According to some scholars, the high levels of lead exposure may have been responsible

for the health issues of men and could have played a role in the decline of the Roman Empire [2]. Although the immediate effects of metal consumption were understood, it wasn't until the 19th century that medical professionals gained a complete understanding of the long-term harm caused by lead poisoning. With the rise of the Industrial Revolution, the use of metals in manufacturing became more common, leading to an increase in cases of chronic metal poisoning among workers [8].

The workers were exposed to lead through various means such as inhaling fine lead dust or fumes, consuming contaminated food at the workplace, or through skin absorption [8]. By the 20th century, the majority of the lead was utilized as an additive in gasoline and as the main pigment in house paint, while some quantities were used as solder in plumbing and in various household items [2].

The accumulation of lead in the body over several months or years leads to lead poisoning, which can cause severe health complications. In adults, lead exposure can have lasting negative effects such as a higher risk of high blood pressure, cardiovascular issues, reproductive system issues, and kidney damage [9]. Additionally, pregnant women who are exposed to high levels of lead are at risk of miscarriage, stillbirth, and premature birth [10].

Children are especially vulnerable to the negative effects of lead exposure because their nervous system is still developing and susceptible to damage. This exposure can lead to reduced intelligence quotient (IQ), altered behavior such as shorter attention span and increased antisocial tendencies, and decreased educational success [10]. Lead exposure can also result in anemia, high blood pressure, renal impairment, immunological issues, and harm to reproductive organs [9]. Lead exposure in adults and children typically occurs through inhalation of air-borne lead particles from gasoline and dust particles from lead-based paint,

food, as well as drinking water delivered through lead-based pipes [11]. Even though leaded gasoline was completely phased out by 1996 and lead-based paint was prohibited by 1978, the environment still contains about 7 million tons of lead from burnt gasoline [2]. Moreover, there are approximately 38 million houses and apartments built before 1978 that still contain some lead paint [2]. Lead exposure in children can occur through ingestion of food or water containing lead, inhalation of lead dust from lead-based paint or contaminated soil. Although lead levels in ground and surface water are usually low, they may rise once the water enters the water distribution system. Although the Safe Drinking Water Act (SDWA) prohibited the use of lead-based pipes, solder, or flux in plumbing system, houses built before 1986 still have lead pipes. Highly acidic water source or water with low mineral content can corrode the pipes and fixtures and leach lead into the drinking water [12]. The existence of long-lasting lead hazards in the environment means that lead exposure continues to be a major public health issue. The Flint, MI crisis is an example of how lead exposure can have catastrophic consequences when proper precautions are not taken [13]. The Flint water crisis occurred in Flint, Michigan, USA, from 2014 to 2019. In an effort to save money, Flint's city officials switched the city's water supply from Lake Huron (treated by the Detroit Water and Sewerage Department) to the Flint River. The inadequately tested corrosive river water caused lead from aging pipes to leach into the city's drinking water, leading to dangerous levels of lead contamination.

The water was also found to have dangerous levels of bacteria and other contaminants. Even though Flint residents had reported that the water being piped into their homes for a year and a half was causing skin rashes, hair loss, and itchy skin due to its foul smell, discoloration, and unpleasant taste, the government refused to acknowledge the issue initially. It took more than a year for the state to finally accept that there was a problem. The

crisis caused widespread health problems, particularly in children exposed to lead, and led to a state of emergency being declared. The crisis drew national attention and sparked public outrage and protests. The government eventually switched back to the Detroit water supply and began replacing the city's lead pipes, but the damage was already done, and the long-term effects of the crisis are still being felt by the community [14]. According to EPA's 7th Drinking Water Infrastructure Needs and Survey Assessment (April 2023) report, lead service lines account for more than 9% of the overall service line infrastructure in the United States, potentially exposing a significant portion of the country's drinking water to the risks associated with lead contamination. Government has undertaken several initiatives to replace the lead service lines. However, this Flint Water Crisis had been the motivation of this dissertation to investigate the viability of using biochar as a sustainable method for removing Pb(II) from contaminated water sources, with a focus on exploring alternative solutions to address emergency situations like the one that occurred in Flint, MI.

Biochar, a porous material derived from the thermal treatment of biomass in the absence of oxygen, has emerged as a promising solution for capturing pollutants from soil and aqueous environments. Biochar can be found naturally by the occurrence of vegetation fires. For over 2,500 years, humans have been producing and utilizing biochar (in the form named as "Terra preta" soils) in traditional agricultural methods in the Amazon Basin region of South America. Terra preta or black earth was formed over thousands of years through a process of human activity and natural decomposition [15]. Indigenous people in the Amazon Basin of South America practiced a form of slash-and-burn agriculture, where they would clear areas of forest and burn the trees and brush to create fertile soil for farming [16]. However, instead of allowing the burned materials to decompose and release carbon back into the atmosphere, they would mix

the charcoal and other organic matter into the soil [17]. The charcoal in the soil, also known as biochar, acted as a stable form of carbon sequestration, locking carbon in the soil for hundreds or even thousands of years [18].

Chapter 2 was focused on the studies conducted over the past few decades which have demonstrated the impressive capacity of biochar to adsorb Pb(II) from water and wastewater. Various strategies explored by the researchers to enhance its adsorption potential, such as activation or modification through synthesis with other compounds or combining it with different materials were also discussed.

Chapter 3 is a fixed-bed adsorption study using biochar as an adsorbent to remove Pb(II) from water to address the lack of column study in this field. This chapter presents the experimental set-up, methodology, and results obtained from the fixed-bed adsorption study. The study aims to provide insight into the effectiveness of biochar as an adsorbent for Pb(II) removal from contaminated water and its potential application in real-world scenarios. The findings of this study will contribute towards the development of sustainable and efficient technologies for water treatment and management.

Chapter 4 presents a collaborative research paper with University of Padova, Italy team on the bioremediation of industrial effluents, specifically tannery wastewater, using biochar as a pretreatment measure. Tannery wastewater is known to contain toxic compounds such as chromium (Cr), which can inhibit the growth of microorganisms. Biochar was used to remove Cr from tannery wastewater and to facilitate the growth of microalgae in this pretreated water utilizing other nutritional compounds presents in the water. Characterization of commercial biochar and pinewood biochar prepared by lab-scale pyrolysis method, comparative adsorption kinetics and best fitted isotherm models based on batch adsorption study were investigated as

part of this collaboration effort. The findings align with the objectives of the dissertation, which aims to explore the potential of biochar as an adsorbent for heavy metal removal from contaminated water. The study's results provide valuable insights into the use of biochar for wastewater treatment.

Finally, Chapter 5 discussed the future scope of this dissertation and identifies potential areas for further investigation in the field of biochar for lead removal from water. This dissertation aims to provide an in-depth analysis of the opportunities and engineering challenges associated with biochar's application in Pb removal, serving as a valuable resource for future researchers in this field.

REFERENCES

(1) Lead (Element). https://pubchem.ncbi.nlm.nih.gov/element/Lead.

(2) Lead: Versatile Metal, Long Legacy. https://sites.dartmouth.edu/toxmetal/more-metals/lead-versatile-metal-long-legacy/#:~:text=The%20Babylonians%20and%20the%20Assyrians,their%20fists%20with%20leaden%20knuckles.

(3) Periodic Table Element : Lead. https://www.rsc.org/periodic-table/element/82/lead.

(4) Lead: PubChem CID 5352425. https://pubchem.ncbi.nlm.nih.gov/compound/Lead.

(5) Somobrata Acharya; Acharya, S. Lead between the Lines. *Nat. Chem.* **2013**, *5* (10), 894–894. https://doi.org/10.1038/nchem.1761.

(6) Jack Lewis. Lead Poisoning: A Historical Perspective. **1985**.

(7) Sven Hernberg; Hernberg, S. Lead Poisoning in a Historical Perspective. *Am. J. Ind. Med.* **2000**, *38* (3), 244–254. https://doi.org/10.1002/1097-0274(200009)38:3<244::aid-ajim3>3.0.co;2-f.

(8) Michele Augusto Riva; Michele Augusto Riva; Riva, M. A.; Berretta, M.; Alessandra Lafranconi; Lafranconi, A.; M D'Orso; M D'Orso; D'Orso, M.; Giancarlo Cesana; Cesana, G. Lead Poisoning: Historical Aspects of a Paradigmatic "Occupational and Environmental Disease." *Saf. Health Work* **2012**, *3* (1), 11–16. https://doi.org/10.5491/shaw.2012.3.1.11.

(9) *Learn about Lead | US EPA*. https://www.epa.gov/lead/learn-about-lead (accessed 2023-07-30).

(10) Lead Poisoning, 2023. https://www.who.int/news-room/fact-sheets/detail/lead-poisoning-and-health#:~:text=Lead%20also%20causes%20long%2Dterm,birth%20and%20low%20birth%20weight.

(11) Sally Robertson. *Lead Poisoning History*.

(12) US EPA, O. *Basic Information about Lead in Drinking Water*. https://www.epa.gov/ground-water-and-drinking-water/basic-information-about-lead-drinking-water (accessed 2023-07-30).

(13) Chinaro Kennedy; Kennedy, C.; Ellen E. Yard; Yard, E. E.; Timothy Dignam; Dignam, T.; Sharunda Buchanan; Buchanan, S.; Suzanne K. Condon; Condon, S.; Mary Jean Brown; Brown, M. J.; Jaime Raymond; Raymond, J.; Helen Schurz Rogers; Rogers,
H. S.; John Sarisky; Sarisky, J.; Rey de Castro; de Castro, R.; Ileana Arias; Arias, I.; Patrick N. Breysse; Breysse, P.; Breysse, P. N. Blood Lead Levels Among Children Aged <6 Years - Flint, Michigan, 2013-2016. *Morb. Mortal. Wkly. Rep.* **2016**, *65* (25), 650–654. https://doi.org/10.15585/mmwr.mm6525e1.

(14) Melissa Denchak. *Flint Water Crisis: Everything You Need to Know*; 2018.

(15) Lehmann, J. Terra Preta Nova – Where to from Here? **2009**, 473–486. https://doi.org/10.1007/978-1-4020-9031-8_28.

(16) Heckenberger, M. J.; Kuikuro, A.; Afukaka Kuikuro; Afukaka Kuikuro; Kuikuro, U. T.; Russell, J. C.; Schmidt, M. J.; Fausto, C.; Franchetto, B. Amazonia 1492: Pristine Forest or Cultural Parkland? *Science* **2003**, *301* (5640), 1710–1714. https://doi.org/10.1126/science.1086112.

(17) Glaser, B.; Lehmann, J.; Zech, W. Ameliorating Physical and Chemical Properties of Highly Weathered Soils in the Tropics with Charcoal – a Review. *Biol. Fertil. Soils* **2002**, *35* (4), 219–230. https://doi.org/10.1007/s00374-002-0466-4.

(18) Lehmann, J.; Gaunt, J. L.; Rondón, M. A. BIO-CHAR SEQUESTRATION IN TERRESTRIAL ECOSYSTEMS - A REVIEW. *Mitig. Adapt. Strateg. Glob. Change* **2006**, *11* (2), 395–419. https://doi.org/10.1007/s11027-005-9006-5.

CHAPTER 2

A Review on Biochar as an Adsorbent for Pb(II) Removal from Water

Note: The contents of this chapter were adapted from the review article published in the journal 'Biomass.'

Pushpita Kumkum and Sandeep Kumar

biomass

MDPI

Review

A Review on Biochar as an Adsorbent for Pb(II) Removal from Water

Pushpita Kumkum and Sandeep Kumar *

Department of Civil and Environmental Engineering, Old Dominion University, Norfolk, VA 23529, USA; pkumk001@odu.edu
* Correspondence: skumar@odu.edu

Abstract: Heavy metal contamination in drinking water is a growing concern due to its severe health effects on humans. Among the many metals, lead (Pb), which is a toxic and harmful element, has the most widespread global distribution. Pb pollution is a major problem of water pollution in developing countries and nations. The most common sources of lead in drinking water are lead pipes, faucets, and plumbing fixtures. Adsorption is the most efficient method for metal removal, and activated carbon has been used widely in many applications as an effective adsorbent, but its high production costs have created the necessity for a low-cost alternative adsorbent. Biochar can be a cost-effective substitute for activated carbon in lead adsorption because of its porous structure, irregular surface, high surface-to-volume ratio, and presence of oxygenated functional groups. Extensive research has explored the remarkable potential of biochar in adsorbing Pb from water and wastewater through batch and column studies. Despite its efficacy in Pb removal, several challenges hinder the real application of biochar as an adsorbent. These challenges include variability in the adsorption capacity due to the diverse range of biomass feedstocks, production processes, pH dependence, potential desorption, or a leaching of Pb from the biochar back into the solution; the regeneration and reutilization of spent biochar; and a lack of studies on scalability issues for its application as an adsorbent. This manuscript aims to review the last ten years of research, highlighting the opportunities and engineering challenges associated with using biochar for Pb removal from water. Biochar production and activation methods, kinetics, adsorption isotherms, mechanisms, regeneration, and adsorption capacities with process conditions are discussed. The objective is to provide a comprehensive resource that can guide future researchers and practitioners in addressing engineering challenges.

Keywords: biochar; heavy metals; lead; adsorption; pollutant removal; biomass; desorption; regeneration; scalability

Citation: Kumkum, P.; Kumar, S. A Review on Biochar as an Adsorbent for Pb(II) Removal from Water. *Biomass* **2024**, *4*, 0–29. https://doi.org/

Academic Editor: Maurizio Volpe

Received: 21 January 2024
Revised: 7 March 2024
Accepted: 15 March 2024
Published: 22 March 2024

1. Introduction

1.1. Biochar

Biochar is a carbon-rich material known for its stability and long-lasting nature, which refers to its resistance to breakdown or decomposition over long periods of time [1].

From mitigating water pollution to serving as a potential source of energy and combating climate change, biochar has proven to be an invaluable resource in the quest for sustainable solutions [2,3].

Biochar is produced through the pyrolysis process, which involves subjecting biomass or organic waste to high temperatures (ranging from 400 to 600 °C) in the absence of oxygen [4]. During pyrolysis, the biomass is decomposed into three basic components, the solid product, biochar; the liquid, bio-oil, which is formed by the condensation of volatile matters; and the gaseous component, called syngas, which includes carbon monoxide, methane, and carbon dioxide [5–7]. The ratio of these individual components depends on the pyrolysis temperature, heating rate, residence time, etc. [8]. All of these products

originate from cellulose, hemicellulose, and lignin, which is the basic composition of lignocellulosic biomass [9]. The pyrolysis process can be categorized into three classes: slow, fast, and gasification [10]. Due to its ability to produce a higher solid yield (ranging from 25% to 35%) compared to other pyrolysis processes, slow pyrolysis is widely considered as the primary method for biochar production [11]. Biochar International described the stages of pyrolysis [12] as follows: (a) drying and conditioning—at this stage, at ~100 °C, the chemically bound water starts getting driven off the biomass and at above 150 °C, the biomass starts to breakdown; [9] (b) torrefaction—when the biomass is heated to temperatures ranging from 200 to 280 °C, the chemical bonds present in the biomass start to break down, and the formation of oxygen-containing functional groups (OFGs), i.e., hydroxide, carboxyl, carbonyl, lactone, lactol, quinine, chromene, anhydride, phenol, ether, pyrone, pyridine, pyridone, and pyrrole, etc., starts [13]. This process is endothermic, which means that it requires heat input to raise the temperature of the dry biomass and break the molecular bonds; [5] (c) exothermic pyrolysis—at this stage, between 250 and 300 °C, a combustible mixture of gases and tars starts releasing, resulting in cracks, increasing the surface area, and shrinking the particles, and this self-sustaining process keeps on going up to 400 °C, leaving a carbon-enriched residue [14]; however, external heat input is needed to maintain the temperature, and a maximum yield is obtained before the end of exothermic pyrolysis [12]; at this stage, the biochar has an ash content of 1.5–5%, around 25–35% of volatiles, and 60–70% of fixed carbon [12]; (d) endothermic pyrolysis—to increase the fixed carbon content, surface area, and porosity of the biochar, further heating is necessary to decompose more of the volatiles, which is typically achieved at a temperature of 550–600 °C, resulting in a fixed carbon content of 80–85% and a volatile content of 12% [15]; and (e) activation and gasification—at temperatures above 600 °C, a small amount of air and steam can activate the surface of the biochar, increasing its surface area and cation exchange by adding acidic functional groups but reducing its yield through the release of more volatiles [16], or, alternatively, adding more air and/or steam can initiate a gasification process with a low biochar yield (often less than 20%) and high ash content [17]. These physical and chemical properties generated due to varying pyrolysis conditions make biochar a promising tool for a variety of applications. The high surface area and porosity [18,19], presence of oxygen-containing functional groups etc. [17,20] of biochar provide it the benefit of adsorbing a variety of substances, including heavy metals and organic pollutants, making it useful for water treatment [21–23] and soil remediation [10,24]. The high cation exchange capacity of biochar allows it to retain nutrients, making it an effective soil amendment for agriculture [25–29].

1.2. Pb(II)

Lead (Pb(II)) is a naturally existing toxic heavy metal of bluish-grey color that is present in trace quantities in the earth's crust and can have serious health consequences when it enters the human body [30].

In the late 1800s, the use of lead pipes for water distribution became increasingly common in major cities across the United States [31]. Even though Pb(II) was more costly compared to iron, the durability and malleability made it a widespread preference for using as pipes [32]. According to the United States Environmental Protection Agency's (USEPA) 7th Drinking Water Infrastructure Needs and Survey Assessment (April 2023) report, there are an estimated number of 9.2 million lead service lines (LSLs) supplying water in US homes [33]. Lead-contaminated drinking water is often the result of corrosion in plumbing materials that contain lead [34]. This is especially common in areas where the water has high acidity or low mineral content, which can cause the corrosion of pipes and fixtures [35].

Children are particularly vulnerable to the harmful effects of lead exposure due to their developing bodies, which absorb more lead than adults [32]. Their brains and nervous systems are also more sensitive to the damaging effects of lead [32]. Children can experience a range of health issues even at low levels of lead exposure, such as behavior and learning

problems, lower IQs, hyperactivity, slowed growth, and hearing problems [36]. In some cases, lead ingestion can also lead to anemia [37]. Severe cases of lead exposure may result in seizures, comas, and even death, although such cases are rare [38]. In adults, lead exposure is linked with harmful effects on cardiovascular health, such as an increased blood pressure and proneness to hypertension [39], deteriorated kidney functions, and reproductive issues in both men and women [40]. Lead exposure in pregnant women is linked to premature births and a reduced growth of the fetus [33]. Replacing the existing lead service lines requires billions of dollars. An ambitious plan was put into place in 2021 to replace all lead service lines within the next ten years under the Bipartisan Infrastructure Law [41]. However, the costs associated with this undertaking are substantial. According to an EPA report, approximately USD 625 billion will be required over the next two decades to address the issues related to drinking water infrastructures [33].

Pb(II) contamination in drinking water has been identified as a significant public health concern, necessitating the exploration of alternative solutions to safeguard human health [42]. Biochar has emerged (as is evident by the numerous articles cited here) as a promising alternative for reducing point-of-use lead concentrations in water [43–46]. In this review, we aimed to capture recent advancements in using biochar for Pb(II) removal from water. We limited our search to studies conducted only from 2012 to 2022 and excluded any research on other metals, soil, or other biosorbents to ensure that our findings were specific to Pb(II), water, and biochar. To compile only the most relevant research within the selected time frame, we used Research Rabbit, a citation-based literature mapping tool for scientific literature that allows for a more targeted search. Figure 1 shows an example of the interface of the tool identifying literature on the relevant topic.

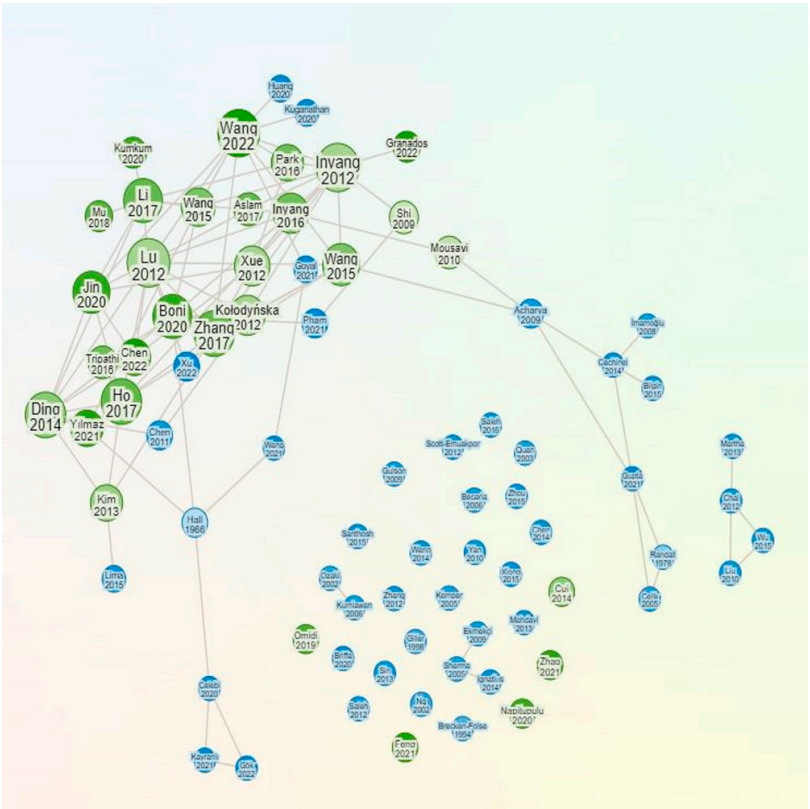

Figure 1. Example of the map generated by Research Rabbit to identify the relevant literature [1–14]. Green circles represent the literatures already in the collection and blue circles indicate similar work.

This review article provides several contributions to the field of Pb(II) removal using biochar. Firstly, our study specifically focuses on Pb(II), which allows us to provide additional knowledge in the field of exploring sustainable materials for tackling the Pb(II)-

contamination issue. Additionally, this study discusses the regeneration of Pb(II)-loaded biochar and also the possibility of adsorbed Pb(II) leaching back into the solution by desorption, which has not been typically covered in existing review papers. Furthermore, our study identifies two key gaps in the current literature on the use of biochar for lead removal. Firstly, there is a lack of research on the potential disposal options for Pb(II)-loaded biochar. Secondly, there is a lack of research on column-flow setups, which could provide more knowledge in the real-life application of biochar for Pb(II) removal. By highlighting these gaps and by providing valuable insights, this review article can help guide future research and serve as a vital tool for developing practical solutions to this pressing public health issue.

2. Pb(II) Removal Using Pristine Biochar

2.1. Feedstock

Researchers have conducted numerous studies to explore the Pb(II)-removing potential of biochar produced from different feedstocks under various pyrolysis conditions. The types of feedstocks they used are agricultural and forest residues, such as wheat and rice [21], wood and bark [21], cinnamon, cannabis [47], sesame straw [22], date seed [48], etc.; industrial by-products, such as anaerobically digested sludge, waste-activated sludge [49], digested whole-sugar beets [50]; and non-conventional materials, such as tire waste [51], etc. The physical and chemical properties of these feedstocks play an important role in defining the adsorption capacity and background mechanism of Pb(II) removal. They appeared to show a high content of oxygen-containing functional groups (OFGs) that provide negatively charged bonding sites on the biochar surface for Pb(II) [52], and some of them have high levels of Na, K, and Mg, which is related to the cation exchange capacity (CEC) and facilitates the ion exchange mechanism when reacting with Pb(II) in a low pH (6.0–7.0) environment [9]. Additionally, the high ash and mineral components present in these biomass feedstocks also promote creating mineral precipitates. which is one of the major dominant mechanisms of removing Pb(II) from water [53].

About 78% of these studies utilized agricultural and forest residues, 18% of these studies explored Pb(II) adsorption by animal waste/industrial by-products, and 4% of these studies investigated non-conventional/synthetic materials as feedstocks to produce biochar to remove Pb(II) from water.

Figure 2 demonstrates the fractions of the different categories of feedstocks utilized to produce biochar.

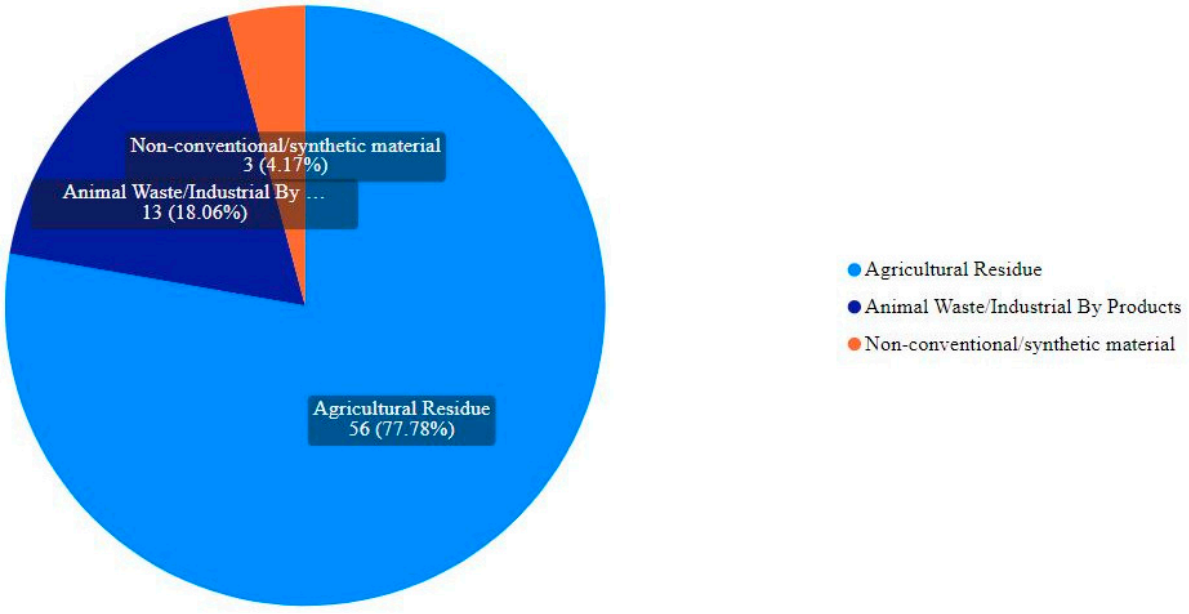

Figure 2. Different categories of feedstocks used for biochar.

2.2. Pyrolysis Temperatures/Conditions

A wide range of temperatures (300–700 °C) have been utilized to produce biochar, which resulted in the biochar of various physicochemical properties that played a critical role in removing Pb(II) from water. A low pyrolysis temperature (300–450 °C) typically retains the OFGs, i.e., carboxylic and hydroxylic/phenolic (-COOH, -OH, and C-OH) groups that are present on the biochar surface, which contributes to surface complexation or the electrostatic interaction between biochar and Pb(II) by influencing the protonation and deprotonation of the surface and thereby removing it from the water [21]. As the temperature increases, the volatile matters occupying the pores of the surface starts releasing out of the biomass, creating an increased number of pores and thereby increasing the surface area and pore volume that facilitates the physical adsorption of Pb(II) [47]. Biochar produced by a high pyrolysis temperature showed an increased pH, increased ash/mineral content, decreased number of OFGs, and increased aromaticity and hydrophobicity [4]. These variations in the physicochemical properties correlated with pyrolysis temperatures determine the governing adsorption mechanism.

2.3. Experimental Method

Batch experiments and column experiments are two commonly used laboratory methods for studying Pb(II) adsorption using biochar. A batch study is simple and utilizes a static environment. Certain doses of biochar are introduced in a Pb(II)-aqueous solution in reactors of different concentrations. The reactors are then shaken for different reaction times to achieve adequate contact/equilibrium. At the end of the reaction time, the Pb(II) concentration is measured using specific analytical instruments, such as a Flame Absorption Atomic Spectrophotometer (FAAS) or an Inductively Coupled Plasma (ICP) Spectroscope. Wang et al. investigated the Pb(II)-adsorption potential of biochar from peanut shell and from the residue of Chinese medicine materials [54]. A dosage of 4 g/L of biochar was introduced to a Pb(II) solution of with a concentration of 450 mg/L and 900 mg/L and agitated at 140 rpm on a mechanical shaker. Aliquots were collected at certain time intervals within a duration of 2 to 60 h, and the Pb(II) concentrations were measured in the filtrate using FAAS. The Pb(II)-adsorbed biochar were collected using centrifuge and characterized to study surface-property changes using various analytical instruments, such as a scanning electron microscope (SEM), an energy dispersive spectrometer (EDS), Fourier transform infrared spectroscopy (FTIR), a thermogravimetric analysis (TGA), an X-ray diffractometer (XRD), and X-ray photoelectron spectroscopy (XPS) [49,55]. Batch experiments, following a similar procedure, were conducted by Mu et al., Omidi et al., Zhang et al., and Aslam et al. [19,47,56,57]. For column studies, a fixed bed of the adsorbent, biochar, is set up, and a Pb(II)-aqueous solution of various concentrations passes through, using a peristaltic pump, and samples are collected at different times to measure the concentrations of Pb(II). Ding et al. conducted a column study where hickory wood biochar was used to evaluate the Pb(II)-adsorption potential in a fixed-bed setting [58]. Two layers of quartz sand were used, sandwiching the biochar bed to facilitate the uniform distribution of flow. The column was first flushed with DI water for approximately 2 h, and then the metal solution was employed at the bottom inlet of the column to conduct the flow in an upward direction for 140 min. Aliquots were collected at certain intervals and analyzed to measure the Pb(II) concentration. Column studies appear to provide more realistic results that mimic the real-world scenario of the potential of biochar being used as an adsorbent to remove Pb(II). Fixed-bed filtration systems are frequently utilized in large-scale industrial operations to eliminate pollutants from wastewater streams [21]. In a study conducted by Xue et al., hydrochars packed in laboratory filtration columns were found to be highly effective in removing Pb(II) [59]. However, column studies were performed in only 9% of the reviewed literature. This could be explored further to gain more knowledge and insight regarding the interaction of biochar and Pb(II) in a fixed-bed system.

2.4. Kinetic Modeling

An adsorption process typically involves three steps: (1) the external mass transfer of the adsorbate from the bulk solution to the external surface of the adsorbent, (2) the internal diffusion of the adsorbate to the sorption sites, and (3) the sorption itself. Various models have been developed to describe the kinetics of adsorption, and these models are based on different assumptions about which step is the rate-limiting one [60]. Some models assume that the sorption step is the rate-limiting one, while others assume that the diffusion step is the rate-limiting one. By fitting experimental data to these models, it is possible to determine which step is the rate-limiting one and to gain insights into the underlying mechanisms of the adsorption process. Understanding the rate-limiting step is important for optimizing the design of adsorption systems and for predicting the performance of these systems under different operating conditions [61].

Pseudo-first and pseudo-second order and intraparticle diffusion are the models that typically have been employed [47,62].

According to the pseudo-first order (PFO) kinetic model introduced by Lagergren (1898), adsorption is primarily governed by the difference in the concentration of metal ions in the solution and the adsorbent surface [63]. This model is commonly used to describe the kinetics of metal adsorption in the early stages of the process, assuming that the adsorption occurs via diffusion through the interface. However, this model fails to explain the effect of intraparticle diffusion or other mass transfer limitations that may occur during the later stages of the adsorption process. The pseudo-first order kinetic model equation is as follows:

$$q_t = q_e(1 - e^{-k_1 t}) \quad (1)$$

Here, q_t = the amount of Pb(II) sorbed at time t;
q_e = the amount of Pb(II) sorbed at equilibrium;
k_1 = the second-order rate constant.

Physisorption (sorption by intermolecular forces) is the main mechanism involved in this model.

The pseudo-second-order (PSO) model by Ho and McKay (1998) implies that the adsorption rate is dependent on the available adsorption capacity of the adsorbent and not on the concentration of the adsorbate itself [64]. This model considers that the rate at which adsorption sites are filled is directly proportional to the square of the number of available activated sites on the surface of the adsorbent. This suggests that the rate of adsorption is limited by the number of available adsorption sites on the adsorbent surface rather than the concentration of the adsorbate in the solution. Therefore, this model can be applicable to the entire timeline of the sorption process, especially when chemisorption is the rate-limiting mechanism [21]. The pseudo-second-order equation can be written as follows:

$$q_t = \frac{k_2 q_e^2 t}{1 + k_2 q_e^2 t} \quad (2)$$

Here, q_t = the amount of Pb(II) sorbed at time t;
q_e = the amount of Pb(II) sorbed at equilibrium;
k_2 = the second-order rate constant.

The Elovich model assumes that the rate of adsorption of a solute decreases exponentially as the amount of adsorbed solute increases. This indicates that as more solute is adsorbed onto the surface of the adsorbent material, the availability of active sites on the surface decreases, leading to a slower adsorption rate. Despite its initial development for gaseous systems, the Elovich model has proven to be a useful tool for understanding the kinetics of adsorption in wastewater processes and for predicting the performance of adsorption systems under different operating conditions [65]. The model can be expressed by Equation (3):

$$q_t = \frac{1}{\beta} = \ln(\alpha\beta t + 1) + b \quad (3)$$

Here, q_t = the amount of Pb(II) sorbed at time t;
α = the initial adsorption rate;
β = the desorption constant at time t.

The intraparticle diffusion model is a useful tool for describing adsorption processes in which the rate of adsorption is influenced by the rate of diffusion of the adsorbate towards the adsorbent surface [66]. This suggests that the process is controlled by the diffusion rate of the adsorbate [18]. The equation can be expressed as Equation (4):

$$q_t = k_3 t^{\frac{1}{2}} + b \quad (4)$$

Here, q_t = the amount of Pb(II) sorbed at time t;
k_3 = the intraparticle diffusion rate constant;
b = the intercept.

After fitting the experimental data with this model, the resulting value of b indicates how the thickness of the boundary layer of the biochar can influence the adsorption process [54].

Table 1 summarizes the different kinetic models investigated in the reviewed studies, along with the corresponding feedstocks, pyrolysis conditions, and pre-/post-treatments.

2.5. Isotherm Modeling

Researchers have adopted mathematical approaches, such as isotherm models, to study the adsorption behavior of Pb(II) onto biochar under different conditions, such as a differing pH, temperature, initial Pb(II) concentration, flow, etc. [67,68]. There are several different isotherm models that are used by researchers including the Langmuir, Freundlich, Temkin, Thomas, Yoon–Nelson, Bohart–Adams, Prausnite–Radke, Redlich–Peterson, Toth, and Sips isotherms, etc. [48,69]. Each of these models has a different mathematical form and is used to describe different aspects of the adsorption behavior.

The Langmuir isotherm model is a commonly used approach for characterizing the adsorption of solutes onto solid surfaces [70,71]. This model is based on the assumption that the adsorbent surface is uniform and homogeneous in nature, which means that all the adsorption sites have the same energy [72]. Additionally, the model assumes that there is no interaction between adsorbed molecules on different sites and that each site can accommodate only one adsorbed molecule at a time [51].

By utilizing the Langmuir isotherm model, it is possible to gain insights into the adsorption process and obtain essential information about the adsorption capacity of the adsorbent material, the affinity of the adsorbate for the adsorbent surface, and the maximum adsorption capacity of the adsorbent [50,54]. This information can be used to optimize the design and operating conditions of adsorption systems and ensure their optimal performance. The model can be expressed as Equation (5):

$$q_e = \frac{q_{m_{ax}} K_L c_e}{1 + K_L c_e} \quad (5)$$

Here, q_{max} = the maximum amount of adsorbed Pb(II) by the unit weight of biochar;
q_e = the amount of Pb(II) adsorbed at an equilibrium concentration;
K_L = the Langmuir constant;
Ce = the concentration of Pb(II) in the solution at equilibrium.

The Freundlich isotherm model assumes that the adsorbent surface is heterogenous and that adsorption happens in a multilayer sorption, where adsorbate molecules tend to preferentially attach to sites that have a stronger affinity (higher bonding energy) for them, resulting in the formation of multiple layers of the adsorbate molecules on the adsorbent surface [21]. In contrast to the Langmuir model, this model accounts for the non-uniform distribution of the adsorption heat and affinity toward the heterogeneous

surface. It assumes that the adsorption process occurs on sites with varying properties, resulting in a non-uniform distribution of the adsorption [73]. The Freundlich equation can be expressed as Equation (6):

$$q_e = K_F C_e^n \quad (6)$$

Here, q_e = the amount of Pb(II) adsorbed at an equilibrium concentration;
K_F = the adsorption coefficient of the Freundlich model.

Table 1 summarizes the different isotherm models investigated in the reviewed studies, along with the corresponding feedstocks, pyrolysis conditions, and pre-/post-treatments.

2.6. Sorption Mechanisms

The adsorption and removal of Pb(II) from water by biochar involves various mechanisms, including surface complexation, electrostatic interaction/ion exchange, and mineral precipitation.

2.6.1. Physical Sorption

Biochar is composed of micropores (<2 nm), mesopores (2–50 nm), and macropores (>50 nm), which have the capacity to capture Pb(II) ions and remove them from the solution through the process of physical sorption [74]. The amount of Pb(II) adsorbed onto these sites is determined by the number of available sites, which is influenced by the type of feedstock used and the pyrolysis temperature during biochar production [6]. The unique pore structure of biochar provides a large surface area for adsorption, making it an effective adsorbent for Pb(II) removal. Physical sorption occurs as Pb(II) ions are attracted to and captured by the available sites within the biochar pores [75]. This process is influenced by various factors, such as the size and shape of the pores [15], the chemical composition of the biochar, and the concentration of Pb(II) ions in the solution [76–78]. The pore volume and surface area of biochar can be quantified using a BET surface analyzer [79]. Increasing the temperature during pyrolysis leads to an increase in the specific surface area [80]. This happens when the volatile matters present in the feedstock starts escaping the pores as the temperature increases and, therefore, the surface area increases [81]. However, a non-woody biomass appeared to have high nutrient and ash contents, which volatized and increased the surface area and porosity of biochar under a high pyrolysis temperature [57]. While it is generally true that elevating the temperature to above 400 °C can lead to an increase in the surface area, there have been some studies that have observed the opposite effect. This can be attributed to factors such as tar blocking the pores, partial ash fusions, or a decomposition of the porous structure [82,83].

2.6.2. Surface Complexation with Functional Groups

This process is facilitated by the presence of oxygen-containing functional groups on the biochar surface, which can be identified by Fourier Transform Infrared Spectroscopy (FTIR). The presence and position of carboxyl and hydroxyl groups in the FTIR spectrum can provide insights into their role in the adsorption process. The content of these functional groups is dependent on the feedstock properties of the biochar, the pyrolysis conditions, and the pH of the solution. Although a woody biomass has a lower surface area compared to a non-woody biomass, the presence of OFGs makes it favorable for them to adsorb Pb(II) from water. These woody biomasses, and also agricultural and forest residues, have an abundant amount of oxygen-containing groups (carboxyl COOH, carbonyl C=O, and hydroxyl OH) that provide negatively charged surface binding sites and that facilitate creating surface complexation with Pb(II) [53,77,84].

These functional groups participate in the cation exchange mechanism, whereby they either gain protons (at a low pH) or donate protons (at a high pH) in the presence of Pb(II) [20]. The extent of cation exchange is determined by the concentration of the exchangeable cations on the biochar surface and their affinity for the adsorbed cations [4]. The content of the functional groups in biochar decreases with temperature due to higher

carbonization [76]. This is because the dehydration of cellulose and lignin begins at 300 °C, and their transformation occurs at 400 °C [83].

2.6.3. Electrostatic Interaction

Pb(II) adsorption by electrostatic interaction occurs when positively charged Pb(II) ions are attracted to the negatively charged surface of the biochar [49,85]. This attraction is due to the electrostatic forces between the ions and the surface [50]. When the biochar has a net negative charge, it can attract and bind positively charged ions, such as Pb(II) [86]. The strength of this interaction depends on the magnitude of the charge on the biochar surface, the size and charge of the ions, and the ionic strength of the solution [29,85]. When the pH of the net solution is zero, no interaction happens [47]. But when the pH of the solution is greater than the pH at the point of zero charge (pHPZC) [83], then the biochar surface becomes negatively charged by releasing H^+ and facilitates the adsorption of the positively charged Pb(II) [87]. When the pH of the solution is less than the pH at the point of zero charge, then the biochar surface becomes positively charged by gaining H^+ and repulsing the positively charged Pb(II) [19]. At a high pyrolysis temperature (>500 °C), the content of the negatively charged surface functional groups decreases, causing a reduction in the negative surface charge and an increase in the pH at the point of zero charge [83]. Also, a high temperature increases the ash content, which facilitates an increase in the pH of the solution when the biochar is introduced [83]. Similarly, a low pyrolysis temperature is attributed with a high amount of oxygen functional groups, which thereby promotes an increased chance of surface complexation [88].

2.6.4. Mineral Precipitation

Pb(II) adsorption by mineral precipitation occurs when these ions react with the minerals present in the biochar to form insoluble precipitates [19]. The formation of these precipitates is influenced by several factors, including the pyrolysis temperature and the mineralogy and surface chemistry of the biochar [89]. Biochar with an alkaline nature [90], which is produced by the thermal degradation of cellulose and hemicellulose at temperatures above 400 °C, can facilitate the precipitation of metals [91]. Also, biochar derived from animal waste is rich in minerals such as Ca and K, which can participate in the precipitation of metals on the biochar surface [91]. Mineral components can take part in removal through a competitive ion exchange as well [83]. Increasing the temperature during biochar production leads to a higher content of mineral components [4,80]. However, the water-soluble fraction of these minerals stops increasing beyond 200 °C. This is due to the fact that at temperatures above 200 °C, the minerals start to crystallize [92], resulting in reduced solubility. This is attributed to the facilitation of the removal of Pb(II) through mineral precipitation [83].

2.6.5. Ion Exchange

Cation exchange is another important mechanism that plays a role when removing Pb(II) from water using biochar [18,93]. Biochar properties consist of cations such as Na, K, Ca, Mg, etc. [9]. While in a solution, these are released, and due to the competitive affinity of different ions on the binding active sites of biochar, Pb(II) ions may be exchanged with these mineral ions and thereby may be removed from the solution [72,87]. High levels of Na, K, and Mg are associated with an increased Cation Exchange Capacity (CEC). A high CEC promotes ion exchange under acidic pH by the biochar releasing these in the solution and creating bonding with Pb(II) [53,94]. Figure 3 demonstrates the different sorption mechanisms, and Table 1 summarizes the key findings of the different studies.

Table 1. Removal mechanisms and key findings: Pb(II) removal using pristine biochar.

Feedstock	Production Method/ Pyrolysis Condition	Removal Mechanism/Kinetic Model/Isotherm Model	Maximum Adsoprtion	Key Findings/Notes	Reference
Carbon Wheat Straw and Natural Straw	300 °C for 60 min	• Langmuir • PSO • Endothermic	149.7 mg/g	• Increased dosage of biochar showed increased Pb(II)-removal percentage. • Adsorption Capacity$_{\text{Carbon wheat straw}}$ > Adsorption Capacity$_{\text{Natural straw}}$. • Carbon wheat straw biochar reached equilibrium faster than natural straw.	[56]
Cinnamon cannabis	300, 400, and 600 °C for 120 min	• Surface complexation • Ion exchange • Electrostatic interaction • Langmuir	135.68–168.05 mg/g	• Increased pyrolysis temperature resulted in higher surface area. • Average pore size indicated that adsorbent has mesoporous structure.	[47]
Phyllostachys pubescens (PP)	0–4% oxygen content atmosphere—slow pyrolysis—450 °C and 700–60 min	• Precipitation • Surface complexation through Pb(II)–π interaction and functional groups	67.4 mg/g	• Increased oxygen content showed increased contribution of mineral precipitation in Pb(II) removal. • Increase in pyrolysis temperature increased surface area, porosity through aromatization (related to decreased functional groups), and π chemical bond. • Under an oxygen-rich atmosphere and low pyrolysis temperature (450 °C), the lactonic functional group (i.e., carboxylic esters), pore volume, and surface area of the pyrolysis product increased, which in turn created additional adsorption sites. • As the temperature increased, the number of oxygen-containing functional groups decreased, while the ash content increased. The ash was composed of various inorganic compounds, including calcium carbonate, which aided in the precipitation-based removal process.	[19]

Table 1. *Cont.*

Feedstock	Production Method/ Pyrolysis Condition	Removal Mechanism/Kinetic Model/Isotherm Model	Maximum Adsoprtion	Key Findings/Notes	Reference
Rice husk Dairy manure	350 °C for 4 h	• Surface complexation • Precipitation	Not quantified	• The decomposition of cellulose and hemicellulose in rice husk biochar occurred at a temperature of around 300 °C, resulting in the production of organic acid and phenolic compounds that can cause a decrease in pH. • Dairy manure biochar exhibited a higher pH level, owing to the minerals that initiate separation beyond the temperature threshold of 300 °C.	[29]
Sesame straw	700 °C for 4 h	• Langmuir	• 102 mg/g (monometal) • 88 mg/g (multimetal)	• The adsorption characteristics of the multimetal solution were not the same as those of the monometal. • Among the cations present in the multimetal solution, Pb(II) exhibited the highest level of adsorption. This aligns with the results of other studies.	[22]
Peanut hull	450 °C	• Surface complexation • Precipitation • Electrostatic interaction	63.09 mg/g	• Adsorption capacity increased with the increase in temperature, which means this was an endothermic process. • The adsorption capacity was found to be greater in particles with a size of less than or equal to 2 mm compared to those with a size greater than 2 mm. This is due to the fact that smaller particle sizes have a larger surface area, which facilitates greater adsorption.	[72]

Table 1. *Cont.*

Feedstock	Production Method/ Pyrolysis Condition	Removal Mechanism/Kinetic Model/Isotherm Model	Maximum Adsoprtion	Key Findings/Notes	Reference
• Avocado seed • Avocado peel • Grapefruit peel • Brown seaweed	• Laboratory tube furnace (300 °C 1 h) • DIY biochar maker (BioCharlie Log—ASB, APB, GPB, and BSB)	This study did not discuss the adsorption mechanism, but the authors guessed the chemisorption processes—precipitation, ion exchange, electrostatic attraction, and surface complexation. However, in this study is unique in a sense that the authors compared lab-made biochar and home-made (temperature uncontrolled) biochar	Not quantified; used % removal	• Land-based biochar (Avocado and Grapefruit): high carbon content, and oxygen-containing functional groups were the dominating factor in Pb(II) adsorption. • Marine-based biochar (seaweed): high ash content, which played a governing role in adsorption. • The typical trend of an increased pH with an increased pyrolysis temp was not found in this study, which the authors attributed with the biomass-specific characteristics. • Lab-produced biochar showed better adsorption efficiency.	[62]
• Green waste biochar (GWB) (consists of Bermuda Grass—Cynodondactylon) • Popular twigs biochar (PTB)	350 °C and 650 °C at 8–9 °C min^{-1}	• Surface complexation • Precipitation • Cation exchange	44.42 mg/g	• In this study, the authors discussed the correlation between the O:C ratio and biochar stability, which is not quite typical with regards to the discussion points of other studies. • A higher pH was found for a higher temp, which is in agreement with other studies that suggest that a high pH is associated with a low O and H and a low amount of oxygen functional groups. • A low temp and a high CEC were found as well as a high surface area and a high amount of functional groups, which is because at a high temp, oxygen-containing functional groups become volatilized.	[57]
Grape pomance	300–700 °C at 10 °C min^{-1}	• Physisorption and chemisorption	134 mg/g	Uniqueness: experiment with low Pb(II) concentration to mimic practical scenarios.	[87]

Table 1. *Cont.*

Feedstock	Production Method/ Pyrolysis Condition	Removal Mechanism/Kinetic Model/Isotherm Model	Maximum Adsoprtion	Key Findings/Notes	Reference
• Waste-activated sludge • Anaerobic digestion sludge	400–800 °C at 15 °C min^{-1}	• Precipitation (dominant: 53.5%) • Ion exchange • Surface complexation • Electrostatic interaction	53.96 mg/g	• The ion exchange capacity and precipitation tendency were found to be higher in the biochar prepared at a higher temperature, as compared to those prepared at a lower temperature (400 °C). Additionally, the biochar prepared at a lower temperature contained fewer functional groups than the biochar prepared at 800 °C. These findings are in agreement with other studies. • At high temperatures, low H:C and O:C ratios indicated a high carbon content due to increased carbonization and aromaticity, resulting in greater resistance to decomposition. This means that a high temperature provides increased thermal stability.	[49]
• Peanut shell • Residue of Chinese medicine materials	300–600 °C	• Surface complexation • Pb(II)–π interaction • Precipitation	82.5 mg/g	• For the peanut shell, the adsorption efficiency was higher with low temperatures and the medicine residue biochar showed higher adsorption efficiency with high temperatures. • Precipitation was the dominant mechanism in all cases, except Pb(II)–π interactions in the peanut shell biochar which was the dominant one with a high temp.	[54]
Sugarcane bagasse	250, 400, 500, and 600 °C at 10 °C min^{-1}	• Surface complexation • Precipitation	21 mg/g	• Sorption capacity decreased with increasing temp.	[95]

Table 1. *Cont.*

Feedstock	Production Method/ Pyrolysis Condition	Removal Mechanism/Kinetic Model/Isotherm Model	Maximum Adsoprtion	Key Findings/Notes	Reference
Sludge	550 °C for 2 h	• Surface complexation • Precipitation • Ion exchange	30.88 mg/g	• Presence of carboxyl and hydroxyl groups facilitated co-ordination with Pb(II) by acting as a proton donor. • Higher pH levels created more sites for surface complexation, since more carboxylic groups deprotonated and thus helped in sorption. • As the pH level rose beyond 5, co-precipitation mechanisms started playing their roles.	[96]
Wheat straw	400 °C for 2 h	• Surface complexation	185.19 mg/g	This study explored the potential of hydroxide complex formation at higher pH levels, although it did not delve into the possibility of metal precipitation as a result of this mechanism.	[85]
• Digested animal waste • Digested whole sugar beet	600 °C for 2 h	• Precipitation	200 mg/g	• Somewhat similar FTIR spectra of pre- and post-sorption indicated that lead adsorption was not governed by an interaction with the surface functional groups. • Even though Pb(II) had the highest surface electronegativity compared to other metals, it still did not show the highest tendency for adsorption. This is not in agreement with other studies [23].	[50]
Red fruit peel	300 °C for 2 h	• Physical sorption	61.86 mg/g	• This study found that a higher ash content led to lower adsorption rates, likely due to clogging of the biochar pores. • These researchers also observed a peak in adsorption, followed by a decrease, which they attributed to desorption, since adsorption is a reversible process.	[86]

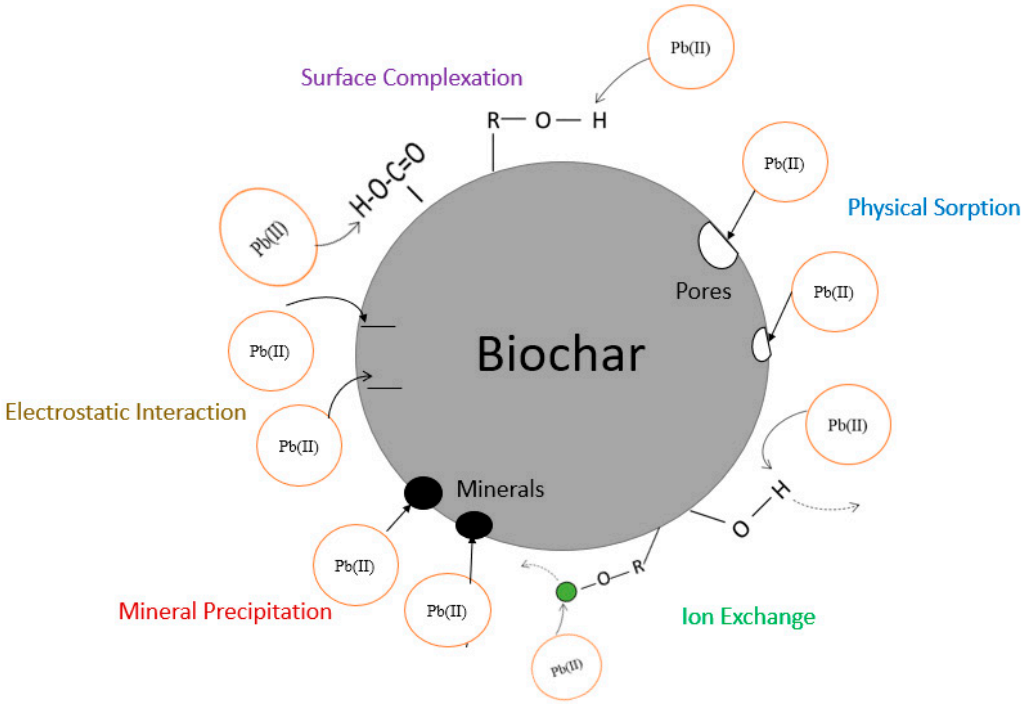

Figure 3. Sorption mechanisms involved in Pb(II) removal.

Omidi et al. investigated the adsorption of Pb(II) by biochar using cinnamon and cannabis as feedstocks [47]. Similar to other studies, they also found that the adsorption capacity increases with an increase in the biochar dose until a certain point, after which it starts to decrease. This can be attributed to the fact that, initially, there are numerous bonding sites available which get occupied rapidly, leading to an increase in the adsorption capacity. However, as the dose is further increased, the rate of available active sites exceeds the rate of adsorption, resulting in a decrease in capacity. To strike a balance between these two factors, an optimum dose was identified. In this study, the increase in the initial concentration of Pb(II) was observed to enhance the adsorption capacity while reducing the removal percentage. This can be attributed to the higher availability of the adsorbate for adsorption. However, since more ions are available for adsorption, the rate at which they get adsorbed decreases, leading to a reduction in the removal percentage. The adsorption rate happened to be faster in the initial stage of reaction due to the abundance of active binding sites, and, as time progresses, the number of available sites for adsorption decreases as they become occupied. Consequently, the rate of adsorption reduces [47]. A further analysis of how functional groups affect the adsorption process could have greatly enhanced the value of this research.

Xu et al. conducted their comparative adsorption study using rice husk (RHBC) and dairy manure biochar (DMBC) [29]. DMBC is more effective than RHBC in removing Pb(II) due to its ability to use both ionized phenolic O- group complexation and mineral precipitation with CO_3^{2-} and PO_4^{3-}. In contrast, RHBC only utilizes complexation with ionized phenolic O- groups to remove metal. These researchers examined the sorption of metals in mono- and multimetal solutions and at low and high metal concentrations. They discovered that RHBC exhibited greater competition in both low and high concentrations due to its reliance on a single mechanism—complexation with phenolic groups. Meanwhile, DMBC was less affected by competition due to its ability to use multiple mechanisms. The competition was greater for both types of biochar in the high concentration, because more metals compete for the available sites [29]. Cui et al. investigated Pb(II) adsorption using peanut hull-derived biochar [72]. This study explored the effects of the particle size of biochar on the adsorption process, which is not a very typical practice. The adsorption

capacity showed a similar pattern of increase with an increasing pH, until it reached a pH of 5.5. After 5.5, the rate of the capacity increase slowed down and reached equilibrium. However, the adsorption capacity remained high due to the precipitation mechanism, in addition to complexation. These results align with findings from other studies.

Wang et al. explored the adsorption of Pb(II) using peanut shell and the residue of Chinese medicine materials as biochar feedstocks [54]. In this study, a weak correlation was found between the reduction in Pb(II) sorption and ash content. The results suggest that precipitation is not solely dependent on the mineral content, which is different from the findings of other studies. Instead, the morphology of minerals, specifically the crystallization of minerals, was found to have an influence on the adsorption of Pb(II).

3. Pb(II) Removal by Modified/Functionalized Biochar

Researchers have explored the removal of Pb(II) by modifying or functionalizing biochar to either increase the removal capacity or to target specific contaminants, which shows a low adsorption potential by pristine biochar. They have studied modifications by metal oxides, such as hydrous manganese oxide (HMO) [97], MnO_2 [98], and $KMnO_4$ [99], and metal salts, such as $MgCl_2$ [100,101], $FeCl_3$ [102,103], $MnSO_4$, and $KHCO_3$ [104]. They have also studied activations by gases, such as CO_2 [105], and complex organics like chitosan [106], as well as modifications by nanoparticle composites, such as ZnO [107] and nanoscale Zero-Valent Iron (nZVI) [108]. These studies were able to show a 2–49-time increase in adsorption capacity.

Figure 4 demonstrates that a majority of the studies utilized metal salts or oxides for modifying the biochar. Table 2 summarizes the key findings of the different studies.

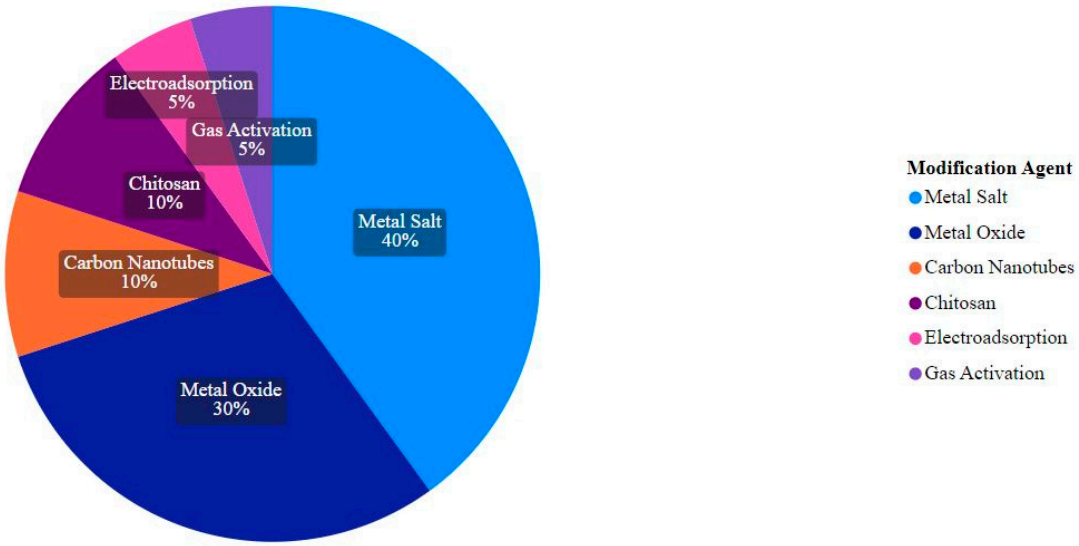

Figure 4. Different modification agents used for functionalizing biochar.

Table 2. Removal mechanisms and key findings: Pb(II) removal using modified biochar.

Feedstock	Modifying Agent/Compound	Pre-Pyrolysis/ Post-Pyrolysis	Production Method	Sorption Increase	Maximum Adsorption	Removal Mechanism/Kinetic Model/Isotherm Model	Key Findings/Notes	Reference
Pinewood	Hydrous manganese oxide (HMO)	Post	Feedstock was first converted to biochar by pyrolysis—100 °C for 1 h and then 700 °C for 3 h. Prepared biochar was then modified by manganese nitrate and $KMnO_4$.	92.50%	Not specified	• Surface complexation • Electrostatic interaction • PSO (rate was proportional to the number of active sites) • Langmuir • Endothermic (with an increased temperature, sorption increased)	Modification increased the number of hydroxyl groups, decreased pH at point of zero charge (pH_{PZC}), and increased the number of mesopores and macropores.	[97]
Coconut shell	$MgCl_2$	Pre	Feedstock was first impregnated with $MgCl_2$ and then pyrolyzed at 400 °C.	20 times	532.28 mg/g	• Ion exchange • Mineral precipitation • Interaction with OFGs • Metal–π electron co-ordination • Langmuir	Modification increased the OFG content.	[55]
Corn straw	$MgCl_2$	Post	Feedstock was first converted to biochar by pyrolysis—250 °C for 2 h. Prepared biochar was then modified by $MgCl_2$.	More than 2 times	5.15 mg/g	• Freundlich • PSO	Physical/chemical property changes associated with the modification were not investigated. No comparative analysis based upon the characteristic features were explored.	[101]
Swine manure	MnO_2	Post	Feedstock was first converted to biochar by pyrolysis—400 °C for 2 h. Prepared biochar was then modified by $KMnO_4$.	2 times	268 mg/g	• Electrostatic interaction • Surface complexation • Ion exchange	Adsorption was dependent on pH, which is similar to other studies. Modification increased the surface area and pore volume.	[98]
Oak wood and Oak bark	Metal salt impregnation followed by alkali (NaOH) treatment	Post	$Fe_2(SO_4)_3.nH_2O$ and $FeSO_4$ were used to make Fe^{2+}/Fe^{3+} SO_4^{2-}, 400–450 °C. Fast pyrolysis.	2.5 times	55.91 mg/g	• PSO • Langmuir–Freundlich • Endothermic	Introduction of iron oxide on the surface of biochar influenced the adsorption process.	[109]
Antibiotic residue	CO_2 gas activation	During pyrolysis	300–800 °C for 2 h	3 times	454 mg/g	Highest Pb(II) adsorption occurred by the biochar produced at 700 °C	Study focused on increasing the carbon and ash component (carbonate and phosphate) of biochar to improve Pb(II) removal through mineral precipitation.	[105]

Table 2. *Cont.*

Feedstock	Modifying Agent/Compound	Pre-Pyrolysis/ Post-Pyrolysis	Production Method	Sorption Increase	Maximum Adsorption	Removal Mechanism/Kinetic Model/Isotherm Model	Key Findings/Notes	Reference
Lotus leaf	$(NH_4)_2HPO_4$ (diammonium hydrogen phosphate)	Pre	600 °C for 1 h	2 times	1936.2 mg/g	• Freundlich • Complexation and precipitation	Modified biochar (NP-BC) had -COOH, -NH_2, P=O, and -OH, which co-ordinated with Pb(II) to form complexation.	[110]
Date seed	Electro-adsorption	Post	Pyrolyzed biochar was used as an electrode—550 °C for 3 h	21%	179.64 mg/g	• Electrostatic interaction • Physical adsorption • Surface complexation	Electro-assistance improved adsorption by increasing the surface charge density and bringing ions into closer contact with the biochar. Additionally, the electric current increased the pore structure.	[111]
Rice husk	Metal salt and metal oxide: rice husk biochar (BC) ---> magnetic rice husk biochar (FBC) ---> KMnO4-treated magnetic biochar (FMBC)	Pre and post	Pre-pyrolysis (600 °C for 1.5 h) magnetization and post-pyrolysis (600 °C for 0.5 h) $KMnO_4$ activation.	7 times	148 mg/g	• Surface complexation • PSO • Langmuir	$KMnO_4$ treatment increased OFGs, because $KMnO_4$ oxidized and produced more OFGs, and MnO has a greater affinity for heavy metals (HMs).	[79]
Cassava root husk	ZnO Nanoparticles	Post	Pyrolysis (400 °C for 2 h) and wet impregnation.	28% or 1.39 times	42.05 mg/g	• Precipitation • Surface complexation	Modification increased the number of -OH, which dropped after adsorption, indicating that precipitation took part in Pb(II) removal. It also increased the -CO- that took part in surface complexation. Modification reduced aromaticity, which is favorable for Pb(II) adsorption.	[107]
Sugarcane straw	$FeCl_3$	Post	Pyrolysis: 350 and 750 °C at 5 °C min^{-1}. Modification: wet impregnation.	2–11%	92.81 mg/g	• Precipitation (due to higher ash content) • Electrostatic interaction	Modification increased the specific surface area and exposed functional groups.	[102]

Table 2. *Cont.*

Feedstock	Modifying Agent/Compound	Pre-Pyrolysis/ Post-Pyrolysis	Production Method	Sorption Increase	Maximum Adsorption	Removal Mechanism/Kinetic Model/Isotherm Model	Key Findings/Notes	Reference
• Nut shield • Wheat straw • Grape stalk • Grape husk	$FeCl_3$	Post	Pyrolysis: 600 °C for 30 min. Modification: wet impregnation.	461%	179 mg/g	• Surface complexation	Magnetization increased sorption by improving the structure of biochar. Fe oxides promoted stronger chemical bonds with Pb(II). Fe oxides increased CEC value significantly, and CEC is an important feature for Pb(II) adsorption.	[103]
Raw cypress sawdust (RCS)	$MgCl_2$	Pre	600 °C for 1 h	7.4 times	202.2 mg/g	• Surface complexation • Precipitation	Modification increased the surface area, amount of OFGs, and the CEC associated with Mg ions.	[112]
Commercial biochar	$FeSO_4$ and $FeCl_3$	Post	Pyrolysis: 500 °C. Magnetization: chemical precipitation and wet impregnation.	Modification decreased adsorption	35 mg/g	• Ion exchange • Precipitation	This study showed a decrease in adsorption capacity.	[89]
Pinewood	$MnCl_2.4H_2O$ and birnessite ($KMnO_4$ precipitate)	Pre and post	Pyrolysis in the presence of $MnCl_2.4H_2O$ (MPB): 600 °C for 1 h. Impregnated with birnessite via precipitation following pyrolysis (BPB).	2–20 times	17 mg/g	• Physical sorption on sites provided by birenssite • Precipitation	The modification process using $MnCl_2$ resulted in an increase in the surface area and pore volume, potentially due to the formation of Mn-bearing minerals.	[113]
Silkworm excrement	Chitosan combined with pyromellitic dianhydride (GBC)	Post	• Pyrolysis: 600 °C for 2 h---> BC. • Chitosan-BC: wet impregnation. • Chitosan-BC-PD: wet impregnation (GBC).	12%	9.54 mg/g	• Surface complexation • Ion exchange • Electrostatic interaction	Modification increased the surface area pore volume, and OFG content.	[114]
Hickory wood	NaOH	Post/during	Wet impregnation, followed by pyrolysis at 600 °C for 2 h.	4.7 times	19.1 mg/g	• Physical adsorption • Surface complexation	Modification promoted more adsorption sites and increased OFGs.	[58]
Rice straw	$KMnO_4$	Post	Wet impregnation.	2.5 times	304.5 mg/g	• Surface complexation	Modification increased OFGs, surface area, and pore volume.	[99]
Hickory wood	$KMnO_4$	Pre	Wet impregnation.	3.5 times	153.1 mg/g	• Surface complexation	Modification provided more binding sites and introduced more OFGs.	[115]

Table 2. *Cont.*

Feedstock	Modifying Agent/Compound	Pre-Pyrolysis/ Post-Pyrolysis	Production Method	Sorption Increase	Maximum Adsorption	Removal Mechanism/Kinetic Model/Isotherm Model	Key Findings/Notes	Reference
Hickory wood and sugarcane bagasse	Carbon nanotubes (CNT) with the aid of a surfactant	Pre	Pyrolysis: 600 °C for 1 h and wet impregnation of surfactant and CNT.	25–28%	15 mg/g	• Surface complexation • Electrostatic interaction	Sodium dodecylbenzenesulfonate (SDBS), the surfactant, played a crucial role in preventing the aggregation of CNTs and promoting their distribution and stabilization on the BC surface. This resulted in the provision of binding sites for Pb(II) adsorption through CNT nanoparticle interactions.	[116]
• Bamboo • Sugarcane bagasse • Hickory wood • Peanut hull	Chitosan	Post	Feedstock was first converted to biochar by pyrolysis—600 °C for 2 h. Prepared biochar was then modified by chitosan.	5 times	71.5 mg/g	• Surface complexation	Chitosan enhanced the adsorption process by providing binding sites.	[106]
Corncob	$MgCl_2$	Pre	450 °C for 1 h	9.34 times	526.20 mg/g	• Precipitation • Complexation • Ion exchange	Modification increased the crystalline $CaCO_3$ and OFGs, as well as the surface area and pore volume.	[100]
Peanut shell	$MnSO_4$ and $KHCO_3$	Pre and post	Pyrolysis: 600 °C for 1 h. Wet impregnation.		225 mg/g	• Physical adsorption • Freundlich isotherm • Intraparticle diffusion	Although MnO is used to provide additional adsorption advantages, its micropores can sometimes hinder the diffusion of heavy metals within them. To overcome this limitation, $KHCO_3$ was added to increase the pore channel of biochar. This facilitated the adsorption of Pb(II) by the formation of a new composite, HMO-K-BC.	[104]

Biochar-based composites can be produced by impregnation or coating by metal oxides, clay minerals, carbonaceous structures (graphene oxide or carbon nanotubes), complex organics, or by inoculation with micro-organisms where biochar can act as a scaffold for embedding new materials [90,99,100,102,117–119]. Wu et al. conducted their modification study using coconut shell as a feedstock and $MgCl_2$ as a modifying agent [55]. Modification increased the pore volume to some extent but not significantly enough to demonstrate physical adsorption as the dominant mechanism. The modified biochar was more capable of exchanging Mg for Pb(II) compared to the unmodified biochar, which resulted in a 49-time increase in the ion exchange capacity. In addition to naturally present minerals, impregnation with $MgCl_2$ resulted in the generation of MgO and Mg(OH)Cl after pyrolysis, which increased the extent of mineral precipitation. Modification increased the intensity of the aromatic C=C unit, and after the adsorption of Pb(II), there was a decrease in the aromatic C=C intensity. It is well established that cyclic aromatic functional groups serve as donors of π electrons during the adsorption process [120]. Therefore, alterations in these groups are indicative of their involvement in the adsorption mechanism. This study also investigated the adsorption of Pb(II) in the presence of other metals and found that the sorption of Pb(II) was unaffected by the presence of other metals (K, Na, and Ca^{2+}), except for Cd, which showed a significant decrease in sorption when Pb(II) was present. This observation was attributed, by with the researchers, with the fact that Pb(II) is a hard Lewis acid, resulting in a greater affinity for hydroxyl and carboxyl groups present on the biochar surface (which act as hard Lewis bases) towards Pb(II) compared to Cd or other metals [55]. Wang et al. modified biochar using hydrous manganese oxide and found that an optimum impregnation of 3.65% of Mn yielded an increased Pb(II) adsorption [115]. Figure 5 demonstrates the average sorption increase, in terms of percentage, achieved by different modification methods, with metal salts being the highest contributor.

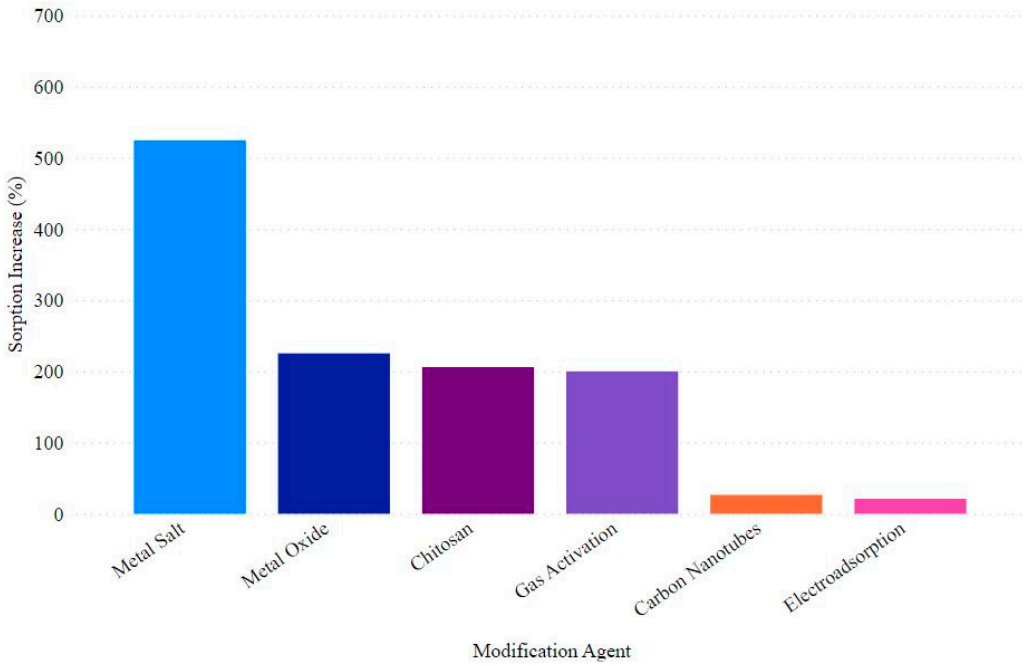

Figure 5. Sorption increase (%) by modification agent.

Liu et al. [105] conducted a modification study by CO_2 activation. Their intention was to increase the carbon and ash component (in form of carbonate and phosphate) of biochar to improve Pb(II) removal through mineral precipitation. Cassava Root Husk-derived biochar was combined with ZnO nanoparticles, which increased the adsorption by up to 28% [107]. The adsorption model followed both PFO and PSO, which indicates that chemisorption also occurred by interactions among the involved components, such as

ion exchange and surface precipitation [64]. However, modification did not significantly increase the surface area and porous structure; therefore, physical adsorption was not significant [107]. In this study, modification increased the number of -OH, which appeared to be dropped after adsorption, indicating that precipitation took part in Pb(II) removal. Tho et al. [107] also found that modification increased the -CO group, which was evident in an FTIR spectrum that took part in surface complexation [55]. Mohan et al. conducted a study of magnetizing biochar by the ferrous and ferric salt impregnation of oak wood and oak bark, followed by a NaOH treatment [109], and showed that the distribution of the magnetic iron oxide particles on the surface of biochar has an impact on the accessibility of aqueous Pb(II) ions to the active sites and pores present on the char. This, in turn, affects the number of sites that are available for the adsorption of Pb(II). Therefore, both the kinetic and equilibrium behavior of the adsorption process are influenced by the extent of dispersion of magnetic particles on the biochar surface. Several other researchers [103,107,114,116,119] have investigated the comparative adsorption capacity between magnetic biosorbents and nanoparticle modifications and found that nanoparticles are less favorable for adsorption compared to magnetic biosorbents. This is partly due to the fact that magnetization causes a decrease in pHZPC, which reduces the difference between the pH and pHZPC. This difference in decrease is particularly favorable for the adsorption of heavy metals [92]. Mahdi et al. conducted a study where they used date seed biochar (DSB) as a cathode, copper wire as an anode, a Pb(II) solution as a cell electrolyte, and a DC power supply to employ 0.1 V for 1 h [111]. They observed an initial rapid adsorption, which was attributed to the fast external mass on the highly porous DSB due to the abundance of vacant surface sites. The electric current applied during the DSB-electro process was believed to be responsible for the observed increase in pore structure. This was thought to be due to the repulsion of negatively charged impurities, which in turn led to the opening of pores. Soares et al. investigated Pb(II) removal by modifying sugarcane straw using $FeCl_3$ [102]. The authors noted that the modification process resulted in an increase in the surface area and an exposure of functional groups due to the deposition of Fe and Cl. However, they did not elaborate on the specific mechanism behind this outcome. The authors suggested that the modification process could have led to the oxidation of Fe^{2+} to $FeCl_3$, which may have supplied free electrons to the system. These electrons could have potentially contributed to the generation of a negative charge on the biochar surface, leading to enhanced adsorption. However, further research is needed to confirm this hypothesis and better understand the underlying mechanism. Han et al. [89] conducted a study where they modified commercial biochar by magnetite impregnation using $FeSO_4$ and $FeCl_3$ and found that although the magnetization process increased the surface area and pore volume of the biochar, the adsorption for Pb(II) reduced from 50 mg/g to 29 mg/g. A reduction in the pH (1.5) during the magnetization process appeared to dissolute the calcite present on the biochar surface, creating pore spaces as well as increasing the pore volume. However, this reduction in adsorption, despite the increase in the surface area and pore volume, indicated that Pb(II) sorption is more related to the OFGs than the surface area [89].

A study was conducted by Bian et al. where they used silkworm excrement as the feedstock, which was pyrolyzed at 600 °C for 2 h and was followed by wet impregnation using chitosan combined with pyromellitic dianhydride [114]. Chitosan is a polymer with amino and hydroxyl groups that can be used to functionalize the surface of biochar and enhance its adsorption properties. When combined with Pyromellitic Dianhydride (PD), the resulting synergistic compound contains functional groups, such as -CONH2-, and carboxyl groups that can interact with heavy metals through mechanisms like ion exchange, electrostatic attraction, and surface complexation [114]. While these compounds were used to modify the silkworm excrement, the resulting biochar showed an increased surface area and pore volume and increased OFG content. The synergistic effect of chitosan and PD creates N-C=O, which is responsible for the removal of Pb through complexation. Modification increased the functional groups but decreased the mineral components, so the role of ion exchange and the precipitation mechanism in Pb removal were not significant;

therefore, complexation played a dominant role. This counterbalancing effect is the reason adsorption did not significantly increase after modification [114].

4. Regeneration/Desorption Study

Various researchers [121–124] have conducted studies on the desorption of Pb(II) from biochar to assess its potential for regeneration, which is critical for cost effectiveness and for ensuring the sustainability of biochar as a solution for Pb(II) removal. Another important reason for conducting desorption studies is to investigate the potential hazard of Pb(II) leaching from biochar, if not disposed of in a manner that aligns with sound environmental practices.

Once the biochar reaches full saturation with metal contaminants, desorption can be achieved through the use of desorbents, such as $NaNO_3$, HNO_3, or KNO_3 solutions, at varying concentrations. By providing a substantial quantity of cations, these compounds can effectively substitute the Pb(II) bonded on the biochar and facilitate the regeneration of the adsorbent [90].

Trakal et al. investigated the desorption of Pb(II) from a magnetically modified nut shield, wheat straw, grape stalk, and husk biochar using $NaNO_3$, $CaCl_2$, and HNO_3 [103]. They found that after magnetically modifying the biochar, the desorption of Pb(II) was reduced for all chemicals. However, this also demonstrated that the main sorption mechanism was ion exchange and not precipitation. Wu et al. conducted a regeneration experiment of $MgCl_2$-modified biochar using NaOH as an eluent [55]. These researchers then conducted five consecutive cycles of adsorption and desorption using the regenerated biochar and found a 25% reduction in the adsorption capacity. This reduction in adsorption is likely attributed to the precipitation caused by the elution, which leads to the blockage of the pores, hindering the adsorption process. Wang et al. investigated the regeneration of biochar from the residue of a magnetic eucalyptus leaf using EDTA-2Na [123] and found a ~21% reduction in the adsorption capacity after the first cycle. Pan et al. explored the regeneration of nitrogen-phosphorous-modified biochar, which demonstrated only a slight decrease in adsorption, even after the 4th cycle. This can be attributed to the deactivation of the functional groups and the blockage of pores, which hinders the sorption process [110]. Mahdi et al. regenerated biochar by reversing the external electric field, and no significant desorption was observed [111]. Sun et al. found about a 50–60% reduction in the adsorption capacity after the 3rd cycle, which can be attributed to structural degradation and the loss of surface minerals [79]. Ding et al. [95] were able to achieve 85% of Pb(II) recovery using HCl. Bian et al. demonstrated only a 7.28% reduction in the adsorption capacity of the silkworm excrement biochar, even after the 5th cycle when NaOH was used as an eluent [114]. Ding et al. investigated the regeneration of hickory wood biochar using HCl [58]. The reduction in adsorption was only 6%, which can be attributed to the other metals not being leached and, therefore, not creating space for adsorption sites for Pb(II). The desorption of Pb(II) from biochar is a critical factor in assessing the potential for its regeneration and sustainability as a solution for Pb(II) removal. Various studies [115,117,125] have investigated the use of different desorbents, such as $NaNO_3$, HNO_3, KNO_3, $CaCl_2$, NaOH solutions, at varying concentrations and found that the effectiveness of desorption and regeneration varies depending on the type of biochar, desorbent, and regeneration method used. Some studies [96,121,124] have shown a reduction in the adsorption capacity after multiple cycles of regeneration due to precipitation, the deactivation of functional groups, and structural degradation. Nevertheless, some studies have demonstrated the successful regeneration of biochar with minimal reduction in the adsorption capacity, such as the use of HCl as a desorbent. Overall, further research is needed to identify optimal methods for the regeneration of biochar and to ensure its sustainable use for Pb(II) removal.

5. Limitation of Studies and Future Scope of Work for Using Biochar as an Adsorbent

The use of biochar for the removal of Pb(II) presents several engineering challenges and opportunities for future research. To date, limited studies [126,127] have investigated

the potential disposal options for Pb(II)-loaded biochar if it is not regenerated, highlighting the need for a comprehensive analysis of toxic Pb(II) leaching from the biochar to identify the most viable management solution for spent biochar. Furthermore, only a few number of studies [43,48,69,101] have explored the column adsorption behavior of biochar that is shown in Figure 6.

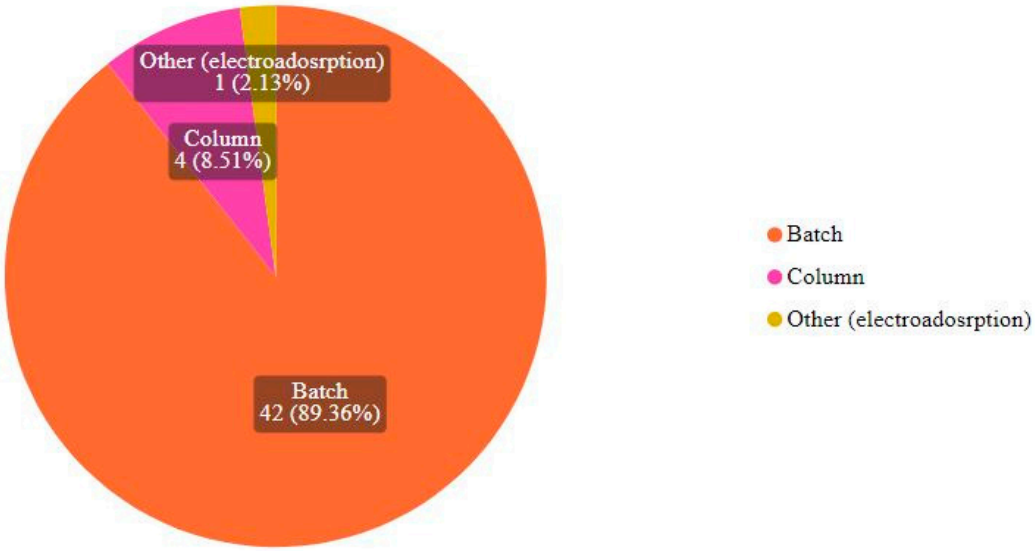

Figure 6. Experimental methods adopted by Pb(II) adsorption studies.

The lack of studies conducted on column flow setups presents a critical knowledge gap that must be addressed to advance the technology. More specifically, a thorough understanding of the mechanisms underlying Pb(II) sorption behavior is required to establish design criteria for scaling up the system. It is important to note that the majority of studies [49,66,70,128] to date have focused on monometal solutions, where only one metal is required to be removed. However, in real-world applications, water and wastewater contain a variety of components and contaminants that can significantly affect the Pb(II) sorption behavior of biochar. Thus, a more realistic approach that considers the presence of these compounds is necessary to advance the technology [129]. Biochar is a fluffy low bulk density powder. Batch studies can use this power directly; however, engineering challenges are encountered when it is to be designed for a column study [67,68]. For a real application, column design is preferred. The packing of fluffy biochar does not seem to be a feasible solution as it may get compacted with time, which would reduce porosity and increase pressure drops across the column. Additionally, if it is not granulated, the chances of biochar leaching out with flow is real. Therefore, there is a need for studying an engineered column set up and bringing an innovative solution such that it becomes a viable alternative of activated carbon for adsorption applications [130].

6. Conclusions and Recommendations

In conclusion, this review paper has summarized the last decade of research (2012–2022) on the use of biochar as a metal adsorbent, with a specific focus on Pb. The objective of this review was to provide a comprehensive resource that can guide future researchers in this field. This paper discussed the pyrolysis conditions that can alter the properties of feedstock and convert them to a sorbent called biochar. The physical and chemical properties that play a significant role in the adsorption mechanism were also explored in detail. Additionally, different modification methods were reviewed, with a focus on functionalizing biochar for the specific or enhanced removal of Pb(II).

While the potential of biochar as a metal adsorbent has been widely recognized, this review also highlighted the gaps and limitations in the current literature. For example, limited studies have investigated the potential disposal options for Pb(II)-loaded biochar

and the regeneration of biochar, and there is a lack of studies conducted on column flow setups. Furthermore, the majority of studies have focused on monometal solutions, which may not reflect the complexities of real-world applications.

Moving forward, future research should address these limitations and knowledge gaps by conducting a comprehensive analysis of toxic Pb(II) leaching from the biochar to identify the most viable management solution for spent biochar. Moreover, more studies are needed to establish design criteria for scaling up the system, including a thorough understanding of the mechanisms underlying Pb(II) sorption behavior. Overall, this review highlights the opportunities and engineering challenges associated with using biochar as a metal adsorbent and provides a valuable resource for researchers in this field.

Author Contributions: Conceptualization, P.K. and S.K.; methodology, P.K.; software, P.K.; validation, P.K.; formal analysis, P.K.; investigation, P.K.; resources, S.K.; data curation, P.K.; writing—original draft preparation, P.K.; writing—review and editing, P.K. and S.K.; visualization, P.K.; supervision, S.K.; project administration, S.K.; funding acquisition, not applicable. All authors have read and agreed to the published version of the manuscript.

Funding: This research received no external funding.

Conflicts of Interest: The authors declare no conflict of interest.

References

1. Lehmann, J.; Joseph, S. *Biochar for Environmental Management: Science, Technology and Implementation*; Routledge: Oxfordshire, UK, 2015. [CrossRef]
2. Hornung, A.; Stenzel, F.; Grunwald, J. Biochar—Just a Black Matter Is Not Enough. *Biomass Convers. Biorefinery* **2021**, 1–12. [CrossRef]
3. Woolf, D.; Lehmann, J.; Cowie, A.; Cayuela, M.L.; Whitman, T.; Sohi, S. Biochar for Climate Change Mitigation: Navigating from Science to Evidence-Based Policy. *Nat. Geosci.* **2018**, 219–248. [CrossRef]
4. Tomczyk, A.; Sokołowska, Z.; Boguta, P. Biochar physicochemical properties: Pyrolysis temperature and feedstock kind effects. *Rev. Environ. Sci. Biotechnol.* **2020**, *19*, 191–215. [CrossRef]
5. Kambo, H.S.; Dutta, A. A comparative review of biochar and hydrochar in terms of production, physico-chemical properties and applications. *Renew. Sustain. Energy Rev.* **2015**, *45*, 359–378. [CrossRef]
6. Jahirul, M.I.; Rasul, M.G.; Chowdhury, A.A.; Ashwath, N. Biofuels Production through Biomass Pyrolysis—A Technological Review. *Energies* **2012**, *5*, 4952–5001. [CrossRef]
7. Mishra, R.K.; Misra, M.; Mohanty, A.K. Value-Added Bio-carbon Production through the Slow Pyrolysis of Waste Bio-oil: Fundamental Studies on Their Structure-Property-Processing Co-relation. *ACS Omega* **2022**, *7*, 1612–1627. [CrossRef] [PubMed]
8. Cheah, S.; Jablonski, W.S.; Olstad, J.L.; Carpenter, D.L.; Barthelemy, K.D.; Robichaud, D.J.; Andrews, J.C.; Black, S.K.; Oddo, M.D.; Westover, T.L. Effects of thermal pretreatment and catalyst on biomass gasification efficiency and syngas composition. *Green Chem.* **2016**, *18*, 6291–6304. [CrossRef]
9. Yaashikaa, P.R.; Kumar, P.S.; Varjani, S.; Saravanan, A. A critical review on the biochar production techniques, characterization, stability and applications for circular bioeconomy. *Biotechnol. Rep.* **2020**, *28*, e00570. [CrossRef] [PubMed]
10. Ahmad, M.; Rajapaksha, A.U.; Lim, J.E.; Zhang, M.; Bolan, N.; Mohan, D.; Vithanage, M.; Lee, S.S.; Kim, K.-H. Biochar as a sorbent for contaminant management in soil and water: A review. *Chemosphere* **2014**, *99*, 19–33. [CrossRef] [PubMed]
11. Song, W.; Guo, M. Quality variations of poultry litter biochar generated at different pyrolysis temperatures. *J. Anal. Appl. Pyrolysis* **2012**, *94*, 138–145. [CrossRef]
12. Basic Principles of Biochar Production. Available online: https://biochar.international/guides/ (accessed on 17 February 2024).
13. Cárdenas-Aguiar, E.; Gascó, G.; Paz-Ferreiro, J.; Méndez, A. The effect of biochar and compost from urban organic waste on plant biomass and properties of an artificially copper polluted soil. *Int. Biodeterior. Biodegrad.* **2017**, *124*, 223–232. [CrossRef]
14. Rafiq, M.K.; Bachmann, R.T.; Rafiq, M.T.; Shang, Z.; Joseph, S.; Long, R. Influence of Pyrolysis Temperature on Physico-Chemical Properties of Corn Stover (*Zea mays* L.) Biochar and Feasibility for Carbon Capture and Energy Balance. *PLoS ONE* **2016**, *11*, e0156894. [CrossRef]
15. Li, X.; Shen, Q.; Zhang, D.; Mei, X.; Ran, W.; Xu, Y.; Yu, G. Functional Groups Determine Biochar Properties (pH and EC) as Studied by Two-Dimensional 13C NMR Correlation Spectroscopy. *PLoS ONE* **2013**, *8*, e65949. [CrossRef]
16. Ippolito, J.A.; Laird, D.A.; Busscher, W.J. Environmental benefits of biochar. *J. Environ. Qual.* **2012**, *41*, 967–972. [CrossRef] [PubMed]
17. Panwar, N.L.; Pawar, A.; Salvi, B.L. Comprehensive review on production and utilization of biochar. *SN Appl. Sci.* **2019**, *1*, 1–19. [CrossRef]

18. Wang, C.; Wang, X.; Li, N.; Tao, J.; Yan, B.; Cui, X.; Chen, G. Adsorption of Lead from Aqueous Solution by Biochar: A Review. *Clean Technol.* **2022**, *4*, 629–652. [CrossRef]
19. Zhang, C.; Shan, B.; Tang, W.; Zhu, Y. Comparison of cadmium and lead sorption by Phyllostachys pubescens biochar produced under a low-oxygen pyrolysis atmosphere. *Bioresour. Technol.* **2017**, *238*, 352–360. [CrossRef]
20. Qiu, M.; Liu, L.; Ling, Q.; Cai, Y.; Yu, S.; Wang, S.; Fu, D.; Hu, B.; Wang, X. Biochar for the removal of contaminants from soil and water: A review. *Biochar* **2022**, *4*, 19. [CrossRef]
21. Inyang, M.; Gao, B.; Yao, Y.; Xue, Y.; Zimmerman, A.R.; Mosa, A.; Pullammanappallil, P.; Kim, K.-H.; Ok, Y.S.; Cao, X. A review of biochar as a low-cost adsorbent for aqueous heavy metal removal. *Crit. Rev. Environ. Sci. Technol.* **2016**, *46*, 406–433. [CrossRef]
22. Park, J.H.; Ok, Y.S.; Kim, S.H.; Cho, J.S.; Heo, J.S.; Delaune, R.D.; Seo, D.C. Competitive adsorption of heavy metals onto sesame straw biochar in aqueous solutions. *Chemosphere* **2016**, *142*, 77–83. [CrossRef]
23. Shi, T.; Jia, S.; Chen, Y.; Wen, Y.; Du, C.; Du, C.; Guo, H.; Wang, Z. Adsorption of Pb(II), Cr(III), Cu(II), Cd(II) and Ni(II) onto a vanadium mine tailing from aqueous solution. *J. Hazard. Mater.* **2009**, *169*, 838–846. [CrossRef] [PubMed]
24. Scott, H.L.; Ponsonby, D.; Atkinson, C.J. Biochar: An improver of nutrient and soil water availability-what is the evidence? *Cab Rev. Perspect. Agric. Vet. Sci. Nutr. Nat. Resour.* **2014**, *9*, 1–19. [CrossRef]
25. Jindo, K.; Mizumoto, H.; Sawada, Y.; Sánchez-Monedero, M.Á.; Sonoki, T. Physical and chemical characterization of biochars derived from different agricultural residues. *Biogeosciences* **2014**, *11*, 6613–6621. [CrossRef]
26. Lehmann, J.; Joseph, S. *Biochar for Environmental Management: Science and Technology*; Routledge: London, UK, 2009; pp. 321–332. [CrossRef]
27. Lu, T.; Yuan, H.; Wang, Y.; Huang, H.; Chen, Y. Characteristic of heavy metals in biochar derived from sewage sludge. *J. Mater. Cycles Waste Manag.* **2016**, *18*, 725–733. [CrossRef]
28. Singh, B.P.; Hatton, B.J.; Singh, B.; Cowie, A.L.; Kathuria, A. Influence of biochars on nitrous oxide emission and nitrogen leaching from two contrasting soils. *J. Environ. Qual.* **2010**, *39*, 1224–1235. [CrossRef]
29. Xu, X.; Cao, X.; Zhao, L. Comparison of rice husk- and dairy manure-derived biochars for simultaneously removing heavy metals from aqueous solutions: Role of mineral components in biochars. *Chemosphere* **2013**, *92*, 955–961. [CrossRef]
30. Collin, M.S.; Venkatraman, S.K.; Vijayakumar, N.; Kanimozhi, V.; Arbaaz, S.M.; Stacey, R.S.; Anusha, J.; Choudhary, R.; Lvov, V.; Tovar, G.I.; et al. Bioaccumulation of lead (Pb) and its effects on human: A review. *J. Hazard. Mater. Adv.* **2022**, *7*, 100094. [CrossRef]
31. Rabin, R. The lead industry and lead water pipes "A Modest Campaign". *Am. J. Public Health* **2008**, *98*, 1584–1592. [CrossRef]
32. Wani, L.; Ara, A.; Usmani, J.A. Lead toxicity: A review. *Interdiscip. Toxicol.* **2015**, *8*, 55–64. [CrossRef] [PubMed]
33. States with the Most Lead Pipes | Best States | U.S. News. Available online: https://www.usnews.com/news/best-states/articles/states-with-the-most-lead-pipes (accessed on 30 July 2023).
34. U.S. Environmental Protection Agency. Basic Information about Lead in Drinking Water. Available online: https://www.epa.gov/ground-water-and-drinking-water/basic-information-about-lead-drinking-water (accessed on 30 July 2023).
35. How Can Lead Get into My Drinking Water? | US EPA. Available online: https://www.epa.gov/lead/how-can-lead-get-my-drinking-water (accessed on 30 July 2023).
36. Health Effects of Lead Exposure. 2022. Available online: https://www.cdc.gov/nceh/lead/prevention/health-effects.htm (accessed on 10 February 2024).
37. Markowitz, M.; Knollmann-Ritschel, B.E.C. Educational Case: Lead Poisoning. *Acad. Pathol.* **2017**, *4*, 2374289517700160. [CrossRef]
38. Learn about Lead | US EPA. Available online: https://www.epa.gov/lead/learn-about-lead (accessed on 30 July 2023).
39. Navas-Acien, A.; Guallar, E.; Silbergeld, E.K.; Rothenberg, S.J. Lead exposure and cardiovascular disease—A systematic review. *Environ. Health Perspect.* **2007**, *115*, 472–482. [CrossRef]
40. Florea, A.M.; Taban, J.; Varghese, E.; Alost, B.T.; Moreno, S.; Büsselberg, D. Lead (Pb^{2+}) neurotoxicity: Ion-mimicry with calcium (Ca^{2+}) impairs synaptic transmission. A review with animated illustrations of the pre- and post-synaptic effects of lead. *J. Local Glob. Health Sci.* **2013**, *2013*, 4. [CrossRef]
41. *Biden-Harris Administration Announces New Get the Lead Out Initiative*; USEPA: Washington, DC, USA, 2023.
42. WHO. Lead in Drinking-Water. 2003. Available online: https://iris.who.int/handle/10665/75370 (accessed on 11 February 2024).
43. Komkiene, J.; Baltrenaite, E. Biochar as adsorbent for removal of heavy metal ions [Cadmium(II), Copper(II), Lead(II), Zinc(II)] from aqueous phase. *Int. J. Environ. Sci. Technol.* **2016**, *13*, 471–482. [CrossRef]
44. Qu, J.; Zhang, B.; Tong, H.; Liu, Y.; Wang, S.; Wei, S.; Wang, L.; Wang, Y.; Zhang, Y. High-efficiency decontamination of Pb(II) and tetracycline in contaminated water using ball-milled magnetic bone derived biochar. *J. Clean. Prod.* **2023**, *385*, 135683. [CrossRef]
45. Zhao, R.; Wang, B.; Wu, P.; Feng, Q.; Chen, M.; Zhang, X.; Wang, S. Calcium alginate-nZVI-biochar for removal of Pb/Zn/Cd in water: Insights into governing mechanisms and performance. *Sci. Total Environ.* **2023**, *894*, 164810. [CrossRef]
46. Ahmed, W.; Mehmood, S.; Mahmood, M.; Ali, S.; Shakoor, A.; Núñez-Delgado, A.; Asghar, R.M.; Zhao, H.; Liu, W.; Li, W. Adsorption of Pb(II) from wastewater using a red mud modified rice-straw biochar: Influencing factors and reusability. *Environ. Pollut.* **2023**, *326*, 121405. [CrossRef]
47. Omidi, A.H.; Cheraghi, M.; Lorestani, B.; Sobhanardakani, S.; Jafari, A. Biochar obtained from cinnamon and cannabis as effective adsorbents for removal of lead ions from water. *Environ. Sci. Pollut. Res.* **2019**, *26*, 27905–27914. [CrossRef] [PubMed]

48. Saravanakumar, K.; Sathyamoorthy, M.; Prasad, D.M.; Senthilkumar, R.; Prasad, B.S. Prasad Continuous removal of cadmium and lead ions by biochar derived from date seeds in a packed column reactor. *Desalination Water Treat.* **2022**, *250*, 126–135. [CrossRef]
49. Ho, S.H.; Yang, Z.K.; Nagarajan, D.; Chang, J.S.; Ren, N.Q. High-efficiency removal of lead from wastewater by biochar derived from anaerobic digestion sludge. *Bioresour. Technol.* **2017**, *246*, 142–149. [CrossRef]
50. Inyang, M.; Gao, B.; Yao, Y.; Xue, Y.; Zimmerman, A.R.; Pullammanappallil, P.; Cao, X. Removal of heavy metals from aqueous solution by biochars derived from anaerobically digested biomass. *Bioresour. Technol.* **2012**, *110*, 50–56. [CrossRef] [PubMed]
51. Mousavi, H.Z.; Hosseynifar, A.; Jahed, V.; Dehghani, S.A.M. Removal of lead from aqueous solution using waste tire rubber ash as an adsorbent. *Braz. J. Chem. Eng.* **2010**, *27*, 79–87. [CrossRef]
52. Mohan, D.; Singh, P.; Sarswat, A.; Steele, P.H.; Pittman, C.U. Lead sorptive removal using magnetic and nonmagnetic fast pyrolysis energy cane biochars. *J. Colloid Interface Sci.* **2015**, *448*, 238–250. [CrossRef] [PubMed]
53. Uchimiya, M.; Lima, I.M.; Klasson, K.T.; Chang, S.; Wartelle, L.H.; Rodgers, J.E. Immobilization of Heavy Metal Ions (CuII, CdII, NiII, and PbII) by Broiler Litter-Derived Biochars in Water and Soil. *J. Agric. Food Chem.* **2010**, *58*, 5538–5544. [CrossRef] [PubMed]
54. Wang, Z.; Liu, G.; Zheng, H.; Li, F.; Ngo, H.H.; Guo, W.; Liu, C.; Chen, L.; Xing, B. Investigating the mechanisms of biochar's removal of lead from solution. *Bioresour. Technol.* **2015**, *177*, 308–317. [CrossRef] [PubMed]
55. Wu, J.; Wang, T.; Wang, J.; Zhang, Y.; Pan, W.P. A novel modified method for the efficient removal of Pb and Cd from wastewater by biochar: Enhanced the ion exchange and precipitation capacity. *Sci. Total Environ.* **2020**, *754*, 142150. [CrossRef] [PubMed]
56. Mu, R.M.; Wang, M.X.; Bu, Q.W.; Liu, D.; Zhao, Y.L. Adsorption of Pb(II) from aqueous solutions by wheat straw biochar. *IOP Conf. Ser. Earth Environ.* **2018**, *191*, 012041. [CrossRef]
57. Aslam, Z.; Khalid, M.; Naveed, M.; Shahid, M.A.; Aon, M. Evaluation of Green Waste and Popular Twigs Biochar Produced at Low and High Pyrolytic Temperature for Efficient Removal of Metals from Water. *Water. Air. Soil Pollut.* **2017**, *228*, 432. [CrossRef]
58. Ding, Z.; Ok, Y.S.; Hu, X.; Wan, Y.; Wang, S.; Gao, B. Removal of lead, copper, cadmium, zinc, and nickel from aqueous solutions by alkali-modified biochar: Batch and column tests. *J. Ind. Eng. Chem.* **2016**, *33*, 239–245. [CrossRef]
59. Xue, Y.; Gao, B.; Yao, Y.; Inyang, M.; Zhang, M.; Zimmerman, A.R.; Ro, K.S. Hydrogen peroxide modification enhances the ability of biochar (hydrochar) produced from hydrothermal carbonization of peanut hull to remove aqueous heavy metals: Batch and column tests. *Chem. Eng. J.* **2012**, *200*, 673–680. [CrossRef]
60. Saleh, T.A. Surface Science of Adsorbents and Nanoadsorbents. In *Interface Science and Technology*; Academic Press: Cambridge, MA, USA, 2022. [CrossRef]
61. Largitte, L.; Pasquier, R.J. Pasquier A review of the kinetics adsorption models and their application to the adsorption of lead by an activated carbon. *Chem. Eng. Res. Des.* **2016**, *109*, 495–504. [CrossRef]
62. Granados, P.; Mireles, S.; Pereira, E.; Cheng, C.-L.; Kang, J. Effects of Biochar Production Methods and Biomass Types on Lead Removal from Aqueous Solution. *Appl. Sci.* **2022**, *12*, 5040. [CrossRef]
63. Lagergren, S. About the theory of so-called adsorption of soluble substances. *K. Sven. Vetenskapsakademiens Handl.* **1898**, *24*, 1–39.
64. Ho, Y.S.; McKay, G. A Comparison of Chemisorption Kinetic Models Applied to Pollutant Removal on Various Sorbents. *Process Saf. Environ. Prot.* **1998**, *76*, 332–340. [CrossRef]
65. Kajjumba, G.W.; Emik, S.; Öngen, A.; Özcan, H.K.; Aydın, S. Modelling of Adsorption Kinetic Processes—Errors, Theory and Application. In *Advanced Sorption Process Applications*; IntechOpen: London, UK, 2018. [CrossRef]
66. Kołodyńska, D.; Wnetrzak, R.; Leahy, J.J.; Hayes, M.H.B.; Kwapinski, W.; Hubicki, Z. Kinetic and adsorptive characterization of biochar in metal ions removal. *Chem. Eng. J.* **2012**, *197*, 295–305. [CrossRef]
67. Gwenzi, W.; Chaukura, N.; Noubactep, C.; Mukome, F.N. Mukome Biochar-based water treatment systems as a potential low-cost and sustainable technology for clean water provision. *J. Environ. Manag.* **2017**, *197*, 732–749. [CrossRef]
68. Rosales, E.; Meijide, J.; Pazos, M.; Sanromán, M.Á. Challenges and recent advances in biochar as low-cost biosorbent: From batch assays to continuous-flow systems. *Bioresour. Technol.* **2017**, *246*, 176–192. [CrossRef] [PubMed]
69. Boni, M.R.; Chiavola, A.; Marzeddu, S. Remediation of Lead-Contaminated Water by Virgin Coniferous Wood Biochar Adsorbent: Batch and Column Application. *Water. Air. Soil Pollut.* **2020**, *231*, 1–16. [CrossRef]
70. Chen, X.; Zhu, X.; Fan, G.; Wang, X.; Li, H.; Li, H.; Xu, X. Enhanced adsorption of Pb(II) by phosphorus-modified chicken manure and Chinese medicine residue co-pyrolysis biochar. *Microsc. Res. Tech.* **2022**, *85*, 3589–3599. [CrossRef]
71. Yılmaz, C.; Güzel, F. Performance of wild plants-derived biochar in the remediation of water contaminated with lead: Sorption optimization, kinetics, equilibrium, thermodynamics and reusability studies. *Int. J. Phytoremediation* **2021**, *24*, 177–186. [CrossRef]
72. Cui, L.; Yan, J.; Li, L.; Quan, G.; Ding, C.; Chen, T.; Yin, C.; Gao, J.; Hussain, Q. Does Biochar Alter the Speciation of Cd and Pb in Aqueous Solution. *Bioresources* **2014**, *10*, 88–104. [CrossRef]
73. Kalam, S.; Abu-Khamsin, S.A.; Mahmoud, M.; Kamal, M.S.; Patil, S. Surfactant Adsorption Isotherms: A Review. *ACS Omega* **2021**, *6*, 32342–32348. [CrossRef]
74. Fahmi, A.H.; Jol, H.; Singh, D. Physical modification of biochar to expose the inner pores and their functional groups to enhance lead adsorption. *RSC Adv.* **2018**, *8*, 38270–38280. [CrossRef]
75. Chatterjee, A.; Abraham, J. Desorption of heavy metals from metal loaded sorbents and e-wastes: A review. *Biotechnol. Lett.* **2019**, *41*, 319–333. [CrossRef] [PubMed]
76. Mukherjee, A.; Patra, B.R.; Podder, J.; Dalai, A.K. Dalai Synthesis of Biochar From Lignocellulosic Biomass for Diverse Industrial Applications and Energy Harvesting: Effects of Pyrolysis Conditions on the Physicochemical Properties of Biochar. *Front. Mater.* **2022**, *9*, 870184. [CrossRef]

77. Mohan, D.; Pittman, C.U., Jr.; Bricka, M.; Smith, F.; Yancey, B.; Mohammad, J.; Steele, P.H.; Alexandre-Franco, M.F.; Gómez-Serrano, V.; Gong, H. Sorption of arsenic, cadmium, and lead by chars produced from fast pyrolysis of wood and bark during bio-oil production. *J. Colloid Interface Sci.* **2007**, *310*, 57–73. [CrossRef] [PubMed]
78. Conz, R.F.; Abbruzzini, T.F.; Andrade, C.D.; Milori, D.M.; Cerri, C.E. Effect of Pyrolysis Temperature and Feedstock Type on Agricultural Properties and Stability of Biochars. *Agric. Sci.* **2017**, *8*, 914–933. [CrossRef]
79. Sun, C.; Chen, T.; Huang, Q.; Wang, J.; Wang, J.; Wang, J.; Lu, S.; Yan, J. Enhanced adsorption for Pb(II) and Cd(II) of magnetic rice husk biochar by KMnO 4 modification. *Environ. Sci. Pollut. Res.* **2019**, *26*, 8902–8913. [CrossRef]
80. Major, J.; Steiner, C.; Downie, A.; Lehmann, J. Biochar Effects on Nutrient Leaching. In *Biochar for Environmental Management*; Routledge: London, UK, 2012; pp. 303–320.
81. Muoghalu, C.C.; Owusu, P.A.; Lebu, S.; Nakagiri, A.; Semiyaga, S.; Iorhemen, O.T.; Manga, M. Biochar as a novel technology for treatment of onsite domestic wastewater: A critical review. *Front. Environ. Sci.* **2023**, *11*, 1095920. [CrossRef]
82. Jin, J.; Li, Y.; Zhang, J.; Wu, S.; Cao, Y.; Liang, P.; Zhang, J.; Wong, M.H.; Wang, M.; Shan, S.; et al. Influence of pyrolysis temperature on properties and environmental safety of heavy metals in biochars derived from municipal sewage sludge. *J. Hazard. Mater.* **2016**, *320*, 417–426. [CrossRef]
83. Li, H.; Dong, X.; da Silva, E.B.; de Oliveira, L.M.; Chen, Y.; Ma, L.Q. Mechanisms of metal sorption by biochars: Biochar characteristics and modifications. *Chemosphere* **2017**, *178*, 466–478. [CrossRef]
84. Cao, X.; Ma, L.; Liang, Y.; Gao, B.; Harris, W. Simultaneous Immobilization of Lead and Atrazine in Contaminated Soils Using Dairy-Manure Biochar. *Environ. Sci. Technol.* **2011**, *45*, 4884–4889. [CrossRef]
85. Zhao, Q.; Wang, Y.; Xu, Z.; Yu, Z.; Yu, Z. Removal mechanisms of Cd(II) and Pb(II) from aqueous solutions using straw biochar: Batch study, Raman and X-ray photoelectron spectroscopy techniques. *Desalination Water Treat.* **2021**, *220*, 199–210. [CrossRef]
86. Napitupulu, M.; Walanda, D.K.; Simatupang, M. Utilization of red fruit's peel (freycinetia arborea gaudich) as biochar for lead (Pb) adsorption. *J. Phys. Conf. Ser.* **2020**, *1434*, 012033. [CrossRef]
87. Jin, Q.; Wang, Z.; Feng, Y.; Kim, Y.T.; Stewart, A.C.; O'Keefe, S.F.; Neilson, A.P.; He, Z.; Huang, H. Grape pomace and its secondary waste management: Biochar production for a broad range of lead (Pb) removal from water. *Environ. Res.* **2020**, *186*, 109442. [CrossRef] [PubMed]
88. Keiluweit, M.; Kleber, M. Molecular-Level Interactions in Soils and Sediments: The Role of Aromatic π-Systems. *Environ. Sci. Technol.* **2009**, *43*, 3421–3429. [CrossRef] [PubMed]
89. Han, Z.; Sani, B.; Mrozik, W.; Obst, M.; Beckingham, B.; Karapanagioti, H.K.; Werner, D. Magnetite Impregnation Effects on the Sorbent Properties of Activated Carbons and Biochars. *Water Res.* **2015**, *70*, 394–403. [CrossRef]
90. Ahmed, M.B.; Zhou, J.L.; Ngo, H.H.; Guo, W.; Chen, M. Progress in the preparation and application of modified biochar for improved contaminant removal from water and wastewater. *Bioresour. Technol.* **2016**, *214*, 836–851. [CrossRef]
91. Cao, X.; Harris, W.G. Properties of dairy-manure-derived biochar pertinent to its potential use in remediation. *Bioresour. Technol.* **2010**, *101*, 5222–5228. [CrossRef]
92. Hassan, M.; Naidu, R.; Du, J.; Liu, Q.; Liu, Y.; Liu, Y.P.; Qi, F. Critical review of magnetic biosorbents: Their preparation, application, and regeneration for wastewater treatment. *Sci. Total Environ.* **2020**, *702*, 134893. [CrossRef]
93. Sayyadian, K.; Moezzi, A.; Gholami, A.; Panahpour, E.; Mohsenifar, K. Ohsenifar Effect of Biochar on Cadmium, Nickel and Lead Uptake and Translocation in Maize Irrigated with Heavy Metal Contaminated Water. *Appl. Ecol. Environ. Res.* **2019**, *17*, 969–982. [CrossRef]
94. Duku, M.H.; Gu, S.; Hagan, E.B. Biochar production potential in Ghana—A review. *Renew. Sustain. Energy Rev.* **2011**, *15*, 3539–3551. [CrossRef]
95. Ding, W.; Dong, X.; Ime, I.M.; Gao, B.; Ma, L.Q. Pyrolytic temperatures impact lead sorption mechanisms by bagasse biochars. *Chemosphere* **2014**, *105*, 68–74. [CrossRef]
96. Lu, H.; Zhang, W.; Yang, Y.; Huang, X.; Wang, S.; Qiu, R. Relative distribution of Pb2+ sorption mechanisms by sludge-derived biochar. *Water Res.* **2012**, *46*, 854–862. [CrossRef]
97. Wang, M.C.; Sheng, G.D.; Qiu, Y.P. A novel manganese-oxide/biochar composite for efficient removal of lead(II) from aqueous solutions. *Int. J. Environ. Sci. Technol.* **2015**, *12*, 1719–1726. [CrossRef]
98. Liang, J.; Li, X.; Yu, Z.; Zeng, G.; Luo, Y.; Jiang, L.; Yang, Z.; Qian, Y.; Wu, H. Amorphous MnO2 Modified Biochar Derived from Aerobically Composted Swine Manure for Adsorption of Pb(II) and Cd(II). *ACS Sustain. Chem. Eng.* **2017**, *5*, 5049–5058. [CrossRef]
99. Tan, G.; Wu, Y.; Liu, Y.; Xiao, D. Removal of Pb(II) ions from aqueous solution by manganese oxide coated rice straw biochar A low-cost and highly effective sorbent. *J. Taiwan Inst. Chem. Eng.* **2018**, *84*, 85–92. [CrossRef]
100. Deng, Y.; Li, X.; Ni, F.; Liu, Q.; Yang, Y.; Wang, M.; Ao, T.; Chen, W. Synthesis of Magnesium Modified Biochar for Removing Copper, Lead and Cadmium in Single and Binary Systems from Aqueous Solutions: Adsorption Mechanism. *Water* **2021**, *13*, 599. [CrossRef]
101. Huang, K.; Cai, Y.; Du, Y.; Song, J.; Mao, H.; Xiao, Y.; Wang, Y.; Yang, N.; Wang, H.; Han, L. Adsorption of Pb(II) in Aqueous Solution by the Modified Biochar Derived from Corn Straw with Magnesium Chloride. *Nat. Environ. Pollut. Technol.* **2020**, *19*, 1273–1278. [CrossRef]

102. Soares, M.B.; dos Santos, F.H.; Alleoni, L.R. Iron-Modified Biochar from Sugarcane Straw to Remove Arsenic and Lead from Contaminated Water. *Water. Air. Soil Pollut.* **2021**, *232*, 1–13. [CrossRef]
103. Trakal, L.; Veselská, V.; Šafařík, I.; Vítková, M.; Číhalová, S.; Komárek, M. Lead and cadmium sorption mechanisms on magnetically modified biochars. *Bioresour. Technol.* **2016**, *203*, 318–324. [CrossRef] [PubMed]
104. Wan, S.; Qiu, L.; Tang, G.; Weiyang, C.; Li, Y.; Gao, B.; He, F. Ultrafast sequestration of cadmium and lead from water by manganese oxide supported on a macro-mesoporous biochar. *Chem. Eng. J.* **2020**, *387*, 124095. [CrossRef]
105. Liu, Y.; Zhu, X.; Wei, X.; Zhang, S.; Jie, J.; Chen, J.; Ren, Z.J. CO_2 Activation Promotes Available Carbonate and Phosphorus of Antibiotic Mycelial Fermentation Residue-Derived Biochar Support for Increased Lead Immobilization. *Chem. Eng. J.* **2018**, *334*, 1101–1107. [CrossRef]
106. Zhou, Y.; Gao, B.; Zimmerman, A.R.; Fang, J.; Sun, Y.; Cao, X. Sorption of heavy metals on chitosan-modified biochars and its biological effects. *Chem. Eng. J.* **2013**, *231*, 512–518. [CrossRef]
107. Tho, P.T.; Van, H.T.; Nguyen, L.H.; Hoang, T.K.; Tran, T.N.; Nguyen, T.T.; Nguyen, T.B.; Le Sy, H.; Tran, Q.B.; Sadeghzadeh, S.M.; et al. Enhanced simultaneous adsorption of As(III), Cd(II), Pb(II) and Cr(VI) ions from aqueous solution using cassava root husk-derived biochar loaded with ZnO nanoparticles. *RSC Adv.* **2021**, *11*, 18881–18897. [CrossRef] [PubMed]
108. Liu, S.; Zhang, S.; Fan, M.; Yuan, Y.; Sun, X.; Wang, D.; Xu, Y. High-efficiency adsorption of various heavy metals by tea residue biochar loaded with nanoscale zero-valent iron. *Environ. Prog.* **2021**, *40*, e13706. [CrossRef]
109. Mohan, D.; Kumar, H.; Sarswat, A.; Alexandre-Franco, M.; Pittman, C.U., Jr. Cadmium and lead remediation using magnetic oak wood and oak bark fast pyrolysis bio-chars. *Chem. Eng. J.* **2014**, *236*, 513–528. [CrossRef]
110. Pan, J.; Deng, H.; Du, Z.; Tian, K.; Zhang, J. Design of nitrogen-phosphorus-doped biochar and its lead adsorption performance. *Environ. Sci. Pollut. Res.* **2022**, *29*, 28984–28994. [CrossRef]
111. Mahdi, Z.; Hanandeh, A.E.; Yu, Q.; Yu, Q.J. Electro-assisted adsorption of heavy metals from aqueous solutions by biochar. *Water Sci. Technol.* **2020**, *81*, 801–812. [CrossRef]
112. Jellali, S.; Diamantopoulos, E.; Haddad, K.; Anane, M.; Durner, W.; Mlayah, A. Lead removal from aqueous solutions by raw sawdust and magnesium pretreated biochar: Experimental investigations and numerical modelling. *J. Environ. Manag.* **2016**, *180*, 439–449. [CrossRef]
113. Wang, S.; Gao, B.; Li, Y.; Mosa, A.; Zimmerman, A.R.; Ma, L.Q.; Harris, W.G.; Migliaccio, K.W. Manganese oxide-modified biochars: Preparation, characterization, and sorption of arsenate and lead. *Bioresour. Technol.* **2015**, *181*, 13–17. [CrossRef]
114. Bian, P.; Liu, Y.; Zheng, X.; Shen, W. Removal and Mechanism of Cadmium, Lead and Copper in Water by Functional Modification of Silkworm Excrement Biochar. *Polymers* **2022**, *14*, 2889. [CrossRef]
115. Wang, H.; Gao, B.; Wang, S.; Fang, J.; Xue, Y.; Yang, K.; Yang, K. Removal of Pb(II), Cu(II), and Cd(II) from aqueous solutions by biochar derived from KMnO4 treated hickory wood. *Bioresour. Technol.* **2015**, *197*, 356–362. [CrossRef] [PubMed]
116. Inyang, M.; Gao, B.; Zimmerman, A.R.; Zhou, Y.; Cao, X. Sorption and cosorption of lead and sulfapyridine on carbon nanotube-modified biochars. *Environ. Sci. Pollut. Res.* **2015**, *22*, 1868–1876. [CrossRef] [PubMed]
117. Gupta, S.; Sireesha, S.; Sreedhar, I.; Patel, C.M.; Anitha, K.L. Latest trends in heavy metal removal from wastewater by biochar based sorbents. *J. Water Process Eng.* **2020**, *38*, 101561. [CrossRef]
118. Rajapaksha, A.U.; Chen, S.S.; Kim, K.-H.; Tsang, D.C.W.; Zhang, M.; Zhang, M.; Vithanage, M.; Mandal, S.; Gao, B.; Bolan, N.; et al. Engineered/designer biochar for contaminant removal/immobilization from soil and water: Potential and implication of biochar modification. *Chemosphere* **2016**, *148*, 276–291. [CrossRef]
119. Sizmur, T.; Fresno, T.; Akgül, G.; Frost, H.; Moreno-Jiménez, E. Biochar modification to enhance sorption of inorganics from water. *Bioresour. Technol.* **2017**, *246*, 34–47. [CrossRef] [PubMed]
120. Cui, X.; Siyu, F.; Yiqiang, Y.; Vogt, R.D.; Li, T.; Ni, Q.; Wang, C.-H.; Yang, X.; He, Z. Potential mechanisms of cadmium removal from aqueous solution by Canna indica derived biochar. *Sci. Total Environ.* **2016**, *562*, 517–525. [CrossRef] [PubMed]
121. Lata, S.; Singh, P.K.; Samadder, S.R. Regeneration of adsorbents and recovery of heavy metals: A review. *Int. J. Environ. Sci. Technol.* **2015**, *12*, 1461–1478. [CrossRef]
122. Odega, C.A.; Ayodele, O.O.; Ogutuga, S.O.; Anguruwa, G.T.; Adekunle, A.E.; Fakorede, C.O. Potential Application and Regeneration of Bamboo Biochar for Wastewater Treatment: A Review. *Adv. Bamboo Sci.* **2022**, *2*, 100012. [CrossRef]
123. Wang, S.Y.; Tang, Y.K.; Chen, C.; Wu, J.T.; Huang, Z.; Mo, Y.Y.; Zhang, K.X.; Chen, J.B. Regeneration of magnetic biochar derived from eucalyptus leaf residue for lead(II) removal. *Bioresour. Technol.* **2015**, *186*, 360–364. [CrossRef]
124. Alsawy, T.; Rashad, E.; El-Qelish, M.; Mohammed, R.H. A comprehensive review on the chemical regeneration of biochar adsorbent for sustainable wastewater treatment. *Npj Clean Water* **2022**, *5*, 29. [CrossRef]
125. Wang, B.; Gao, B.; Fang, J. Recent advances in engineered biochar productions and applications. *Crit. Rev. Environ. Sci. Technol.* **2017**, *47*, 2158–2207. [CrossRef]
126. Zhao, J. Valorization and reuse of waste modified biomass. In *Heavy Metal Biosorption Removal from Aqueous Solutions*; Universitat Autònoma de Barcelona: Bellaterra, Spain, 2019.
127. Zhang, W.; Huang, X.; Jia, Y.; Rees, F.; Tsang, D.C.; Qiu, R.; Wang, H. Metal immobilization by sludge-derived biochar: Roles of mineral oxides and carbonized organic compartment. *Environ. Geochem. Health* **2017**, *39*, 379–389. [CrossRef]

128. Tripathi, M.; Sahu, J.N.; Ganesan, P.B. Effect of process parameters on production of biochar from biomass waste through pyrolysis: A review. *Renew. Sustain. Energy Rev.* **2016**, *55*, 467–481. [CrossRef]
129. Uday, V.; Harikrishnan, P.S.; Deoli, K.; Zitouni, F.; Mahlknecht, J.; Kumar, M. Current Trends in Production, Morphology, and Real-World Environmental Applications of Biochar for the Promotion of Sustainability. *Bioresour. Technol.* **2022**, *359*, 127467. [CrossRef]
130. Oliveira, F.R.; Patel, A.K.; Jin, Y.; Jaisi, D.P.; Adhikari, S.; Lu, H.; Khanal, S.K. Environmental application of biochar: Current status and perspectives. *Bioresour. Technol.* **2017**, *246*, 110–122. [CrossRef]

CHAPTER 3

Evaluation of Lead (Pb(II)) Removal Potential of Biochar in a Fixed-bed Continuous Flow Adsorption System

Note: The contents of this chapter were adapted from the research article published in the journal 'Journal of Health & Pollution.'

Pushpita Kumkum and Sandeep Kumar

Evaluation of Lead (Pb(II)) Removal Potential of Biochar in a Fixed-bed Continuous Flow Adsorption System

Pushpita Kumkum
Sandeep Kumar

Department of Civil and Environmental Engineering, Old Dominion University, Norfolk, VA, USA

Corresponding author:
Sandeep Kumar, PhD
skumar@odu.edu

Background. Lead (Pb(II)) exposure from drinking water consumption is a serious concern due to its negative health effect on human physiology. A commercially available filter uses the adsorption potential of activated carbon for removing heavy metals like Pb(II). However, it has some constraints since it uses only surface area for the adsorption of these contaminants. Biochar produced via slow pyrolysis of biomass shows the presence of oxygen-containing functional groups on its surface that take part in the adsorption process, with higher removal potential compared to activated carbon.
Objectives. The current study examined the adsorption kinetics and mechanisms of Pb(II) removing potential of biochar from water using a fixed-bed continuous flow adsorption system.
Methods. The effect of initial Pb(II) concentration, mass of adsorbent (bed depth), and flow rate on adsorption potential were evaluated. The Adams-Bohart model, Thomas model, and Yoon-Nelson model were applied to the adsorption data.
Results. The maximum removal efficiency of Pb(II) was 88.86 mg/g. The result illustrated that the Yoon-Nelson model is the best fit to analyze the adsorption phenomena of Pb(II) in a fixed-bed biochar column.
Conclusions. The breakthrough data obtained from this study can be utilized to design a point of use filter that would be able to effectively remove Pb(II) from drinking water.
Competing Interests. The authors declare no competing financial interests.
Keywords. fixed-bed adsorption, lead, breakthrough curve, Yoon-Nelson model, biochar, Pb(II)
Received July 29, 2020. Accepted October 5, 2020.
J Health Pollution 28: (201210) 2020

Introduction

Lead (Pb) is a naturally occurring heavy metal that can be found in all parts of the environment including homes. Lead and Pb-based compounds were widely used in products such as paint, ceramic, pipes, plumbing materials, solders, gasoline, batteries, ammunition, and cosmetics until the United States federal government started to discontinue its use in 1973 and banned use by 1996 because of serious health effects from Pb exposure. Lead is dangerous to all humans, but children are especially prone to experience negative impacts since their brain and nervous systems are still developing.[1] Lead exposure can cause behavioral problems and learning disabilities, decreased intelligence quotient and hyperactivity, developmental delay, auditory problems, and anemia. Lead can be very harmful to human health even at a very low level which is why the United States Environmental Protection Agency (USEPA) does not specify a safe level of this toxic metal. The federal government banned the use of Pb-based paint in housing in 1978, but Pb-containing solder, service lines, and plumbing features are still in use. The Lead and Copper Rule regulated by the USEPA was established in 1991 and set down various requirements in order to control Pb exposure through drinking water.[2] These regulations have some shortcomings and do not fully prevent exposure to Pb. Lead exposure through household water supply became a life-threatening issue during the Flint, Michigan water crisis. The corrosive water of the Flint river leached out lead from the pipes and contaminated the tap water supply. Some collected water samples had Pb levels more than 100 times the action level.[3] Using an anti-corrosive agent may reduce the leaching of Pb but cannot eliminate the possibility entirely and thus can be considered a temporary solution only. Replacing all existing service lines would require billions of dollars.[4]

Studies have been conducted to evaluate the adsorption of heavy metals using different low-cost biosorbents (bacteria, microalgae, fungi, yeasts, agricultural wastes, natural residues, etc.) and polymer-based synthetic adsorbents.[5] Chemically-treated rice husk appeared to be more efficient in removing heavy metals like Pb, arsenic (As(V)), nickel (Ni(II)), and zinc (Zn(II)) compared

to untreated rice husk due to the presence of polyphenolic functional groups.[6] Sawdust obtained from the wood industry works as a very good low-cost biosorbent and can remove Zn(II), copper (Cu(II)), chromium (Cr(VI)), and cadmium (Cd(II)).[7,8] Khoramzadeh et al. (2013) examined mercury adsorption on sugarcane bagasse and achieved 97.584% removal efficiency.[9] Several studies have investigated the adsorption of Cu(II) and Zn(II) by extracellular polymeric substances (EPS) extracted from sulfate-reducing bacteria and found that adsorption of Zn(II) was higher than that of Cu(II).[10] Microalgae is capable of metal adsorption as a resistance mechanism in the presence of growth-inhibiting toxic compounds. Different species of microalgae showed high removal yield of various metals i.e., Cu(II), Ni(II), Cd(II), Zn(II) within the range of 15.4 – 836.5 mg/g.[11] Adsorption of heavy metals over polymers such as mineral composites, phosphates composites, clay composites, metal oxide composites, were investigated by Zhao et al. (2018) and they found that these composites create strong bonds with metals and strip them off from aqueous solution.[12]

Many studies have investigated the removal of lead nitrate (Pb(II)) using biochar. Inyang *et al.* (2011) conducted a comparative study of Pb(II) adsorption between commercial activated carbon and biochar obtained from anaerobically digested sugarcane bagasse and found that biochar is more efficient in removing Pb(II) from water compared to activated carbon.[13] Biochar has better performance compared to granular activated carbon (GAC) in the removal of Pb(II).[14] According to a study conducted by Alhashimi in 2016,[15] biochar production requires less energy, has less of a negative effect in climate change, and is more economical in removing metal compared to activated carbon. Surface composition (mainly abundance of oxygen-containing functional groups such as carboxyl, carbonyl, hydroxyl) predominates over the surface area in comparison with GAC in metal adsorption.[16] Sugarcane biochar is found to be more effective compared to orange peel biochar in removing Pb(II).[17] Biochar produced from water hyacinth biomass was utilized to investigate the adsorption capabilities of Pb(II) and Cd(II) and the maximum adsorption capacity was 123.37 mg/g for Pb(II) which is significantly higher compared to Cd(II) adsorption at 70.77 mg/g.[18] A comparative analysis was conducted to evaluate the sorption potential of sugarcane bagasse, eucalyptus forest residues, castor meal, green coconut pericarp, and water hyacinth where sorption data reasonably fit with the Freundlich model and the cationic exchange along with specific surface complexation was found to be the dominant sorption mechanism.[19] Xu *et al.* (2017) showed that biochar derived from waste-art-paper removed aqueous Pb(II) with extraordinary sorption capacity.[20] The majority of these studies were conducted with a focus on batch adsorption experiments. The main purpose of running batch adsorption experiments is to evaluate the viability of the adsorbent-adsorbate system. This is more suitable for the optimization of adsorption conditions in a laboratory set-up.[21] However, a fixed-bed column study is needed to design a flow-through adsorption system.[22-24] Data obtained from continuous flow-through processes are able to provide guidance for scaling-up to an industrial system.

The present study was mainly focused on the Pb(II)-removing potential of biochar in a fixed bed continuous flow process to address the issue of Pb(II) contamination of drinking water. This is a novel step towards designing a point-of-use water filter exploiting the benefit of a cost-effective adsorbent like biochar. To the best of our knowledge, this is a unique approach investigating commercially available biochar for adsorbing the neurotoxic heavy metal Pb(II) in a flow-through system. Commercially available biochar can be exploited to remove Pb(II) from water in an emergency. However, biochar can be produced locally using any clean source of biomass. Household recycled items such as food cans can be used as a pyrolizer and use the produced biochar as an adsorbent for removing Pb(II). The resultant data can be utilized to design a water filter for a sustainable low-cost option for many parts of the world. The Adams-Bohart, Thomas, and Yoon-Nelson models are commonly used for predicting adsorption parameters in a column study.[25-27] The Adams-Bohart model envisions a direct relationship between the height of the bed and the time needed for a breakthrough to be achieved. This linear connection makes the design and analysis easier and also works as a simple approach to run pilot tests.[28] The Thomas model is a universally used theoretical model to explain the effectiveness of the column.[29] The Yoon – Nelson model

Abbreviations

FTIR	Fourier-transform infrared spectroscopy	*GAC*	Granular activated carbon

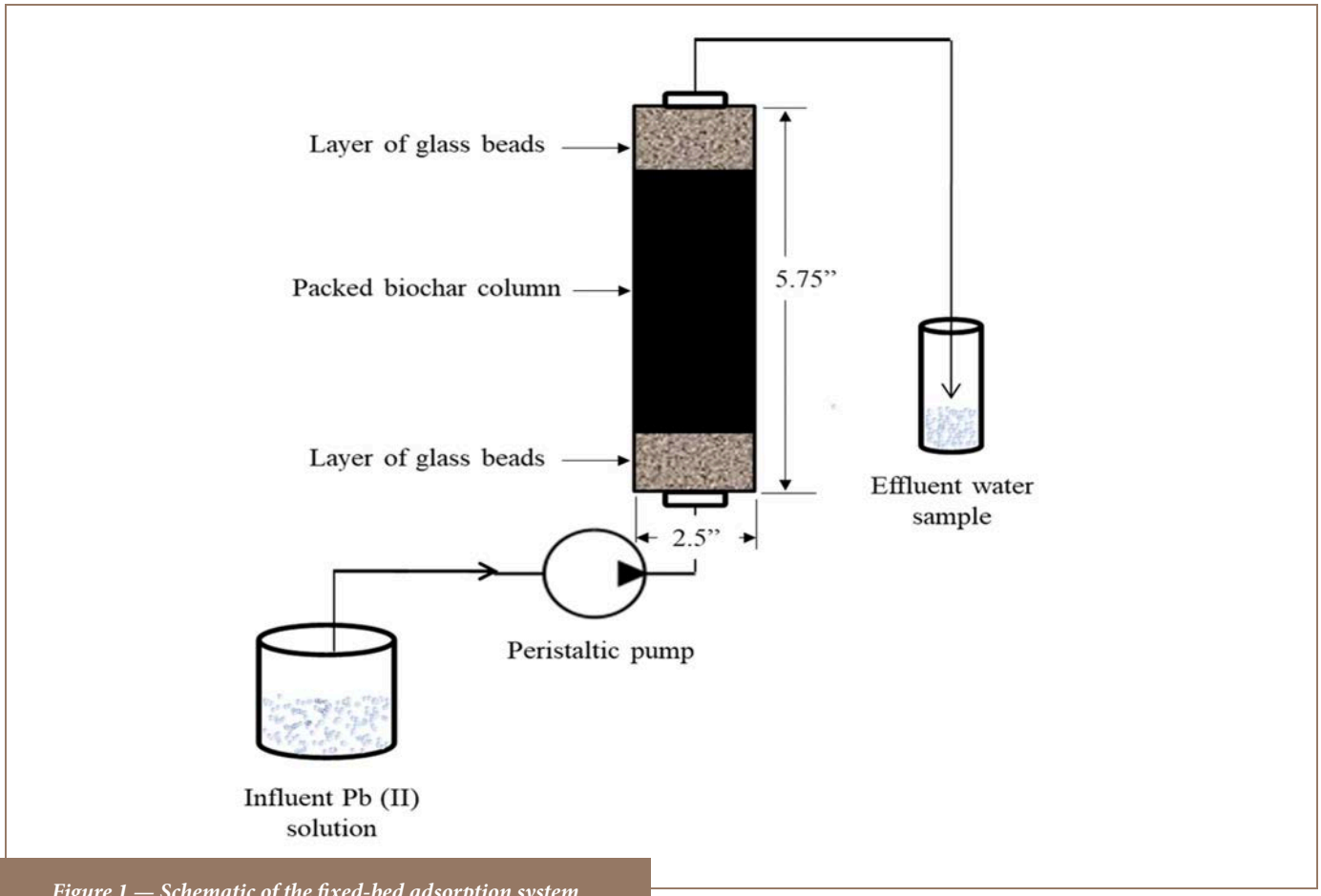

Figure 1 — Schematic of the fixed-bed adsorption system

does not require any comprehensive data on adsorbate and adsorbent properties which makes it a simpler model compared to others.[30] Because of the beneficial aspects of these models, they were applied to data collected from adsorption experiments in the present study.

Methods

A five-gallon bag of commercially produced biochar was procured through Amazon sold by New Hampshire Biochar-The Charcola group. According to the manufacturer, the feedstock was a mix of hardwood and softwood (maple, birch, and pine). It was produced via slow pyrolysis at 500°C. The intent was to run the adsorption experiments using the biochar as-is, with no washing or alkali treatment. In order to have uniform-sized particles, the biochar was passed through 0.02-0.17 µm sieves.

Biochar characterization

The International Biochar Initiative (IBI) developed a protocol to universally and consistently define biochar and to ensure its usability based upon the featured characteristics.[31] "The Standardized Product Definition and Product Testing Guidelines for Biochar That Is Used in Soil" are the IBI Biochar Standards. In the present study, the characterizations of biochar follow these standards.

Elemental analysis

A Flash 2000 elemental analyzer was used to determine the carbon, nitrogen, and hydrogen components of the biochar sample. For quantifying the ash component, approximately 0.5 g of dried sample was weighed into ceramic crucibles and incinerated overnight in a muffle furnace at 575°C.

Fourier-transform infrared spectroscopy analysis

Fourier-transform infrared (FTIR) spectroscopy (4000 – 400 cm^{-1}) analysis was carried out using a Bruker Alpha, Platinum-ATR instrument to identify the surface functional groups of the biochar.

Brunauer-Emmett-Teller surface area measurement

Brunauer-Emmett-Teller (BET) surface area analysis was conducted using the NOVA 4000e surface area and pore size analyzer (Quantachrome Instruments). Raw biochar samples were analyzed for multipoint BET surface area using nitrogen as the adsorbing gas. The analysis involved degassing the sample at 150°C for 4 h.

Chemicals and reagents

All chemicals and reagents used for this study were of analytical grade. The Pb(II) stock solution (1000 mg/L) was prepared by dissolving 1.598 g $Pb(NO_3)_2$ (Sigma-Aldrich, Switzerland) into deionized water in 1000-mL volumetric flasks. Solutions of desired concentrations were prepared by diluting the stock solution using deionized water. The procedure for mixing the stock solution was done according to the Standard Methods for Examination of Water and Wastewater 22nd edition.[32]

Batch experiments

Two sets of batch adsorption experiments were set to evaluate the effect of the initial Pb(II) concentration. Two hundred and fifty (250)-mL Erlenmeyer flasks were used as reactors. A known amount of biochar was added to Pb(II) solutions of varying concentrations. Samples were then agitated at 180 rpm for 4 days and extracted at 0 h, 0.5 h, 1 h, 2 h, 4 h, 24 h, and 96 h using a 0.22-µm polyvinylidene fluoride filter. Collected samples were acidified to pH < 2 using (1:1) nitric acid and analyzed using an atomic absorption spectrophotometer (AA-7000) from Shimadzu. After 4 days, the pH of the solutions were measured. These experiments were performed without adjusting the pH of the mixed solution.

Effect of initial concentration

To evaluate the effect of initial Pb(II) concentration, 250-mL flasks of 40 mg/L, 10 mg/L, and 1 mg/L Pb(II) were chosen with a biochar dosage of 0.5 g/L in each in batch adsorption study.

Effect of biochar dosage

For investigating the effect of biochar dose, 10 mg/L of Pb solution at three different dosages- 0.1 g/L, 0.5 g/L, and 1 g/L of biochar were chosen for the batch adsorption studies.

Column experiments

A fixed bed adsorption system was adopted for column-flow adsorption experiments. A schematic of the system is shown in Figure 1. Biochar was packed inside the glass column as an interlayer between two layers of glass beads. The columns were flushed with di-ionized water for 6 h before running the experiment. The Pb(II) solution prepared using the buffer solution (to keep the pH below the precipitation level) was delivered through the column by a Masterflex peristaltic pump. All the experiments were conducted in an upward flow manner to avoid canalizing in the column. Samples were collected at predetermined sampling times and acidified to pH < 2 using (1:1) nitric acid. Collected samples were analyzed using an atomic absorption spectrophotometer. Column flow experiments were conducted for an extended period of time (29 days) to reach complete saturation of the adsorption bed. Operating condition variables i.e., initial Pb(II) concentration (10 and 20 mg/L), depth of biochar column (5.72 cm, 7.62 cm), and flow rate (2 mL/min and 4 mL/min) were varied.

Effect of initial concentration

The stock solution of Pb(II) was diluted to 10 and 20 mg/L to evaluate the effect of initial Pb(II) concentration on the adsorption of biochar. The flow rate of the influent was adjusted at 2 mL/min and the bed depth of biochar remained at 7.62 cm (15 g biochar). Effluents were collected at certain intervals starting from 0 days to 29 days, acidified, and kept for analysis.

Effect of flow rate

Different flow rates can influence the adsorption of Pb(II) by biochar due to the time of exposure between Pb(II) and biochar. Influent was delivered at two different flow rates including 2 mL/min and 4 mL/min to investigate the effect of flow rate. The initial Pb(II) concentration remained constant at 10 mg/L and bed depth at 7.62 cm (15 g of biochar). Effluents were collected at certain intervals starting from 0 days to 29 days, acidified, and kept for analysis.

Effect of bed depth

To evaluate the effect of bed depth, varying amounts of biochar were packed inside the columns. The bed depths of the packed biochar were measured as 5.72 cm for 10 g of biochar and 7.62 cm for 15 g of biochar. Other parameters i.e., flow rate and initial Pb(II) concentration were set at 2 mL/min and 10 mg/L, respectively. Effluents were collected at certain intervals starting from 0 days to 29 days, acidified, and kept for analysis.

Mathematical expression of batch and fixed-bed column studies

The amount of Pb(II) removed by adsorption was calculated using Equation 1:

Equation 1

$$q_e = V (C_0 - C_e) / M$$

Where q_e is the amount of Pb(II) removed per gram of biochar, C_0 and C_e are the initial and equilibrium Pb(II) concentrations (mg/L) in solution, V is the solution volume (L), and M is the dry weight of biochar in grams.

The effectiveness of the column can be evaluated using the breakthrough curve of the continuous flow system. The breakthrough curve was derived by plotting C/C_0 vs time t, where C_0 and C are the initial and equilibrium Pb(II) concentrations (mg/L) in solution, respectively. Total Pb(II) adsorbed by the biochar column (q_{total}) can be obtained by calculating the area under the plot of the adsorbed concentration ($C_{ad} = C_0 - C$ (mg/L)) versus time t (min) which can be expressed by Equation 2:

Equation 2

$$q_{total} = Q / 1000 \int_{t=0}^{t=total} C_{ad} dt$$

where Q is the volumetric flow rate (mL/min).

The experimental adsorption capacity $q_{eq(exp)}$ (mg/g) can be calculated by Equation 3:

Equation 3

$$q_{eq(exp)} = q_{total} / M$$

where M is the total dry weight of biochar in the column.

Adsorption model for fixed-bed column studies

The breakthrough curves were examined by the commonly used mathematical Adams-Bohart, Thomas, and Yoon-Nelson models.

Adams-Bohart model

The Adams-Bohart model (24) is used for explaining the initial portion of the breakthrough curve. The equation of the Adams-Bohart model can be elaborated as:

$$ln (C_t/C_0) = K_{AB} C_0 t - K_{AB} N_o (Z/U_o)$$

where C_0 is the inlet adsorbate concentration, C_t is the outlet adsorbate concentration (both in mg/L), Z represents the bed depth (cm) of the column, U_o is the superficial or linear velocity (cm/min) calculated by dividing the flow rate by the column cross-section area, N_o is the adsorbate saturation concentration (mg/L), K_{AB} represents the kinetic constant (L/mg/min) of the model. A linear plot of ln (C/C_0) versus time (t) was applied to determine the values of K_{AB} and N_0.

Thomas model

The Thomas model (25) follows the Langmuir isotherm for equilibrium and second-order reversible reaction kinetics. The Thomas model can be expressed as:

$$ln ((C_0/C_t)-1) = K_{Th} q_0 w/Q - K_{Th} C_0 t$$

Here K_{Th} is the Thomas model rate constant (mL/mg/min), q_0 represents equilibrium adsorbate uptake (mg/g), w is the mass of the adsorbent (g) and Q represents flow rate (mL/min). A linear plot of ln ((C_0/C)-1) versus time (t) was applied to determine the values of K_{TH} and q_0.

Yoon-Nelson model

The Yoon-Nelson model[27] is a descriptive model that uses experimental data to estimate breakthrough parameters. The linear equation for the model can be expressed as follows:

$$ln (C/C_0 - C) = K_{YN} t - \tau K_{YN}$$

Where K_{YN} is the Yoon-Nelson rate constant (min^{-1}), and τ represents the time required for 50% adsorbate breakthrough (min). A linear plot of ln (C/C_0 - C) versus time (t) was applied to determine the values of K_{YN} and τ.

Results

The surface characteristics of the biochar used in this study were estimated using a BET surface area analyzer. The specific surface area of the biochar was determined as 285 m^2/g with an average pore diameter of 1.96 nm and a cumulative pore volume of 0.14 cm^3/g which indicates that the biochar is rich in micropores.

The elemental composition of biochar used in this study is shown in Table 1.

Figure 2 shows the FTIR spectra of biochar in the near IR region (wavenumber 4000 – 400 cm^{-1}). The spectra demonstrated the presence of several oxygen-containing functional groups in biochar. The peaks that can be identified and designated were aromatic C=C (~1418 cm-1), aromatic carbonyl/carboxyl C=O, phenolic –OH (~1027 cm-1), and aromatic –CH (~872 cm-1). The presence of several oxygen-containing functional groups was confirmed by Kumar *et al.*[33] in previous research. Aromatic carbonyl/carboxyl groups exhibit high affinity with heavy metals.[16] On the other hand, the FTIR spectra of GAC showed the absence of these functional groups.

Batch studies

The batch experiments *(Figure 3a)* involving different Pb(II) concentration indicated 100% removal of initial Pb(II) concentration within the first few minutes (~ 0 h) and no trace level of Pb(II) was found even

after 96 h. This demonstrates that Pb(II) adsorption to biochar was a rapid phenomenon which result from the strong inclination of Pb(II) ions to biochar leading to the fast diffusion of Pb(II) ions into the pores of the biochar to reach equilibrium.[34] For the initial Pb(II) concentration of 40 mg/L, 10 mg/L and 1 mg/L, the equilibrium adsorption was calculated to be 80 mg/g, 20 mg/g and 2 mg/g, respectively. The experiments involving different dosage of biochar *(Figure 3b)* also showed 100% removal of Pb(II) within the first few minutes (~ 0 h). For the increased dose from 0.1 g/L to 1 g/L, the adsorption uptake decreased from 100 mg/g to 10 mg/g. This indicates that with the increase of dosage, the number of available binding sites increased but remained unsaturated since the initial Pb(II) concentration did not change. A similar phenomenon has been observed in previous studies.[3]

Component name	Values
Surface area (m^2/g)	285.40
Pore volume (cm^3/g)	0.14
Pore diameter (nm)	1.96
pH	7.58[a]
Ash content (%)	35.48
Nitrogen	0
Carbon	44.59
Hydrogen	1.01
Sulphur	0
Oxygen	18.93[b]
H/C Molar Ratio	0.07
O/C Molar Ratio	0.16

[a]Determined following International Biochar Initiative protocol
[b]Determined by differences after retrieving data from carbon hydrogen and nitrogen (CHN) analyzer

Table 1 — Elemental Composition of Biochar

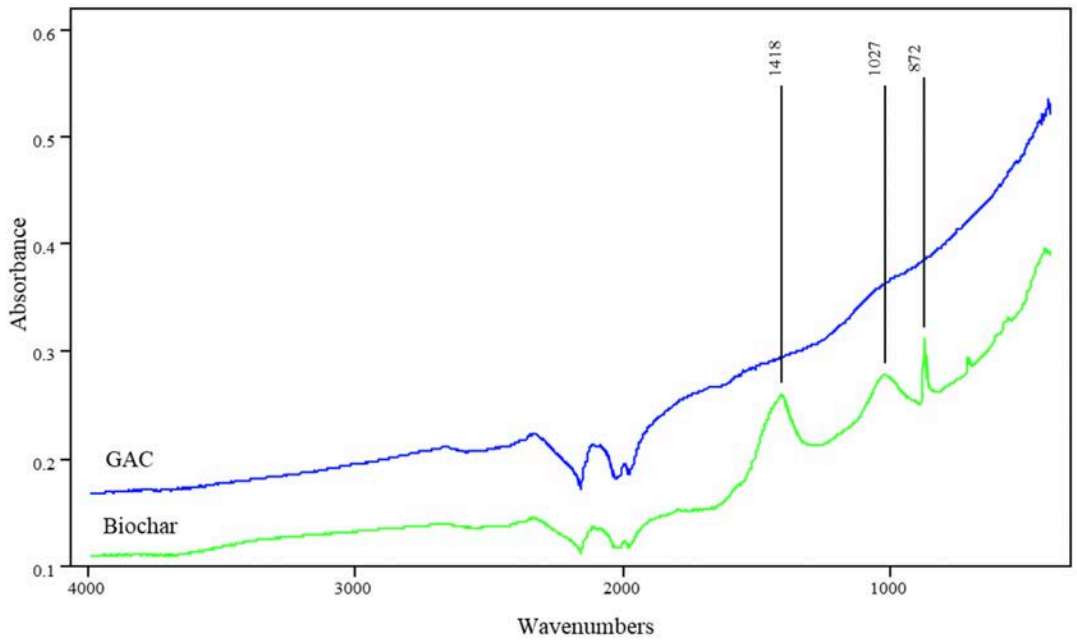

Figure 2 — Fourier-transform infrared spectroscopy spectra of GAC and Biochar

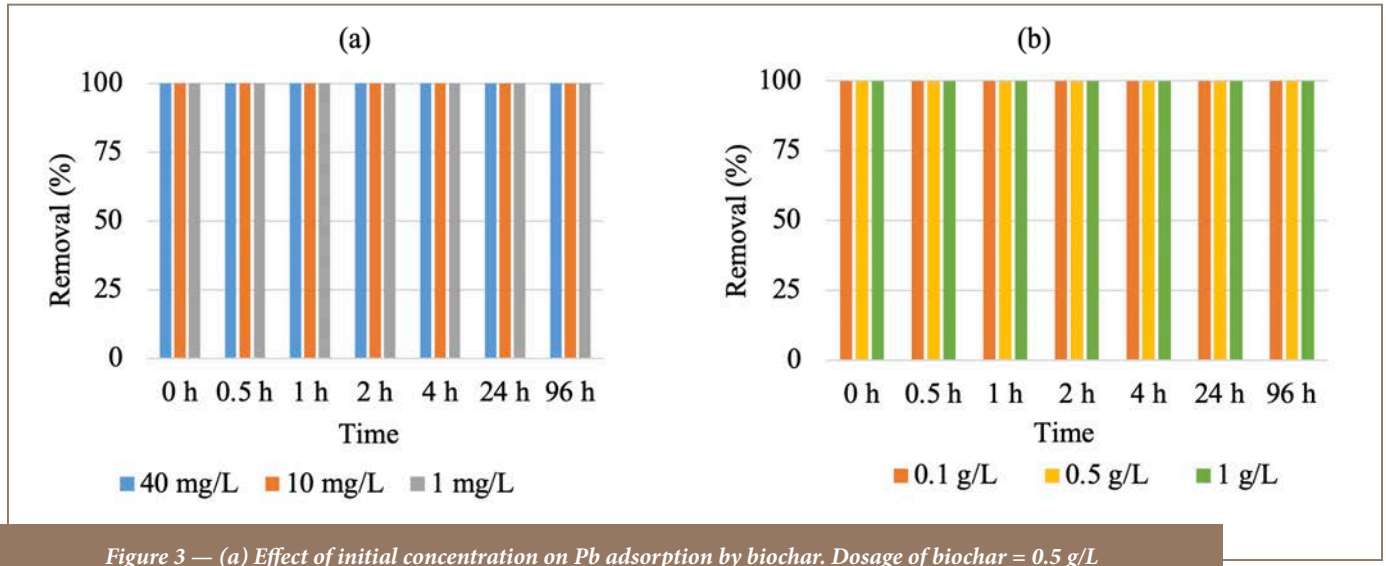

Figure 3 — (a) Effect of initial concentration on Pb adsorption by biochar. Dosage of biochar = 0.5 g/L (b) Effect of biochar dosage on Pb adsorption. Initial Pb concentration = 10 mg/L

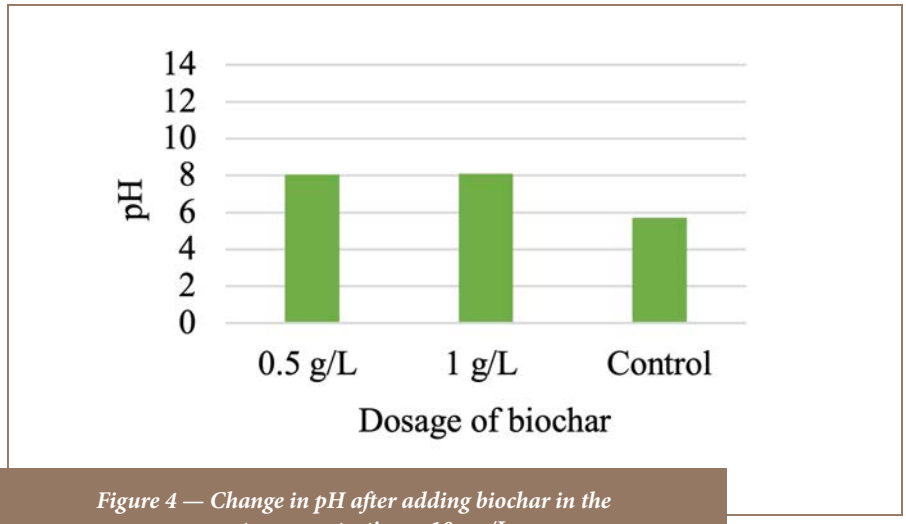

Figure 4 — Change in pH after adding biochar in the reactorconcentration = 10 mg/L

It was also observed *(Figure 4)* that dosing with biochar increased the pH of the solution from ~ 6 to ~ 8. This could occur due to the release of inorganic alkaline species upon adding biochar to the solution. However, the high ash content of the biochar (35.48%) analyzed in this study could also be associated with the presence of these oxides and hydroxides of base cations i.e., CaO, KOH, $Mg(OH)_2$, etc.[36] Lead ions can precipitate as hydroxides at pH ≥ 7 which led many researchers to restrict their experiments within the pH range of 2 to 6 to ensure that Pb(II) removal occurs only by adsorption.[37-39]

Column studies

A fixed-bed column adsorption study can be used to determine the breakthrough capacity and overall life span of the adsorbent bed which can be used to design a reactor for real-time application. The provision of regulating the flow rate can be utilized for filter application and optimization of the process parameters can be useful for designing a fixed-bed adsorbent system.

The effectiveness of a fixed-bed column is evaluated by a breakthrough curve which is a demonstration of the ratio of effluent-influent concentration (C/C_0) against time (t) profile in a continuous flow system.[40] In the present study, the major variables for a breakthrough analysis are the bed height as well as the mass of adsorbent, flow rate, and initial inlet concentration. The soundness of the column is measured by the effects of these variables on the breakthrough curve.

Effect of initial Pb(II) concentration

The effect of the initial Pb(II) concentration on breakthrough

C_0 (mg/L)	Q (mL/min)	Mass of Adsorbent (g)	Z (cm)	pH of the effluent	q_{total} (mg)	$q_{eq(exp)}$ (mg/g)
10	2	10	5.72	4.29	888.55	88.86
10	2	15	5.72	4.45	1238.50	82.57
20	2	15	7.62	4.31	1274.80	84.99
10	4	15	7.62	4.50	481.78	32.12

Table 2 — Experimental Data of the Column Parameters Determined at Various Initial Pb(II) Concentrations

curves was investigated using inlet concentrations of 10 mg/L and 20 mg/L. A constant bed depth of 7.62 cm and a flow rate of 2 mL/min was maintained. The results are shown in Figure 5a and Table 2.

The time to reach the breakthrough point (the point where the ratio of effluent concentration/influent concentration is equal to 0.05) decreased with increasing initial Pb(II) concentration (for 20 mg/L, the breakthrough time was approximately 3.5 days and for 10 mg/L the breakthrough time was approximately 12 days- ref. *(Figure 5a)*) which implies that the bed saturates earlier if higher amounts of Pb(II) ions were fed to the column. Decreasing breakthrough time resulted in a steeper breakthrough curve.

The mass transfer coefficient is proportionately dependent on the concentration gradient of the transporting species. Therefore, increasing the initial Pb(II) concentration would increase the concentration gradient and hence will increase the mass transfer coefficient.

Similar phenomena were observed in other studies.[22,41-43] The equilibrium uptake of Pb(II) q_{eq} decreased and maximum adsorption q_{total} increased with increased initial Pb(II) concentration. This is an exception and not an expected trend. This finding is not in agreement with the observations of other researchers,[43,44] but Canteli *et al.*[42] observed a similar phenomenon in their study investigating the adsorption of benzaldehyde on activated carbon obtained from coconut husk.

Effect of flow rate

The effect of the flow rate on breakthrough curves was investigated using two different flow rates i.e., 2 mL/min and 4 mL/min, when a constant bed depth of 7.62 cm and an initial Pb(II) concentration of 10 mg/L was maintained. The results are shown in Figure 5b and Table 2.

As is evident from the breakthrough curve Figure 5b, increased flow rate resulted in shorter breakthrough time. Variation of the slope of the breakthrough curve for two different flow rates can be explained through mass transfer as well. Increased flow rate resulted in an increased rate of adsorbed Pb(II) onto unit bed depth which increases the mass transfer coefficient implying faster saturation. This trend was similar to other studies in the literature.[21] A higher flow rate provides inadequate contact time between the adsorbent in the column and the Pb(II) ions which resulted in a much lower maximum and equilibrium capacity (32.18 mg/g) compared to that for decreased flow rate (88.86 mg/g). Previous studies also found similar results.[41-43]

Effect of bed depth

The effect of the bed depth on breakthrough curves was investigated using two different amounts of biochar 10 g and 15 g that provided varying bed depths i., e., 5.72 cm, and 7.62 cm, respectively. A constant flow rate of 2 mL/min and an initial Pb(II) concentration of 10 mg/L was maintained. The results are shown in Figure 5c and Table 2.

As seen in Figure 5c, increasing

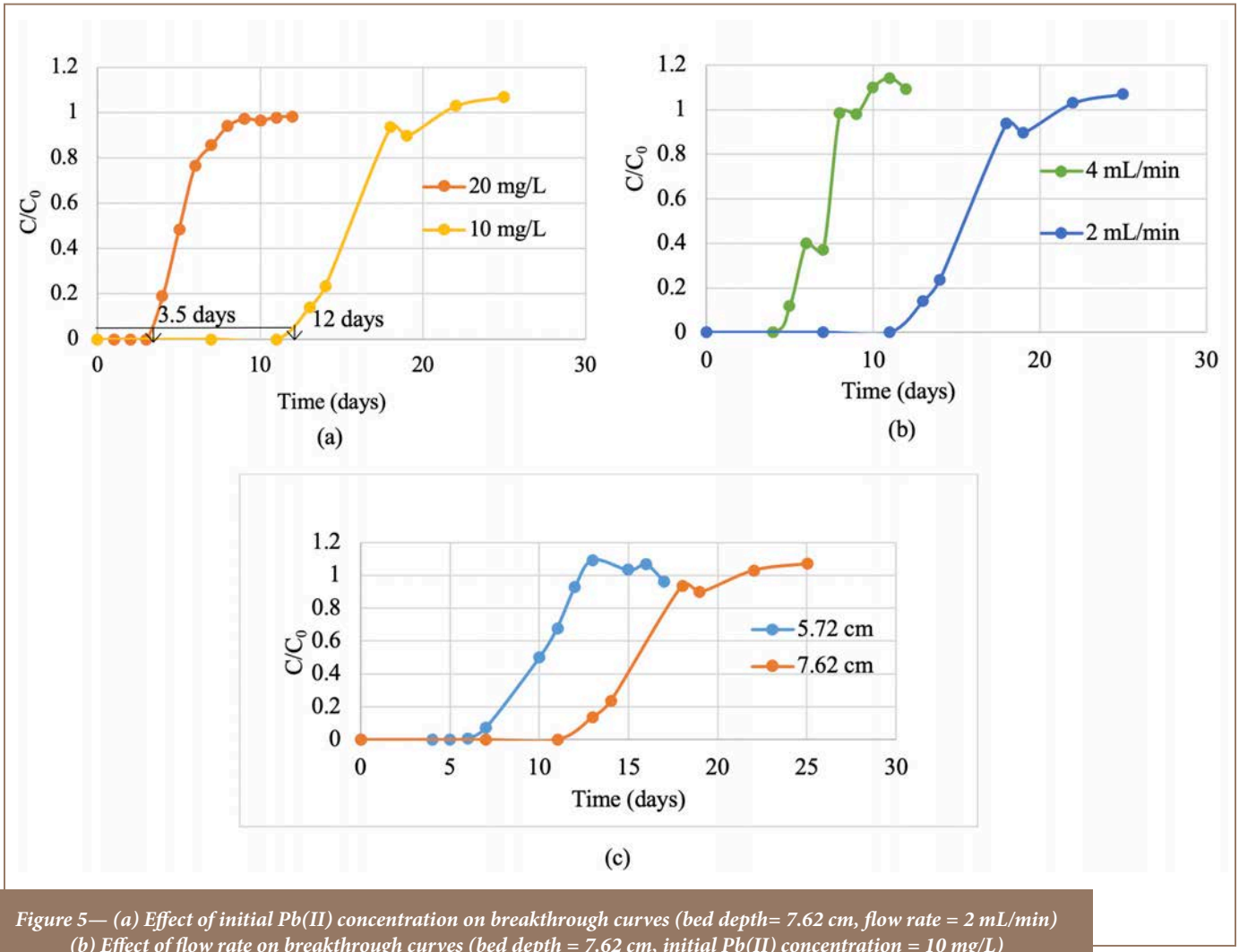

Figure 5— (a) Effect of initial Pb(II) concentration on breakthrough curves (bed depth= 7.62 cm, flow rate = 2 mL/min) (b) Effect of flow rate on breakthrough curves (bed depth = 7.62 cm, initial Pb(II) concentration = 10 mg/L) (c) Effect of bed depth on breakthrough curves (flow rate = 2 mL/min, initial Pb(II) concentration = 10 mg/L)

the bed depth resulted in increased breakthrough time. The slope of the breakthrough curve was slightly decreased. The broadening of the mass transfer zone may explain this.[45] Higher bed depth implies a higher amount of biochar available for the adsorption of Pb(II). A higher amount of biochar indicates a higher surface area to be filled up with Pb(II) ions. Therefore, increasing bed depth significantly increased the breakthrough and saturation time. This observation is in line with findings by other studies.[46]

Adsorption model for fixed-bed column studies

Adams-Bohart model

The Adams-Bohart model can be employed to estimate the fixed-bed parameters of maximum saturation concentration N_0 and the Adams-Bohart rate constant K_{AB}. Linear regression of all the breakthrough curves gives the value of these parameters which were calculated and presented in Table 3.

With increased initial Pb(II) concentration, rate constant K_{AB} decreased and maximum adsorption capacity increased. This observation is in agreement with the results of other studies.[21] The change in concentration gradient induces changes in rate constant and adsorption capacity

C_0 (mg/L)	Q (mL/min)	Z (cm)	K_{AB} (x10^6)(L mg^{-1} min^{-1})	N_0 (x10^{-3})(mg/L)	R^2
20.00	2.00	7.62	5.00	3.53	0.74
10.00	2.00	7.62	20.00	1.95	0.86
10.00	4.00	7.62	20.00	2.41	0.74
10.00	2.00	5.72	20.00	3.30	0.66

Table 3 — Adams-Bohart Variables at Different Conditions by Linear Regression Analysis

C_0 (mg/L)	Q (mL/min)	Z (cm)	K_{TH} (x10^3)(mL mg^{-1} min^{-1})	q_0 (mg/g) (calculated)	q_0 (mg/g) (experimental)	R^2
20.00	2.00	7.62	20.00	28.47	49.92	0.93
10.00	2.00	7.62	50.00	31.08	24.96	0.95
10.00	4.00	7.62	110.00	25.20	49.92	0.84
10.00	2.00	5.72	50.00	56.59	37.44	0.96

Table 4 — Thomas Variables at Different Conditions by Linear Regression Analysis

which implies the diffusion process is concentration-dependent.[47] If the flow rate increases, that implies that adsorbate was getting introduced at a higher rate, which was supposed to be inducing faster saturation, and hence K_{AB} should have decreased (minimal resistance). For this study, an increased flow rate did not show any changes, but validated the observation for increased adsorption capacity, N_0. For varying bed depth, the value of K_{AB} did not change, but maximum adsorption capacity decreased for increased bed depth. This can be explained by the hypothesis that increased bed depth provided an increased number of available binding sites for adsorption.[44] Overall, this model showed that higher initial Pb(II) concentration, flow rate, and bed depth will increase the adsorption potential of biochar. The R^2 values for the Adams-Bohart model are low, ranging from 0.66 to 0.86, which indicates that this model is not a good fit for this study.

Thomas model

The simplified expression of the Thomas model was used to predict the unknown values of the Thomas rate constant. The variables K_{TH} and q_0 and the linear regression coefficient (R^2) are presented in Table 4.

From the calculated values for Thomas model parameters, it can be said that rate constant and equilibrium adsorbate uptake both decreased with the increase of initial Pb(II) concentration, which implies that the concentration gradient was the impelling cause for adsorption. This is similar to studies conducted by other researchers.[44,48,49] With increased flow rate, the rate constant increased which indicates there was a lack of time for the contaminants to transfer from the liquid phase to the solid surface of biochar, and hence adsorbate uptake decreased.[50] Increased bed depth did not have much impact on rate constant, but adsorbate uptake decreased which indicates there were more binding sites available for adsorption. Table 4 provided the comparative values for calculated q_0 using the model and the experimental q_0. According to the Thomas model, lower initial Pb(II) concentration, flow rate, and bed depth will increase the adsorption of Pb(II) on biochar. As seen in the table, there was a 20-50% discrepancy between the predicted and experimental values. Even though

C_0 (mg/L)	Q (mL/min)	Z (cm)	K_{YN} (x10^2)(min^{-1})	τ (min) (calculated)	τ (min) (experimental)	R^2
20.00	2.00	7.62	0.03	12104.30	10080.00	0.93
10.00	2.00	7.62	0.05	23314.00	23040.00	0.95
10.00	4.00	7.62	0.11	9449.09	10800.00	0.84
10.00	2.00	5.72	0.05	28296.00	14400.00	0.96

Table 5 — Yoon-Nelson Variables at Different Conditions by Linear Regression Analysis

this model demonstrated a positive correlation compared to the Adams-Bohart model (R^2 values ranging from 0.84 to 0.96), for this study, the discrepancy between the predicted and calculated value did not support this model being a good fit. According to López-Cervantes *et al.* the main limitation of this model is that it was derived based on the assumption that biosorption follows second-order kinetics and does not depend on the transformation of reactant-product but is dominated by the mass transfer.[21] This assumption might not be valid for processes under all varying conditions.

Yoon-Nelson model

The linearized form of the Yoon-Nelson model was used to estimate the values of rate constant K_{YN} and 50% breakthrough time, . The parameters value and linear regression coefficient are presented in Table 5.

Table 5 provides the 50% breakthrough time achieved by the prediction from the model and the actual experimental 50% breakthrough time is also shown. Increased initial Pb(II) concentration decreased the rate constant and 50% breakthrough time which implies higher feed concentration accelerated the adsorption process that provided a shorter breakthrough time. Increased flow rate gave an increased rate constant and decreased breakthrough time. Increased bed depth shortens the breakthrough time which contradicts experimental data. A comparative analysis can be made between the predicted 50% breakthrough time and experimental 50% breakthrough time which showed that the values were close to each other with no significant difference except for the condition where 10 mg/L of initial Pb(II) concentration, 2 mL/min of flow rate and 10 g of the mass of adsorbent was used. From the predicted and experimental values of the breakthrough time and listed correlation coefficient (R^2) that ranged from 0.84 to 0.96, it can be said that the Yoon-Nelson model demonstrated the most suitable relation to the experimental data and can be utilized to portray the adsorption potential of Pb(II) in a fixed-bed biochar column.

Discussion

Pyrolysis temperature plays an important role in the yield of biochar as well as pore size and volume of the produced biochar.[51,52] Basic components within the biomass such as lignin, cellulose, hemicellulose break down at different stages of pyrolysis. At a temperature range of 200 – 260°C, hemicellulose starts to decompose, cellulose starts breaking down at 240 – 350°C and lignin starts to degrade from 280 – 500°C.[51] It was found that at a lower pyrolysis temperature (300 – 450°C), the specific surface area of produced biochar is typically low (4 – 23 m^2/g)[54] which could be due to the blockage of the residual pores by inorganic material present in biomass.[55] A substantial increase of surface area begins at 400 -500°C[56] (25 – 300 m^2/g) which could be due to the degradation of organic matter and the emergence of porous or narrow passage-like structures.[57,58] The biochar used in this study was produced at 500°C, in accordance with the investigation of temperature needed for yielding high surface area. Biochar produced at a temperature of over 400°C appeared to be more able to adsorb organic and inorganic contaminants owing to its high surface area and appearance of micropores while preserving the oxygen functional groups during pyrolysis.[59] The higher surface area, which is also related to pore volume, influences the capacity of cation adsorption of biochar onto its surface.[60-63] Previous studies conducted by various researchers reported the physical properties of biochar and experimental data of the adsorption experiment. Alhashimi and Aktas[15] conducted a sensitivity analysis focusing on the effect of particle size, surface area, pH, contaminant concentration, adsorbent dose, and contact dose on the adsorption

capacity of such studies. They found surface area to have the most reasonable degree of correlation with adsorption capacity compared to other properties. A similar occurrence was noted in the present study as well. The pH of slow pyrolysis biochar is typically in the range of 4 to 10.[64] Yuan J-H *et al.* observed that biochar pH increases (from 6.5 to 10.8) with increasing pyrolysis temperature (from 300 to 700°C), perhaps owing to the increased accumulation of undecomposed inorganic compounds and the formation of basic surface oxides.[61,65] According to Ronsse *et al.*, Spokas *et al.* and Zhao *et al.*, this increase in pH with increased temperature is correlated with the presence of higher amounts of ash and oxygen-containing functional groups.[54,58,64] The value of pH (7.58) and ash content (35.48%) of the biochar used in the present study (pyrolysis temperature 500°C) are in accordance with their proposition. Rafiq *et al.* found increased ash content (from 5.7 to 18.7%) with an increase of temperature (from 300 – 500°C), which is due to the continuous congregation of minerals and absolute alteration of ligno-cellulosic components.[50,66,67] However, the presence of foreign materials could also be responsible for high ash content, which was also observed by Lee *et al.*[68] The elemental composition of biochar varies widely depending upon the type of feedstock and production process parameters. Slow pyrolysis biochar derived from various feedstock showed carbon content roughly in the range of 6 - 90%, oxygen content ranging from 1 – 37.7%, hydrogen content ranging from 1 – 9.9%, and nitrogen content ranging from 0.1 – 7.4%.[64] Some studies found an increase of carbon content (from 62.2 to 92.4%) with an increase of pyrolysis temperature, which can be attributed to the extended level of chemical change eventually forming robust carbon composition.[69-71] On the other hand, another study by Cantrell *et al.* found a decrease in carbon, hydrogen, and oxygen content ranging from 59.94 to 37.94%, 2.91 to 0.99% and from 2.13 to 0.99%, respectively, with an increase of temperature from 300 to 500°C and attributed this loss to the disappearance of hydroxyl and carboxyl groups of cellulose, hemicellulose, and lignin.[72,73] The H/C molar ratio (0.07) describes the aromaticity and permanence of the biochar, whereas the O/C molar ratio (0.16) explains the hydrophilicity or abundance of polar oxygen-containing surface functional groups of the biochar, which actively take part in adsorption of heavy metals.[73] When comparing two different biochar, lower H/C and O/C ratio indicates higher aromaticity and lower affinity to water.[74]

The intention in the present study was to keep the pH unaltered so experiments were conducted accordingly. Increased pH (up to pH = 8) may have some impact on the Pb(II) removal capacity of biochar. High pH value may facilitate removal through precipitation along with adsorption.[75] Jalali and Aboulghazi showed that at pH ≥ 6.01, more hydroxide complexes i.e., $Pb(OH)^{+}$, $Pb(OH)_2$ easily formed and reduced the concentration of free Pb ions in the solution.[76] Moreover, when solution pH increases, the concentration of H^{+} decreases. To balance the concentration in solution, the oxygen functional groups on the biochar surface release the negative charge and increase the electrostatic attraction for Pb(II).[77] Comprehensive characterization of biochar before and after the experiment could provide a thorough understanding of the adsorption mechanism of Pb(II). According to Li *et al.* net release of cations i. e., Na^{+}, K^{+}, Ca^{2+} and, Mg^{2+} can be measured to estimate the extent of cation exchange during Pb(II) adsorption.[78] Complexation with the oxygen functional groups on the biochar surface can be evaluated by investigating the peak area, peak intensity, and position of the peak in FTIR after Pb(II) adsorption. As stated earlier, precipitation is one of the most important mechanisms in Pb(II) removal and this can be evaluated by X-ray diffraction scanning of Pb(II) loaded biochar.

Batch experiments in this study did not lead to a point where the isotherm model could be plotted or reaction kinetics could be determined since Pb(II) was completely removed by biochar within the very first moment (~ 0 h) of the experiment. A fixed-bed column study was the main focus of this work, hence no further batch adsorption experiments were conducted.

To scale-up the system using the laboratory experimental data, two parameters have significant importance: the superficial velocity and contact time (empty-bed contact time). Both of these parameters need to be the same so that the mass transfer characteristics do not change. Superficial velocity is equal to the flow rate divided by the cross-sectional area. Therefore, using the superficial velocity and flow rate of the lab-scale system, a new value of the cross-sectional area of the packed column can be calculated which will further provide the required diameter of the column. The empty-bed contact time is equal to the volume of the bed occupied by the adsorbent divided by the flow rate and this is a function of both superficial velocity and bed depth. The required mass of the adsorbent can be calculated by multiplying the volume of the packed bed and density. This makes the density of the adsorbent an important variable, because if the particle size changes, density will also

be changed which in turn will change the length of the mass transfer zone. If the mass transfer zone is short, the adsorbent bed will be fully utilized at breakthrough. This is called the point of exhaustion when the bed completely loses the ability to remove adsorbate. The rate of exhaustion can be expressed as the amount of adsorbent used in terms of a unit volume of water treated until the breakthrough. If superficial velocity increases, the length of the mass-transfer zone increases, and the rate of exhaustion decreases. Specific throughput is the volume of water treated per unit mass of adsorbent used. This is a useful variable to determine the adsorption capacity of a fixed-bed system. Thus, the column diameter of the scaled-up system can be calculated from the required throughput and the chosen velocity.

Conclusions

Removal of Pb(II) using biochar is conducted in a fixed-bed column system by varying the initial concentration, flow rate, and bed depth to evaluate the potential of biochar in removing Pb(II) from drinking water. Different parameters effect the breakthrough and saturation capacity for Pb(II) on biochar. Increased initial Pb(II) concentration, flow rate, and decreased bed depth accelerate the process of exhaustion of the column. The column adsorption kinetic models are implemented to the experimental data to further analyze the adsorption mechanism. The Adams-Bohart model does not fit well with the experimental data with respect to both the predicted values and correlation coefficient. The Thomas model shows a good correlation coefficient but the predicted values for equilibrium adsorbate uptake have a 20-50% discrepancy with the experimental data. The Yoon-Nelson model assesses the 50% breakthrough for the column that is close to the values found through the experiment and this model also showed a good correlation between the values.

Acknowledgments

This work was supported by the USEPA P3 Phase I Grant Number (FAIN): 8392660. The authors would also like to thank Dr. James Lee, Department of Chemistry and Biochemistry, Old Dominion University, Norfolk, VA, for the help with the AAS analysis.

References

1. **United States Environmental Protection Agency.** Learn about Lead. epa.gov. Published [Dec. 02, 2013]. Updated [Sept 30, 2020]. Accessed [Jun 08, 2020]. https://www.epa.gov/lead/learn-about-lead
2. **United States Environmental Protection Agency.** Lead and Copper Rule. epa.gov. Published [Oct. 13, 2015]. Updated [Oct 15, 2019]. Accessed [Jul 11, 2020]. https://www.epa.gov/dwreginfo/lead-and-copper-rule
3. **Natural Resources Defense Council.** Flint Water Crisis. nrdc.org. Published [Mar. 29, 2017]. Updated [Aug 18, 2020]. Accessed [Jun 09, 2020]. https://www.nrdc.org/flint.
4. **LaFrance D.** Together, let's get the lead out. AWWA. Published [Mar. 15 2016]. Updated [Mar 17, 2016]. Accessed [Jun. 13 2020]. https://www.awwa.org/AWWA-Articles/together-lets-get-the-lead-out.
5. **Sarkar S., Adhikari S.** Adsorption Technique for Removal of Heavy Metals from Water and Possible Application in Wastewater-Fed Aquaculture. Springer, Singapore; 2018. http://doi-org-443.webvpn.fjmu.edu.cn/10.1007/978-981-10-7248-2_12
6. **Dada AO, Ojediran JO, Olalekan AP.** Sorption of [Pb.sup.2+] from aqueous solution unto modified rice husk: isotherms studies. Adv Phys Chem. Mar 18, 2013. https://doi.org/10.1155/2013/842425
7. **Mansour MS, Ossman ME, Farag HA.** Removal of Cd (II) ion from waste water by adsorption onto polyaniline coated on sawdust. Desalination. 2011;272(1):301-5. https://doi.org/10.1016/j.desal.2011.01.037
8. **Semerjian L.** Removal of heavy metals (Cu, Pb) from aqueous solutions using pine (Pinus halepensis) sawdust: Equilibrium, kinetic, and thermodynamic studies. Environ Technol Innov. 2018;12:91-103. https://doi.org/10.1016/j.eti.2018.08.005
9. **Khoramzadeh E, Nasernejad B, Halladj R.** Mercury biosorption from aqueous solutions by Sugarcane Bagasse. J Taiwan Inst Chem Eng. 2013;44(2):266-9. https://doi.org/10.1016/j.jtice.2012.09.004
10. **Wang J, Li Q, Li M-M, Chen T-H, Zhou Y-F, Yue Z-B.** Competitive adsorption of heavy metal by extracellular polymeric substances (EPS) extracted from sulfate reducing bacteria. Bioresour Technol. 2014;163:374-6. https://doi.org/10.1016/j.biortech.2014.04.073
11. **Monteiro CM, Castro PML, Malcata FX.** Metal uptake by microalgae: Underlying mechanisms and practical applications. Biotechnol Prog. 2012;28(2):299-311. https://DOI: 10.1002/btpr.1504
12. **Zhao G, Huang X, Tang Z, Huang Q, Niu F, Wang X.** Polymer-based nanocomposites for heavy metal ions removal from aqueous solution: a review. Polym Chem. 2018;9(26):3562-82. https://doi.org/10.1039/C8PY00484F
13. **Inyang M, Gao B, Ding W, Pullammanappallil P, Zimmerman AR, Cao X.** Enhanced Lead Sorption by Biochar Derived from Anaerobically Digested Sugarcane Bagasse. Sep Sci Technol. 2011;46(12):1950-6. https://doi.org/10.1080/01496395.2011.584604
14. **Huggins TM, Haeger A, Biffinger JC, Ren ZJ.** Granular biochar compared with activated carbon for wastewater treatment and resource recovery. Water Res. 2016;94:225-32. https://doi.org/10.1016/j.watres.2016.02.059
15. **Alhashimi HA, Aktas CB.** Life cycle environmental and economic performance of biochar compared with activated carbon: A meta-analysis. Resour Conserv Recycl. 2017;118:13-26. https://doi.org/10.1016/j.resconrec.2016.11.016
16. **Regmi P, Garcia Moscoso JL, Kumar S, Cao X, Mao J, Schafran G.** Removal of copper and cadmium

from aqueous solution using switchgrass biochar produced via hydrothermal carbonization process. J Environ Manage. 2012;109:61-9. https://doi.org/10.1016/j.jenvman.2012.04.047

17. **Abdelhafez AA, Li J.** Removal of Pb(II) from aqueous solution by using biochars derived from sugar cane bagasse and orange peel. J Taiwan Inst Chem Eng. 2016;61:367-75. https://doi.org/10.1016/j.jtice.2016.01.005

18. **Ding Y, Liu Y, Liu S, Li Z, Tan X, Huang X, et al.** Competitive removal of Cd(ii) and Pb(ii) by biochars produced from water hyacinths: performance and mechanism. RSC Adv. 2016;6(7):5223-32. https://doi.org/10.1039/C5RA26248H

19. **Doumer ME, Rigol A, Vidal M, Mangrich AS.** Removal of Cd, Cu, Pb, and Zn from aqueous solutions by biochars. Environ Sci Pollut Res. 2016;23(3):2684-92. http://doi: 10.1007/s11356-015-5486-3

20. **Xu X, Hu X, Ding Z, Chen Y, Gao B.** Waste-art-paper biochar as an effective sorbent for recovery of aqueous Pb(II) into value-added PbO nanoparticles. Chem Eng J. 2017;308:863-71. https://doi.org/10.1016/j.cej.2016.09.122

21. **López-Cervantes J, Sánchez-Machado DI, Sánchez-Duarte RG, Correa-Murrieta MA.** Study of a fixed-bed column in the adsorption of an azo dye from an aqueous medium using a chitosan–glutaraldehyde biosorbent. Adsorp Sci Technol. 2017;36(1-2):215-32. https://doi.org/10.1177/0263617416688021

22. **Ahmad AA, Hameed BH.** Fixed-bed adsorption of reactive azo dye onto granular activated carbon prepared from waste. J Hazard Mater. 2010;175(1):298-303. https://doi.org/10.1016/j.jhazmat.2009.10.003

23. **Futalan CM, Kan C-C, Dalida ML, Pascua C, Wan M-W.** Fixed-bed column studies on the removal of copper using chitosan immobilized on bentonite. Carbohydr Polym. 2011;83(2):697-704. https://doi.org/10.1016/j.carbpol.2010.08.043

24. **Han R, Ding D, Xu Y, Zou W, Wang Y, Li Y, et al.** Use of rice husk for the adsorption of congo red from aqueous solution in column mode. Bioresour Technol. 2008;99(8):2938-46. https://doi.org/10.1016/j.biortech.2007.06.027

25. **Bohart GS, Adams EQ.** SOME ASPECTS OF THE BEHAVIOR OF CHARCOAL WITH RESPECT TO CHLORINE.[1]. J Am Chem Soc. 1920;42(3):523-44. https://doi.org/10.1021/ja01448a018

26. **Thomas HC.** Heterogeneous Ion Exchange in a Flowing System. J Am Chem Soc. 1944;66(10):1664-6. https://doi.org/10.1021/ja01238a017

27. **Yoon YH, Nelson JH.** Application of Gas Adsorption Kinetics I. A Theoretical Model for Respirator Cartridge Service Life. Am Ind Hyg Assoc J. 1984;45(8):509-16. https://doi.org/10.1080/15298668491400197

28. **Chu KH.** Breakthrough curve analysis by simplistic models of fixed bed adsorption: in defense of the century-old Bohart-Adams model. Chem Eng J. 2020;380:122513. https://doi.org/10.1016/j.cej.2019.122513

29. **Rozada F, Otero M, García AI, Morán A.** Application in fixed-bed systems of adsorbents obtained from sewage sludge and discarded tyres. Dyes Pigm. 2007;72(1):47-56. https://doi.org/10.1016/j.dyepig.2005.07.016

30. **Aksu Z, Gönen F.** Biosorption of phenol by immobilized activated sludge in a continuous packed bed: prediction of breakthrough curves. Process Biochem. 2004;39(5):599-613. https://doi.org/10.1016/S0032-9592(03)00132-8

31. IBI Biochar Standards 2018. https://biochar-international.org/ibi-biochar-standards/.

32. **Rice EW, Baird RB, Eaton AD, et al.** Standards Methods for Examination of Water and Wastewater. 22nd Edition. American Public Health Association; 2012.

33. **Kumar S, Loganathan VA, Gupta RB, Barnett MO.** An Assessment of U(VI) removal from groundwater using biochar produced from hydrothermal carbonization. J Environ Manage. 2011;92(10):2504-12. https://doi.org/10.1016/j.jenvman.2011.05.013

34. **Li S, Yao Y, Zhao T, Wang M, Wu F.** Biochars preparation from waste sludge and composts under different carbonization conditions and their Pb (II) adsorption behaviors. Water Sci Technol. 2019;80(6):1063-75. http://doi: 10.2166/wst.2019.353

35. **Desta MB.** Batch Sorption Experiments: Langmuir and Freundlich Isotherm Studies for the Adsorption of Textile Metal Ions onto Teff Straw (Eragrostis tef) Agricultural Waste. J Thermodyn. 2013;2013:375830. https://doi.org/10.1155/2013/375830

36. **Fidel RB, Laird DA, Thompson ML, Lawrinenko M.** Characterization and quantification of biochar alkalinity. Chemosphere. 2017;167:367-73. https://doi.org/10.1016/j.chemosphere.2016.09.151

37. **Deng J, Li X, Liu Y, Zeng G, Liang J, Song B, et al.** Alginate-modified biochar derived from Ca(II)-impregnated biomass: Excellent anti-interference ability for Pb(II) removal. Ecotoxicol Environ Saf. 2018;165:211-8. https://doi.org/10.1016/j.ecoenv.2018.09.013

38. **Mishra S, Yadav A, Verma N.** Carbon gel-supported Fe-graphene disks: synthesis, adsorption of aqueous Cr (VI) and Pb (II) and the removal mechanism. Chem Eng J. 2017;326:987-99.

39. **Wan Z, Chen D, Pei H, Liu J, Liang S, Wang X, et al.** Batch study for Pb2+ removal by polyvinyl alcohol–biochar macroporous hydrogel bead. Environmental technology. 2019:1-11. https://doi.org/10.1016/j.cej.2017.06.022

40. **Patel H.** Fixed-bed column adsorption study: a comprehensive review. Appl Water Sci. 2019;9(3):45. https://doi.org/10.1007/s13201-019-0927-7

41. **Biswas S, Mishra U.** Continuous Fixed-Bed Column Study and Adsorption Modeling: Removal of Lead Ion from Aqueous Solution by Charcoal Originated from Chemical Carbonization of Rubber Wood Sawdust. J Chem. 2015;2015:9. https://doi.org/10.1155/2015/907379

42. **Canteli AMD, Carpiné D, Scheer AdP, Mafra MR, Igarashi-Mafra L.** Fixed-bed column adsorption of the coffee aroma compound benzaldehyde from aqueous solution onto granular activated carbon from coconut husk. LWT - Food Sci Technol. 2014;59(2, Part 1):1025-32. https://doi.org/10.1016/j.lwt.2014.06.015

43. **Cruz-Olivares J, Pérez-Alonso C, Barrera-Díaz C, Ureña-Nuñez F, Chaparro-Mercado MC, Bilyeu B.** Modeling of lead (II) biosorption by residue of allspice in a fixed-bed column. Chem Eng J. 2013;228:21-7. https://doi.org/10.1016/j.cej.2013.04.101

44. **Lim AP, Aris AZ.** Continuous fixed-bed column study and adsorption modeling: Removal of cadmium (II) and lead (II) ions in aqueous solution by dead calcareous skeletons. Biochem Eng J. 2014;87:50-61. https://doi.org/10.1016/j.bej.2014.03.019

45. **Singh S, Srivastava VC, Mall ID.** Fixed-bed study for adsorptive removal of furfural by activated carbon. Colloids Surf A Physicochem Eng Asp. 2009;332(1):50-6. https://doi.org/10.1016/j.colsurfa.2008.08.025

46. **Rao JR, Viraraghavan T.** Biosorption of phenol from an aqueous solution by Aspergillus niger biomass. Bioresour Technol. 2002;85(2):165-71. https://doi.org/10.1016/S0960-8524(02)00079-2

47. **Ko DCK, Porter JF, McKay G.** Film-pore diffusion model for the fixed-bed sorption of copper and cadmium ions onto bone char. Water Res. 2001;35(16):3876-86. https://doi.org/10.1016/S0043-1354(01)00114-2

48. **Tofan L, Teodosiu C, Paduraru C, Wenkert R.** Cobalt (II) removal from aqueous solutions by natural hemp fibers: Batch and fixed-bed column studies. Appl Surf Sci. 2013;285:33-9. https://doi.org/10.1016/j.apsusc.2013.06.151

49. **Mantonanaki A, Pellera F-M, Gidarakos E.** Column studies to investigate Cu(II) and Pb(II) removal from aqueous solution using biochar2016. https://www.researchgate.net/publication/308778319_Column_studies_to_investigate_CuII_and_PbII_removal_from_aqueous_solution_using_biochar

50. **Tsai W-C, de Luna MDG, Bermillo-Arriesgado HLP, Futalan CM, Colades JI, Wan M-W.** Competitive Fixed-Bed Adsorption of Pb(II), Cu(II), and Ni(II) from Aqueous Solution Using Chitosan-Coated Bentonite. Int J Polym Sci. 2016;2016:11. https://doi.org/10.1155/2016/1608939

51. **Hassler JW.** Purification with activated carbon; industrial, commercial, environmental. Chemical Publishing Co Inc U S 1974.

52. **Wilson K.** How biochar works in soil. tBJ. 2014;32:25-33. https://www.biochar-journal.org/en/ct/32

53. **Babu B.** Biomass pyrolysis: a state-of-the-art review. Biofuel Bioprod Biorefin. 2008;2(5):393-414. https://doi.org/10.1002/bbb.92

54. **Ronsse F, Van Hecke S, Dickinson D, Prins W.** Production and characterization of slow pyrolysis biochar: influence of feedstock type and pyrolysis conditions. Glob Change Biol Bioenergy. 2013;5(2):104-15. https://doi.org/10.1111/gcbb.12018

55. **Batista EM, Shultz J, Matos TT, Fornari MR, Ferreira TM, Szpoganicz B, et al.** Effect of surface and porosity of biochar on water holding capacity aiming indirectly at preservation of the Amazon biome. Sci Rep. 2018;8(1):1-9. https://doi.org/10.1038/s41598-018-28794-z

56. **Chen Y, Zhang X, Chen W, Yang H, Chen H.** The structure evolution of biochar from biomass pyrolysis and its correlation with gas pollutant adsorption performance. Bioresour Technol. 2017;246:101-9. https://doi.org/10.1016/j.biortech.2017.08.138

57. **Li X, Shen Q, Zhang D, Mei X, Ran W, Xu Y, et al.** Functional groups determine biochar properties (pH and EC) as studied by two-dimensional 13C NMR correlation spectroscopy. PLoS One. 2013;8(6). https://doi.org/10.1371/journal.pone.0065949

58. **Zhao S-X, Ta N, Wang X-D.** Effect of temperature on the structural and physicochemical properties of biochar with apple tree branches as feedstock material. Energies. 2017;10(9):1293. https://doi.org/10.3390/en10091293

59. **Uchimiya M, Wartelle LH, Lima IM, Klasson KT.** Sorption of deisopropylatrazine on broiler litter biochars. J Agric Food Chem. 2010;58(23):12350-6. https://doi.org/10.1021/jf102152q

60. **Fang Q, Chen B, Lin Y, Guan Y.** Aromatic and hydrophobic surfaces of wood-derived biochar enhance perchlorate adsorption via hydrogen bonding to oxygen-containing organic groups. Environ. Sci. Technol. 2014;48(1):279-88. https://doi.org/10.1021/es403711y

61. **Yuan J-H, Xu R-K, Zhang H.** The forms of alkalis in the biochar produced from crop residues at different temperatures. Bioresour Technol. 2011;102(3):3488-97. https://doi.org/10.1016/j.biortech.2010.11.018

62. **Hmid A, Mondelli D, Fiore S, Fanizzi FP, Al Chami Z, Dumontet S.** Production and characterization of biochar from three-phase olive mill waste through slow pyrolysis. Biomass Bioenergy. 2014;71:330-9. https://doi.org/10.1016/j.biombioe.2014.09.024

63. **McHenry MP.** Agricultural bio-char production, renewable energy generation and farm carbon sequestration in Western Australia: Certainty, uncertainty and risk. Agric Ecosyst Environ. 2009;129(1-3):1-7. https://doi.org/10.1016/j.agee.2008.08.006

64. **Spokas KA, Novak JM, Stewart CE, Cantrell KB, Uchimiya M, DuSaire MG, et al.** Qualitative analysis of volatile organic compounds on biochar. Chemosphere. 2011;85(5):869-82. https://doi.org/10.1016/j.chemosphere.2011.06.108

65. **Novak JM, Lima I, Xing B, Gaskin JW, Steiner C, Das K, et al.** Characterization of designer biochar produced at different temperatures and their effects on a loamy sand. Annals of Environ. Sci. 2009. http://hdl.handle.net/2047/d10019637

66. **Rafiq MK, Bachmann RT, Rafiq MT, Shang Z, Joseph S, Long R.** Influence of pyrolysis temperature on physico-chemical properties of corn stover (Zea mays L.) biochar and feasibility for carbon capture and energy balance. PloS one. 2016;11(6). https://doi.org/10.1371/journal.pone.0156894

67. **Cao X, Harris W.** Properties of dairy-manure-derived biochar pertinent to its potential use in remediation. Bioresour Technol. 2010;101(14):5222-8. https://doi.org/10.1016/j.biortech.2010.02.052

68. **Lee JW, Kidder M, Evans BR, Paik S, Buchanan Iii A, Garten CT, et al.** Characterization of biochars produced from cornstovers for soil amendment. Environ Sci Technol. 2010;44(20):7970-4. https://doi.org/10.1021/es101337x

69. **Özçimen D, Ersoy-Meriçboyu A.** Characterization of biochar and bio-oil samples obtained from carbonization of various biomass materials. Renew Energy. 2010;35(6):1319-24. https://doi.org/10.1016/j.renene.2009.11.042

70. **Domingues RR, Trugilho PF, Silva CA, de Melo ICN, Melo LC, Magriotis ZM, et al.** Properties of biochar derived from wood and high-nutrient biomasses with the aim of agronomic and environmental benefits. PloS one. 2017;12(5). https://doi.org/10.1371/journal.pone.0176884

71. **Lehmann J, Joseph S.** Biochar for environmental management: science, technology and implementation: Routledge; 2015.

72. **Cantrell KB, Hunt PG, Uchimiya M, Novak JM, Ro KS.** Impact of pyrolysis temperature and manure source on physicochemical characteristics of biochar. Bioresour Technol. 2012;107:419-28. https://doi.org/10.1016/j.biortech.2011.11.084

73. **Wu Q, Xian Y, He Z, Zhang Q, Wu J, Yang G, et al.** Adsorption characteristics of Pb (II) using biochar derived from spent mushroom substrate. Sci Rep. 2019;9(1):1-11. https://doi.org/10.1038/s41598-019-52554-2

74. **Ahmad M, Lee SS, Rajapaksha AU, Vithanage M, Zhang M, Cho JS, et al.** Trichloroethylene adsorption by pine needle biochars produced at various pyrolysis temperatures. Bioresour Technol. 2013;143:615-22. https://doi.org/10.1016/j.biortech.2013.06.033

75. **Xu X, Cao X, Zhao L, Zhou H, Luo Q.** Interaction of organic and inorganic fractions of biochar with Pb(ii) ion: further elucidation of mechanisms for Pb(ii) removal by biochar. RSC Adv. 2014;4(85):44930-7. https://doi.org/10.1039/C4RA07303G

76. **Jalali M, Aboulghazi F.** Sunflower stalk, an agricultural waste, as an adsorbent for the removal of lead and cadmium from aqueous solutions. J Mater Cycles Waste Manag. 2013;15(4):548-55. https://doi.org/10.1007/s10163-012-0096-3

77. **Qiu Y, Cheng H, Xu C, Sheng GD.** Surface characteristics of crop-residue-derived black carbon and lead (II) adsorption. Water Res. 2008;42(3):567-74. https://doi.org/10.1016/j.watres.2007.07.051

78. **Li H, Dong X, da Silva EB, de Oliveira LM, Chen Y, Ma LQ.** Mechanisms of metal sorption by biochars: Biochar characteristics and modifications. Chemosphere. 2017;178:466-78. https://doi.org/10.1016/j.chemosphere.2017.03.072

CHAPTER 4

Bioremediation of industrial effluents: How a biochar pretreatment may increase the microalgal growth in tannery wastewater

Note: The contents of this chapter were adapted from the collaborative research article published in the journal 'Journal of Water Process Engineering'. Biochar characterization, comparative batch adsorption experiments and analysis using synthetic wastewater, batch kinetic experiments and analysis by varying biochar dose, Cr concentration were conducted by the author of this dissertation.

Eleonora Sforza, Pushpita Kumkum, Elena Barbera, Sandeep Kumar

Journal of Water Process Engineering 37 (2020) 101431

Contents lists available at ScienceDirect

Journal of Water Process Engineering

journal homepage: www.elsevier.com/locate/jwpe

Bioremediation of industrial effluents: How a biochar pretreatment may increase the microalgal growth in tannery wastewater

Eleonora Sforza[a,*], Pushpita Kumkum[b], Elena Barbera[a], Sandeep Kumar[b]

[a] Department of Industrial Engineering DII, University of Padova, Via Marzolo 9, 35131 Padova, Italy
[b] Department of Civil and Environmental Engineering, Old Dominion University, Norfolk, VA, USA

ARTICLE INFO

Keywords:
Chlorella protothecoides
Chromium
Adsorption
Photosynthetic bioremediation
Slow pyrolisis

ABSTRACT

The application of microalgae in wastewater treatment is gaining increasing attention due to the possible environmental benefits of using photosynthetic organisms for bioremediation. Tannery wastewaters, however, may be inhibiting for microorganisms' growth due to the presence of toxic compounds, especially chromium. In this work, we assessed the possibility of combining the application of biochar, as an adsorbent for metals including chromium, with microalgae cultivation for tannery wastewater treatment. Two different types of biochar (pinewood biochar, PB, and a commercial one, CB) were tested as a pretreatment step prior to cultivation of *Chlorella protothecoides*. The application of both types of biochar led to a significant increase in growth rates (61 % and 126 % for PB and CB, respectively) and nutrients removal compared to cultivation in raw wastewaters. Concerning the comparison between different biochars, it resulted that biochar production process and its physiochemical characteristics strongly affect Cr(III) adsorption performances, with CB removing 99.6 % from a synthetic medium in 5 min, compared to 83.4 % of PB in 3 h. Cr(III) adsorption on CB followed Freundlich isotherm model. The kinetics of adsorption was also addressed, and pseudo-second order kinetics was found to be the best fitted model for Cr(III) adsorption on CB. When applied to real tannery effluents, chromium adsorption performances were affected by the complexity of the medium

1. Introduction

The tanning industry is specialized in the production of a wide range of bovine leathers for the footwear, furnishings, clothing and leather goods industries. The impacts of tannery wastes on health and on the environment is potentially dangerous and continuously growing: tannery effluent contains large amounts of pollutants, such as salt, lime sludge, sulfides, and acids [1]. Secondary effluents from wastewater treatment plants also contain large quantities of nutrients, such as nitrogen and phosphorus, which may cause eutrophication in lakes and disrupt the balance of the ecosystem [2]. In addition, water generated during this industrial process has a significant amount of heavy metals, especially chromium, which is harmful for living organisms [3].

The water discharged from tannery industries needs a specific treatment. Conventional wastewater treatment typically includes primary and secondary treatment. Primary treatment comprises sulfide oxidation, solids separation, and chromium precipitation. Various physicochemical methods such as filtration, precipitation or physicochemical coagulation have been used. Other methods for chromium removal or recovery from industrial effluent include advanced treatment such as membrane separation [4], advanced oxidation processes [5], and ion exchange [6]. Secondary treatment is usually accomplished by activated sludge systems [7], which is possible after a proper pretreatment. However, conventional systems, based on activated sludge, result in the generation of a considerable amount of sludge, which requires treatment before final disposal [8].

As an alternative to conventional technologies, the integration of a microalgae-bacteria based process within wastewater treatment plants seems very promising due to the ability of these microorganisms to reduce the concentration of inorganic nutrients such as nitrogen and phosphorus, in a gas self-sustaining system, i.e. avoiding the aeration of the conventional biological process [9].

Another interesting advantage is related to the nitrogen exploitation, that results in the accumulation of such a compound in the biomass, according to a circular economy perspective. Microalgae were also found to reduce the concentration of dissolved heavy metals such as mercury, cadmium and copper, lead, aluminum, and chromium [3]. The applicability of microalgae/bacteria consortia in industrial wastewater is still under preliminary investigation. Several studies demonstrated the capability of microalgal species to survive in tannery

* Corresponding author.
E-mail address: eleonora.sforza@unipd.it (E. Sforza).

https://doi.org/10.1016/j.jwpe.2020.101431
Received 21 April 2020; Received in revised form 3 June 2020; Accepted 8 June 2020
Available online 23 June 2020

wastewater (TWW) [10]. As an example, Da Fontoura et al. [2] showed that *Scenedesmus* species is able to grow in TWW with a biomass production of 1.72 g L^{-1}, obtaining removals of about 95 % of total nitrogen, ammonium, phosphorous and Chemical Oxygen Demand (COD). Generally, phycoremediation has been evaluated by several researchers, and different microalgae and cyanobacteria such as species of *Oscillatoria, Phormidium, Ulothrix, Chlamydomonas, Scenedesmus* have been evaluated for their ability to grow in tannery effluent and accumulate chromium [11–14]. Thus, microalgae can be an alternative in the TWW treatment, reducing the environmental impact caused by their pollutants, converting these nutrients into biomass that can be availed in different applications (e.g. biofuels) [3]. However, one drawback of growing microalgae directly in TWW is that the presence of some pollutants may inhibit the algal growth, besides producing a biomass which in itself is rich in metals and may not be used in some specific commercial products.

This could however be mitigated by integrating a biochar filtration step prior to the algal cultivation system. Biochar is a carbon-rich material characterized by high porosity with oxygen functional groups and aromatic surfaces. It is obtained from the thermal degradation of wood residues, green waste and agricultural remains. Its porous structure with high surface-volume ratio and affinity for non-polar substances (e.g. polyaromatic hydrocarbons) makes it a potential sorbent for organic pollutants and pesticides [15,16]. In the last few years, biochar produced via slow pyrolysis or hydrothermal carbonization has shown potential to remove salts and many metal contaminants from water [17–20]. For example, biochar obtained from hydrothermal carbonization treatment (HTCB) of pinewood [17] and alkali-activated biochar (A-HTCB) from switchgrass [19] can be used as alternatives to powdered activated carbon for the sorption of metal ions and heavy metals from water. Researchers have investigated Cr(VI) removal potential of biochar derived from rice husk, organic solid wastes and sewage sludge [21], as well as from herb-residue [22]. Increased Cr(VI) removal efficiency and stabilization by magnetic iron nanoparticles-assisted biochar has been reported by Zhu et al. [23]. However, the majority of these studies focused on Cr(VI) removal potential of biochar, and only a few are available that involved the evaluation of Cr(III) removal potential, which is a component of current concern in the environmental field.

In this work, we carried out a preliminary assessment of an integrated process comprising biochar-based filtration for secondary effluent TWW and subsequent microalgae cultivation. To our knowledge, this is the first attempt of integrating biochar technology with microalgal application, the latter often characterized by poor results when applied to industrial wastewater. Accordingly, the novel solution could provide an opportunity to minimize inhibitory compounds in algae cultivation, which could significantly enhance the algae productivity and biochemical composition, so that the produced biomass could be exploited for broader applications. The influence of biochar production process on trivalent chromium removal efficiency from tannery effluent was also evaluated by comparing the performances of biochar obtained using different pyrolysis temperature and feedstock. Adsorption isotherm and kinetic studies were carried out to increase the knowledge on adsorption of Cr(III) on biochar, by deepening the influence of metal and adsorbent concentration ratios, as well as the effect of operating variables.

2. Materials and methods

2.1. Experimental plan

Biochar application was tested to specifically remove chromium and other pollutants from tannery wastewater, and to assess its possible use as a pretreatment for algal cultivation in tannery wastewater. Different sets of experiments were carried out, and results are reported in the same order.

The first set of experiments was carried out to assess the applicability of a laboratory made pinewood biochar (PB) in real tannery wastewater as a pretreatment, followed by the growth of the microalga *Chlorella protothecoides*: this algal species was cultivated in such pretreated wastewater as well as in a non-treated sample, as a control. The aim of this section was to prove the applicability of biochar pretreatment to improve algal growth.

The second set of experiments was carried out to specifically test the adsorption potential of laboratory made pinewood biochar (PB) on Cr (III) adsorption, in synthetic solutions. The adsorption performances were also compared to those of a commercial biochar (CB). The adsorption equilibrium was also studied from a kinetic point of view. The experimental conditions (Cr concentration, biochar dosage and time intervals) were chosen according to a literature review [24,25]. The aim of this section was to provide information about the difference in absorption due to pyrolysis operating conditions.

Finally, the commercial biochar (CB) was tested as a pretreatment for microalgae cultivation in real tannery wastewater (third experimental set), and a comparison of the performances with those obtained in the first set of experiments was discussed. For clarity, the experiments are summarized in Table 1.

2.2. Microalgae species and cultivation set-up

Chlorella protothecoides 3380 (SAG-Goettingen), which is a widely investigated algal species for wastewater treatment applications [14,26], was grown in TWW to assess its nutrient uptake effectiveness in this medium. *C. protothecoidesis* is a facultative heterotrophic green alga that can survive in a wide variety of environments [27]. Axenic pre-inocula were maintained in BG-11 cultivation medium in Drechsel bottles under controlled temperature and light conditions. The algae wastewater treatment tests (see section 3.2) were performed in batch photobioreactors, namely 50 mm diameter Drechsel bottles with a total volume of 250 mL (Quickfit® Drechsel), for a duration of five days, starting from a microalgae concentration corresponding to an optical density OD_{750} = 0.3. The temperature of the photobioreactors was kept constant at 24 °C by placing the bottle inside a thermostatic incubator. Cultures were continuously mixed by means of a magnetic stirrer. Artificial light was supplied by means of a LED panel (warm-white), and the light intensity was regulated by varying the distance of the

Table 1
Summary of the three sets of experiments performed: the first set is related to microalgae growth in tannery wastewaters, both raw and after biochar pretreatment; the second set is related to PB and CB adsorption characterization; the third set to microalgae growth in tannery wastewaters, both raw and after biochar pretreatment.

Experimental set	Type of experiment	Experimental conditions	
1	Microalgae growth	TWW-1a TWW-1 + PBb	
2	Biochar adsorption	CBc/PB comparison	3 mg L^{-1} Cr(III) 5 g L^{-1} biochar 5 min – 25 h
		CB adsorption isotherm	1-20 mg L^{-1} Cr (III) 0.5 g L^{-1} biochar 50 min
		CB adsorption kinetics	20-3-1 mg L^{-1} Cr (III) 0.5-2-5 g L^{-1} biochar 25 h
3	Microalgae growth	TWW-2d TWW-2 + CB	

[a]first sample of tannery wastewaters; [b]Pinewood biochar; [c]Commercial biochar; [d]second sample of tannery wastewater.

photobioreactor from the light source. The photon flux (μmol photons m^{-2} s^{-1}) in terms photosynthetically active radiation (PAR, 400 − 700 nm), was measured with a photoradiometer (Delta OHM – HD 2101.1) and set at 100 μmol photons m^{-2} s^{-1}.

To avoid the growth of unwanted bacteria or microalgae strains (lab environment contamination) the photobioreactors and all the tools were sterilized in an autoclave for 20 min at 121 °C, whereas the tannery wastewater was not sterilized, so to maintain the endogenous microflora naturally present, and better exploit the CO_2/O_2 gas exchange between algae and bacteria [28]. For this reason, no external supply of air and CO_2 was provided to the cultures. All the growth experiments were performed with at least two biological replicates.

2.3. Tannery wastewater

Tannery wastewater was collected from the inlet of the industrial-urban wastewater treatment plant of Montebello Vicentino (VI), Italy, which receives wastewater from the tanneries located in the industrial leather districts of Montebello, Zermeghedo and Montorso (Vicenza, Italy), and urban influents coming from the same area. Such waste streams are then treated by conventional activated sludge, where an efficient removal of COD and nitrogen is performed. Besides the other contaminants, the issue of chromium removal is borderline, and more research is needed to lower the concentration of such compound, which, despite being under the law limits, should be reduced to contain the environmental impact.

The TWW, after primary sedimentation, was collected and stored in 1.0 L bottles and preserved at − 20 °C to limit the growth of endogenous microflora and variation of pollutants concentration. No sterilization was carried out on the medium. The TWW was characterized in terms of pH and nutrients content. Two different TWW samples (TWW-1 and TWW-2, respectively) were collected from the treatment plant in two different moments (which were used in the first and the third sets of experiments, respectively, see section 2.1). The analysis of these two samples highlighted a different composition, which was due to the inevitable variability of the wastewater inlet composition to the plant. The values measured are reported in Table 2, for both samples. Total Nitrogen (TN) values were comparable with ammonia concentrations, suggesting that nitrogen is mainly present as ammonium.

In addition, the tannery wastewater samples were analysed by ICP – OES analysis, resulting in the metals composition reported in Table 3. It should be noticed that most of the chromium present in wastewater was easily settleable, so that the soluble fraction resulted in 1.55 ± 0.10 ppm in terms of elemental chromium. The chromium present in the water was mainly in the trivalent form. The Italian law limits (D. Lgs 152/06) are 0.2 mg L^{-1} for hexavalent chromium. Thus, we refer to total chromium, but it can be reasonably assumed that the presence of hexavalent chromium is less than 0.2 mg L^{-1}, as certified by the tannery companies, which have also revamped their processes in the recent past, to avoid the application of such a highly toxic compound.

2.4. Biochar production and characterization

Laboratory produced pinewood biochar (PB), was obtained via slow pyrolysis of pinewood branches using a Parr reactor in laboratory set-up [29]. The biomass was dried in an electric oven at 105 °C for 2 days. The bark was removed, and the branches were chopped into pieces (10 mm x 20 mm). 50 g of the biomass were incubated in the reactor. The chamber was purged with nitrogen (N_2) for 5 min. The highest treatment temperature (HTT) was 400 °C for a 30 min retention time at ambient pressure. The reactor was slowly cooled with internal water coil system. The resulting biochar was collected, and its yield resulted about 35–40 % w/w.

Flash 2000 Elemental Analyzer was used to determine the carbon, hydrogen and nitrogen content of the biochar sample. For quantifying ash component approximately 0.5 g of dried sample was weighed into ceramic crucibles and incinerated overnight in a muffle furnace at 575 °C.

Fourier-transform infrared spectroscopy (FTIR) analysis was carried out: infrared spectra (4000 – 400 cm^{-1}) were recorded using Bruker Alpha, Platinum-ATR. BET analysis was carried out using NOVA 2000e surface area and pore size analyser (Quantachrome Instruments). Raw biochar samples were analysed for multipoint BET surface area using nitrogen as the adsorbing gas. The analysis involved degassing the sample at 150 °C for 4 h.

Another type of biochar (CB) was commercially procured by “New Hampshire Biochar – The Charcola Group”. According to the manufacturer, mixed feedstock of hardwood and softwood such as maple, birch, pine etc. were used to produce this biochar at 500 °C via slow pyrolysis method. Biochar was passed through 0.02 − 0.17 μm sieves prior to its use in the experiment.

2.5. Application of biochar as a pretreatment for microalgal cultivation

In the first and third sets of experiments, PB and CB, respectively, were used as preliminary filtration step before microalgae cultivation in real TWW. For each treatment, the amount of biochar needed was powdered in a mortar grinder, weighted, and added to the TWW. The biochar was maintained in suspension placing the test tube on a laboratory orbital shaker. After the treatment, biochar was separated from the liquid phase by vacuum filtration using a paper filter with a pore diameter of 0.8 μm. The filtrate was collected and analysed. For biochar treatment experiments the volume used was about 100 mL for each single experiment.

2.5.1. Growth measurement

Microalgal/bacterial growth was monitored daily from each wastewater treatment test. Optical density (OD) was measured with a spectrophotometer (Spectronic Unicam UV-500® UV–vis, UK) at a wavelength of 750 nm. Total suspended solids (TSS) concentration were measured as dry weight, by filtering a fixed volume of sample using 0.45 μm (Whatman®, UK) filters. The pre-weighed filters were dried for 2 h at 105 °C. As these analyses do not distinguish between microalgae or bacteria contributions, *C. protothecoides* growth was analysed by cell count with a Bürker chamber, to account for microalgae growth only. Specific growth rate (μ) of microalgae was obtained by the linearization of exponential data in semi-logarithmic graph of cell concentration, according to Malthus model:

$$\ln(C_x/C_{x,in}) = \mu t \quad (1)$$

where C_x is the biomass concentration, $C_{x,in}$ is the initial concentration and t the time considered.

2.5.2. Analytical procedures

To evaluate the TWW treatment performances, initial and final concentration of pollutants were measured for each test. Chemical

Table 2
pH and nutrients average concentrations of filtered TWW (mg L^{-1}).

	pH	COD	N-NH_3	P-PO_4	Cr (total, soluble fraction)
TWW-1	8	1104 ± 21	151 ± 1	1.62 ± 0.32	1.653 ± 0.273
TWW-2	7.67	2,133 ± 78	2,218 ± 12	1.68 ± 0.2	2.139 ± 0.001

Table 3
ICP-OES analysis of tannery wastewater of the two water samples, TWW-1 and TWW-2 respectively.

Element	Average concentration (ppm)		Element	Average concentration (ppm)	
	TWW-1	TWW-2		TWW-1	TWW-2
Ag	0.007 ± 0.001	0.0028 ± 0.05	Mn	0.039 ± 0.007	0.138 ± 0.003
Al	nd	0.0214 ± 0.005	Mo	nd	nd
As	nd	0.0184 ± 0.001	Na	> 1005	90.8
B	0.189 ± 0.045	nd	Ni	0.027 ± 0.026	nd
Ba	0.002 ± 0.002	nd	P	2.093 ± 1.007	2.67 ± 0.04
Be	0.007 ± 0.001	nd	Pb	nd	0.018 ± 0.04
Ca	61.190 ± 23.905	169.92 ± 0.02	S	> 530	> 600
Cd	nd	nd	Sb	0.179 ± 0.028	0.396 ± 0.028
Ce	nd	nd	Se	nd	0.046 ± 0.01
Co	nd	nd	Si	nd	0.455 ± 0.018
Cr	1.653 ± 0.273	2.139 ± 0.001	Sn	0.050 ± 0.003	0.013 ± 0.003
Cu	nd	nd	Sr	0.140 ± 0.048	0.59 ± 0.048
Fe	0.160 ± 0.018	1.3 ± 0.004	Te	0.140 ± 0.081	0.087 ± 0.081
Hg	nd	nd	Ti	0.005 ± 0.002	0.025 ± 0.002
K	46.130 ± 9.247	68.84 ± 0.026	Tl	nd	nd
Li	0.008 ± 0.001	0.011 ± 0.001	V	0.025 ± 0.005	0.025 ± 0.005
Mg	41.957 ± 4.817	76.6 ± 0.03	Zn	nd	0.081 ± 0.005

Oxygen Demand (COD), Orthophosphates (P-PO_4), Ammonia (N-NH_3), Nitrites (NO_2) and Nitrates (NO_3) concentrations were measured with a spectrophotometer, based on colorimetric tests. COD concentration was assessed by a colorimetric method based on the oxidation of organic and inorganic compounds by potassium dichromate ($K_2Cr_2O_7$) in acid conditions. In addition to the latter, the reagent also contains sulfuric acid (H_2SO_4), which works as a catalyst, and mercury sulphate ($HgSO_4$) which prevents interferences due to the presence of chloride ions. Absorbance at 445 nm of a sample reacted for 2 h at 148 °C were then obtained. Orthophosphates were analysed with the molybdate/ascorbic acid method. The colorimetric reaction took place between orthophosphate ions and molybdenum, under reducing conditions, resulting in a blue complex, whose absorbance was measured at 705 nm after 10 min reaction at room temperature. Ammonia concentration was evaluated by measuring the absorbance at 445 nm of a sample reacted for 5 min at room temperature, using a standard test kit (Hydrocheck Spectratest, id 6201), which involves a colorimetric reaction between ammonium ions and the Nessler's solution. Nitrates were evaluated using standard test kits (Hydrocheck Spectratest, id 6227), according to the Griess test, and measuring the absorbance at 520 nm of the sample after 8 min reaction at room temperature. Nitrates analysis was carried out by measuring the absorbance at 445 nm of the sample, reacted for 10 min at room temperature with a standardized volume of powder reagent available in a standard test kit (Hydrocheck Spectratest, id 6223). Metals concentration was measured by inductively coupled plasma optical emission spectrometry (ICP-OES, AMETEK® - SPECTRO GENESIS).

2.6. Batch adsorption experiments with biochar

In the second set of experiments, biochar adsorption performances were characterized in synthetic medium to better understand their trivalent chromium adsorption capabilities. Chromium nitrate, Nonahydrate nitric acid chromium salt (chemical formula - CrN_3O_9; molecular weight – 238.01 g mol^{-1}) supplied by Fisher Scientific, IL, USA, were used for the synthetic medium. The stock solutions of 1 g/L Cr(III) were prepared by dissolving 4.577 g CrN_3O_9 in 1 L DI water. All other chemicals used were of analytical reagent grade. All experiments were carried out in two replicates.

2.6.1. Comparison between adsorption potential of CB and PB

Two reactors were set: one having CB as adsorbent and another one with PB. Each reactor had a 125 mL volume of 3 mg L^{-1} Cr(III) solution (i.e. 0.375 g Cr(III) in total), with 5 g L^{-1} dosage of adsorbent. The concentration of biochar was selected based on the survey of previous literature [24,25,30]. All mixtures were shaken at 180 rpm. Samples were collected at 5 min, 20 min, 40 min, 60 min, 180 min and 25 h using PVDF filter (0.22 μm). Results will be presented in the results and discussion section. Control (no biochar) and blank [no Cr(III)] samples were simultaneously carried through with the adsorption samples.

2.6.2. Batch adsorption isotherm experiment

To investigate the best fitted adsorption isotherm, different reactors with 125 mL of Cr(III) solution having concentration starting from 1 mg L^{-1} to 20 mg L^{-1}, with 0.5 g L^{-1} of biochar dosage at each were set. All mixtures were shaken at 180 rpm. After 50 min. of adsorption equilibrium samples were collected passing through 0.22 μm filter. All experiments were performed in duplicate. The amount of Cr(III) removed by adsorption was calculated using the following equation:

$$q_e = \frac{V(C_0 - C_e)}{M} \quad (2)$$

where q_e is the amount of Cr(III) removed per gram of biochar, C_0 and C_e are the initial and equilibrium Cr(III) concentrations (mg L^{-1}) in solution, V is the solution volume (L), and M is the weight of biochar (g).

Adsorption isotherm can estimate the adsorption capacity and provide knowledge of the physicochemical phenomena involved in the process. Isotherm can describe the equilibrium relationship between adsorbate and the adsorbent surface. Langmuir, Freundlich, Temkin, Dubinin–Radushkevich (D–R), BET adsorption isotherms are some of the commonly used ones. In this study, Langmuir and Freundlich isotherm models were tested to fit the data, as they are the most commonly used to fit the isotherm equilibrium data of heavy metals sorption on biochar. The Langmuir isotherm can be articulated as:

$$\frac{C_e}{q_e} = \frac{C_e}{q_m} + \frac{1}{q_m b_L} \quad (3)$$

q_e = Amount of Cr(III) adsorbed (mg/g)

C_e = Equilibrium solution concentration of Cr(III) (mg/L)

q_m = Langmuir constant related to the maximum adsorption capacity (mg/g)

b_L = Langmuir constant related to the energy of adsorption (L/mg)

A plot of C_e/q_e versus C_e will give a straight line with a slope of $1/q_m$ and intercept $1/q_m b_L$. The Freundlich equation can be expressed as:

$$\log q_e = \log K_f + \frac{1}{n}\log C_e \quad (4)$$

where q_e is the amount of Cr(III) adsorbed (mg/g), K_f is the Freundlich constant related to the relative adsorption capacity of the adsorbent

(mg/g) (mg/L)^n, *1/n* is the heterogeneity factor which is related to the capacity and intensity of the adsorption and C_e the equilibrium solution concentration of Cr(III) (mg/L). A plot of (log q_e) versus (log C_e) will give a straight line with a slope of *1/n* and intercept of (log K_f).

2.6.3. Batch adsorption equilibrium experiment

Batch kinetic experiments involved using three different biochar dose (0.5 g L^{-1}, 2 g L^{-1} and 5 g L^{-1}) and initial Cr(III) concentration (20 mg L^{-1}, 3 mg L^{-1} and 1 mg L^{-1}). Experiments were carried out for 25 h and samples were collected at regular intervals after filtering through 0.22 μm filter. Both experiments had duplicate reactors for each sampling interval. To investigate the possible adsorption mechanism and to analyse the rate of adsorption of Cr(III) on biochar, pseudo first-order and pseudo second-order kinetic models were applied to the adsorption data.

2.7. Statistical analysis

t-student tests were applied to ascertain meaningful differences in nutrient removal with respect to the initial concentration of the wastewater and in specific growth rates of *C. protothecoides* with and without the biochar pretreatment. The level of statistical significance was assumed for $p < 0.05$, and significantly different results are highlighted with an asterisk in the figures. P-values are reported in the text when the corresponding results are discussed.

3. Results and discussion

3.1. Effect of biochar application on tannery wastewater and as a pretreatment for algae cultivation

Pinewood biochar (PB) was used to assess its possible exploitation as an adsorbent in TWW for metals removal, based on the results of a previous study reporting good performances in synthetic solutions [17]. The effects of its application were evaluated by varying the operating conditions, such as contact time and amount of biochar added. The results showing the effect of contact time on relevant metals concentrations, obtained using a biochar concentration of 5 g L^{-1}, are reported in Fig. 1. It is seen that after 5 min of contact about 34 % of the total chromium was removed by the biochar ($p = 0.01$), and that longer contact times did not result in improved performances (Fig. 1A). Besides chromium, other metals present in the tannery wastewaters were found to be affected by the treatment, as reported in Fig. 1B. Metals such as Ni were reduced by 60 % ($p = 0.009$), which could be beneficial for the subsequent algal growth, while K and P were found at slightly higher concentrations after biochar pretreatment.

Additional experiments were carried out by changing the amount of biochar added to the wastewater, ranging between 5 − 50 g L^{-1} (Figure S1, Supplementary Material). No differences were found among the different treatments, resulting in chromium removal values very close to the ones reported in Fig. 1, suggesting that a biochar concentration of 5 g L^{-1} was indeed sufficient, and there could be some other limitation to a higher removal, possibly related to the complexity of the wastewater (see Section 3.5 for detailed discussion). The effect of pH was also assessed, without significant total Cr removal improvement, in the range of viability of microalgae (data not shown). The residual chromium content in the water, even if lower than the current law limit, still represents an environmental issue. In fact, the concerns about the possible effects of releasing such amount of chromium into the environment has led to the resolution of strongly reduced law limits, corresponding to 50 μg L^{-1} of total chromium and 10 μg L^{-1} of the hexavalent form for drinkable water [Dlgs 31 − 2001, https://www.camera.it/parlam/leggi/deleghe/testi/01031dl.htm]. Thus, new methodologies should be applied to accomplish these constraints, starting from the reduction of environmental inputs of the metals in wastewater treatment facilities.

According to the perspective of applying biochar filtration as a first pretreatment for subsequent algal-bacteria cultivation, COD, ammonium and nitrates concentration was also evaluated before and after the adsorption step (Fig. 2). COD and ammonium were not affected by the treatment, while a slight decrease of N-NO_3 was observed at higher contact times. However, the concentration of N-NO_3 was negligible compared to the ammonium form, so that overall soluble nitrogen can be considered almost constant. The only nutrient that was significantly affected was phosphorus, whose concentration, as reported in Fig. 1B, was found increased after biochar treatment ($p = 0.007 - 0.024$ at different contact times). This might indeed possibly have a beneficial effect on the subsequent microalgal growth. This behaviour with respect to nutrients adsorption is in agreement with what reported by other researchers. For example, Zhou et al. [31] reported limited adsorption or even released NO_3^- and P, which is in agreement also with the findings of Zhang et al. [32]. It is suggested that an electrostatic repulsion occurs between the negatively charged surface of biochar and negatively charged NO_3^- and P ions, which makes it difficult for these compounds to be adsorbed. Concerning organic compounds, Kwarciak-Kozłowska et al. [33] found a COD adsorption percentage of 53 %, with a heavy metals adsorption rate up to 96 % from landfill leachate. A possible explanation for the reduced adsorption could be the high affinity of heavy metal ions to biochar compared to COD, ammonium and nitrates. In particular, in this study, pores might be quickly occupied by Cr(III), leaving no binding site available for other compounds. Overall, it can be concluded that adsorption of dominant species/compounds

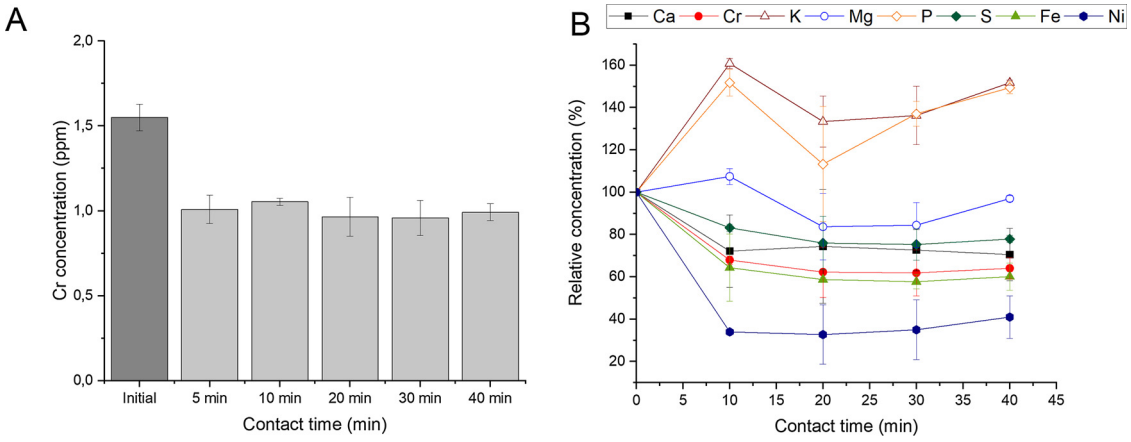

Fig. 1. Metals concentration in tannery wastewaters (TWW-1) as a function of biochar contact time: chromium absolute concentration (A), and other metals relative concentration (B) (see Table 3 for initial concentrations). Error bars represent standard deviation of triplicates.

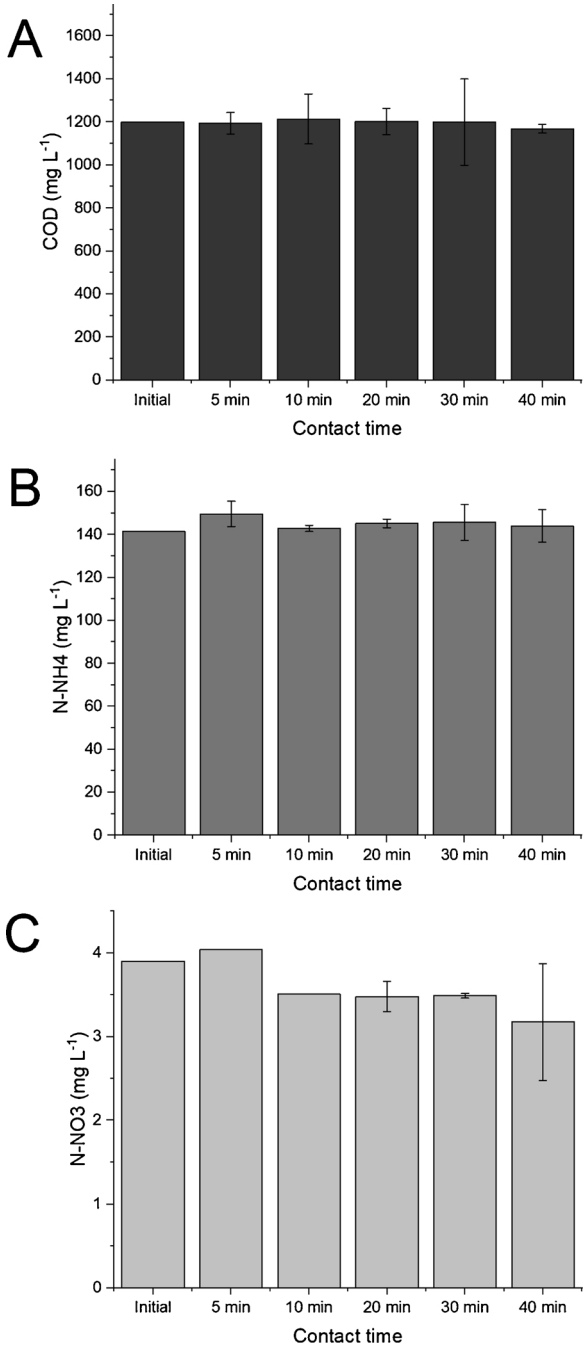

Fig. 2. COD (A), ammonium nitrogen (B) and nitrate nitrogen (C) in tannery wastewater as a function of biochar contact time. Error bars represent standard deviation of triplicates.

requires systematic analysis, which will depend on the type of wastewater and origin of contaminants, as well as on the characteristics of the specific biochar.

After characterizing the adsorption performances of PB on real TWW, its potential as pretreatment for microalgal cultivation was tested. The microalgal species used was *C. protothecoides* which was firstly cultivated in raw tannery wastewater (Fig. 3) to assess the growth performances in this complex substrate. The growth obtained in such medium (0.59 ± 0.02 d^{-1}) was significantly slower compared to the values that are typically reported for this microalgal species in standard synthetic media (about 1 d^{-1}) [34,35].

Thus, even though the species was able to grow in tannery wastewater as such, some inhibition phenomena occurred. Interestingly, a

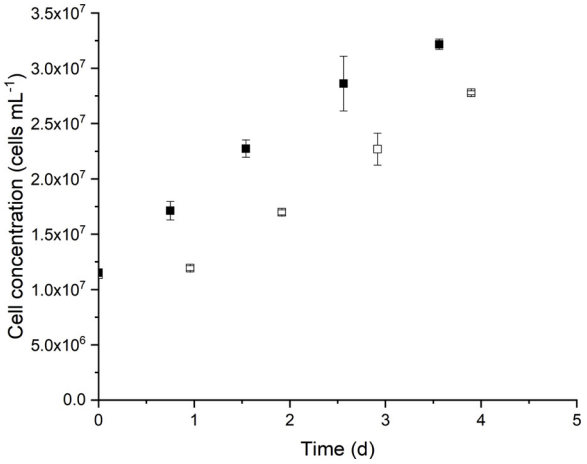

Fig. 3. Growth of *Chlorella protothecoides* in raw tannery wastewaters (TWW-1) (open dots) and after biochar (PB) pretreatment (black dots). Error bars represent the standard deviation of the two biological replicates.

remarkable improvement of the growth rate was observed when microalgae were cultivated after the pre-treatment of the tannery wastewater with biochar, as shown in the same figures. In fact, the growth rate increased from 0.59 ± 0.02 to 0.95 ± 0.02 d^{-1} ($p = 0.002$), very close to the values reported for synthetic media. This suggests that biochar filtration was effective in reducing the concentration of inhibitory compounds in industrial wastewater. It is not clear yet which kind of molecules may have caused the inhibition of microalgal growth, but the improvement in growth rate after biochar treatment is promising in view of a combined application for industrial wastewater treatment. In addition to increased growth rate, the biochar pre-treatment allowed also to partially remove Cr from the medium, hence reducing the amount eventually uptaken by the microalgal biomass.

Nutrients removal was also monitored (Fig. 4): the application of biochar pre-treatment resulted in a slightly increased biological removal, especially for nitrogen, which increased from 38 % to 49 % ($p = 0.022$). This was in agreement with the increased growth reported in Fig. 3. The initial concentration of about 3 mg L^{-1} of $N\text{-}NO_3$ remained constant for all the treatments, suggesting that no nitrification occurred. COD and P removal were instead not significantly affected by the treatment. However, COD removal was also carried out by the endogenous bacteria, while P removal was high in both cases (83 %), as microalgae are very efficient in uptaking this nutrient in a wide variety of environmental conditions [36].

3.2. Biochar characterization: the importance of the biochar properties

As reported in the previous section, the PB biochar was effective as a pretreatment for algal cultivation, but showed a reduced removal of metals, in particular chromium, even though previous studies showed an efficient removal of such a compound. [17] It should be highlighted that the chromium present in TWW is the trivalent one, while usually the adsorption capability reported by other authors is related to the hexavalent species. In this regard, Tan et al. [37]. Reported that adsorption of Cr(III) is stronger compared to Cr(VI). They suggested one of the reasons behind this phenomenon is the higher cation exchange properties of Cr(III) compared to Cr(VI). Of the Ca and Mg elements that are present in the biochar as CaO and MgO forms, some contribute in buffering the pH of the solution, while another portion takes part in cation exchange with Cr^{3+} and H^+, which are hence removed from the solution. Cr(VI) species are instead negative ions ($HCrO_4^-$ and CrO_4^{2-}), and as a result cannot take part in cation exchange. They proved this hypothesis by observing a lower concentration of released Ca^{2+} at equilibrium with Cr(VI) solutions compared to Cr(III). Another reason could be related to $Cr(OH)_3$ precipitation at higher pH, whereas Cr(VI)

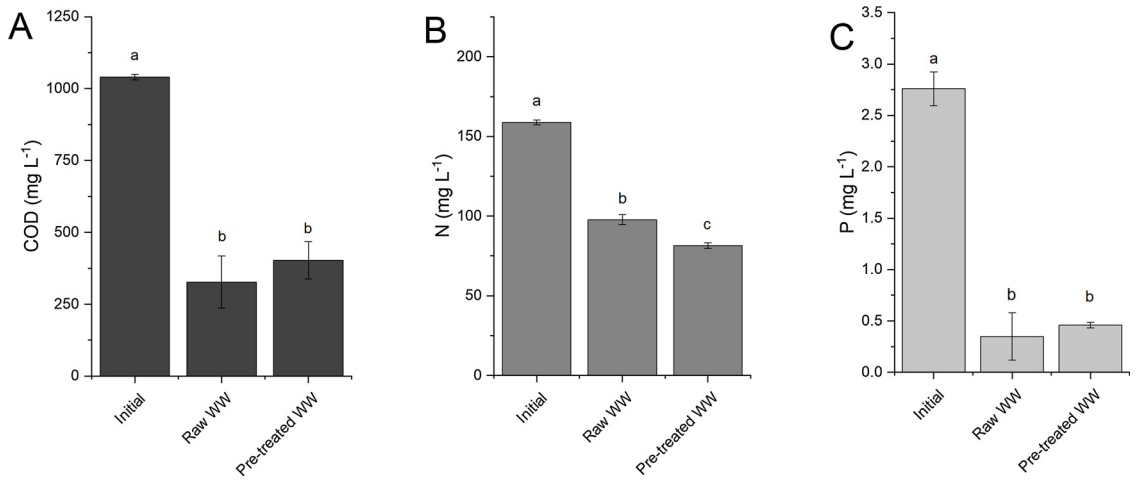

Fig. 4. Nutrient removal from raw and biochar pre-treated tannery wastewaters (TWW-1) by *C. protothecoides*: COD (A), total nitrogen (TN) (B) and phosphorus (C). Different letters indicate statistically different results ($p < 0.05$). Error bars represent standard deviation of triplicate sampling of two biological replicates.

does not precipitate regardless of change of pH.

A possible explanation of reduced removal might be related to the complexity of the wastewater, which contained a huge amount of organic compounds, as well as other metals, possibly causing a competition in the adsorption efficiency of the biochar. To further investigate the possible reasons for reduced Cr adsorption in real tannery wastewaters, it was decided to carry out some additional tests at lab scale, using a synthetic medium with dissolved Cr(III) salts (see section 2.6). Moreover, to investigate whether the type of biochar and its physiochemical properties could be affecting the adsorption performances, PB was compared to a commercial biochar (CB), having different characteristics in terms of raw materials and operating conditions used for their production. The elemental composition and surface area of the two types of biochar is given in Tables 4 and 5 A shows the FTIR (Fourier-Transform Infrared Spectroscopy) spectra of CB. The spectra demonstrate the presence of several oxygen containing functional groups in biochar. The peaks that can be identified and designated were aromatic C═C (~1418 cm-1), aromatic carbonyl/carboxyl C═O, phenolic −OH (~1027 cm-1) and aromatic −CH (~872 cm-1). Fig. 5B shows the FTIR spectra of pinewood biochar (PB). The peaks that can be identified and designated were aromatic C═C (~1585 cm^{-1}), asymmetric stretching of COO- (~1429 cm^{-1}) and peak at ~1171 cm^{-1} can be corresponding to R−OH and phenol groups.

3.3. Adsorption kinetics

Fig. 6 shows the comparative removal percentage of Cr(III) using CB and PB: commercial biochar was able to remove ~99.6 % Cr(III) within 5 min. ($p = 0.22$), whereas the laboratory made pinewood biochar showed ~83.4 % removal after 1500 min (3 h) ($p = 0.16$). However, after 25 h, both of the biochar showed almost similar removal efficiency. Varying surface functionality (carboxylic and other oxygen-containing functional groups) of biochar attributed from feedstock and pyrolysis temperature can play an important role in this regard. Further investigation of this phenomenon could be the scope of future work. It was evident from these studies that CB was more efficient in removing Cr(III) compared to the PB which was utilized for the preliminary investigation.

Table 4
BET Surface area and elemental composition of biochar.

Component name	Commercial biochar (CB)	Pinewood biochar (PB)
Surface area (m^2/g)	285.40	2.10
Ash content (%)	35.48	3.99
Nitrogen	0	< 0.50
Carbon	44.59	81.60
Hydrogen	1.01	2.69
Sulphur	0	0
Oxygen	18.93[a]	15.71[b]
H:C Molar Ratio	0.07	0.15
O:C Molar Ratio	0.16	0.07

[a,b]Determined by differences after retrieving data from CHNS analyzer.

Li et.al. [38] proposed that five basic mechanisms are responsible for heavy metal adsorption on biochar, such as complexation, cation exchange, precipitation, electrostatic interactions and chemical reduction. There is not much research conducted on adsorption of Cr(III) on biochar compared to Cr(VI). However, according to the limited studies available, three basic mechanisms are suggested to be responsible for Cr (III) adsorption on biochar: (a) complexation with oxygen containing functional groups, (b) cation exchange, and (c) electrostatic interaction between Cr(III) ions and biochar [39]. Higher O:C ratio corresponds to the presence of native negative charge from oxygen functional groups [29,40], which can play an important role in creating complexation with positively charged metal ions [41]. O:C was slightly lower for PB compared to CB, which can be related to the lower Cr(III) removal potential of the former compared to that of CB. During the batch experiment, it was observed that the solution pH having CB was slightly higher (8.38) compared to the solution pH having PB (7.18). This little increase could be due to the release of CaO and MgO into the solution upon adding biochar, which suggest that cation exchange could also play some role. Chen et al., and Qian et al., observed a similar phenomenon in their studies [37,42]. According to studies conducted by other researchers, sorption of Cr(III) increases with increasing solution pH [30,43]. Lower solution pH indicates higher H^+ concentration, which can take part in creating electrostatic attraction of positively charged Cr(III) species with negatively charged biochar. However, in this study, the presence of CB in solution inhibited the increase of solution pH beyond 7 (8.38) which might rule out the possibility of sorption of Cr(III) through electrostatic interaction.

It is evident from this discussion that O:C ratio and solution pH seem to have minimal effect in Cr(III) sorption in this study. It can be concluded that the extremely high surface area of CB (approximately 2 orders of magnitude higher i.e., 285.40 m^2/g vs. 2.10 m^2/g) governs the overall sorption capacity. This variation happened mainly due to the difference in feedstock and pyrolysis temperature adopted in the production of biochar.

Accordingly, the following investigations were carried out with respect to the CB only. Onward, a complete set of batch adsorption experiment was conducted to evaluate the best fitted adsorption model and kinetics. The Langmuir and Freundlich isotherm models were used

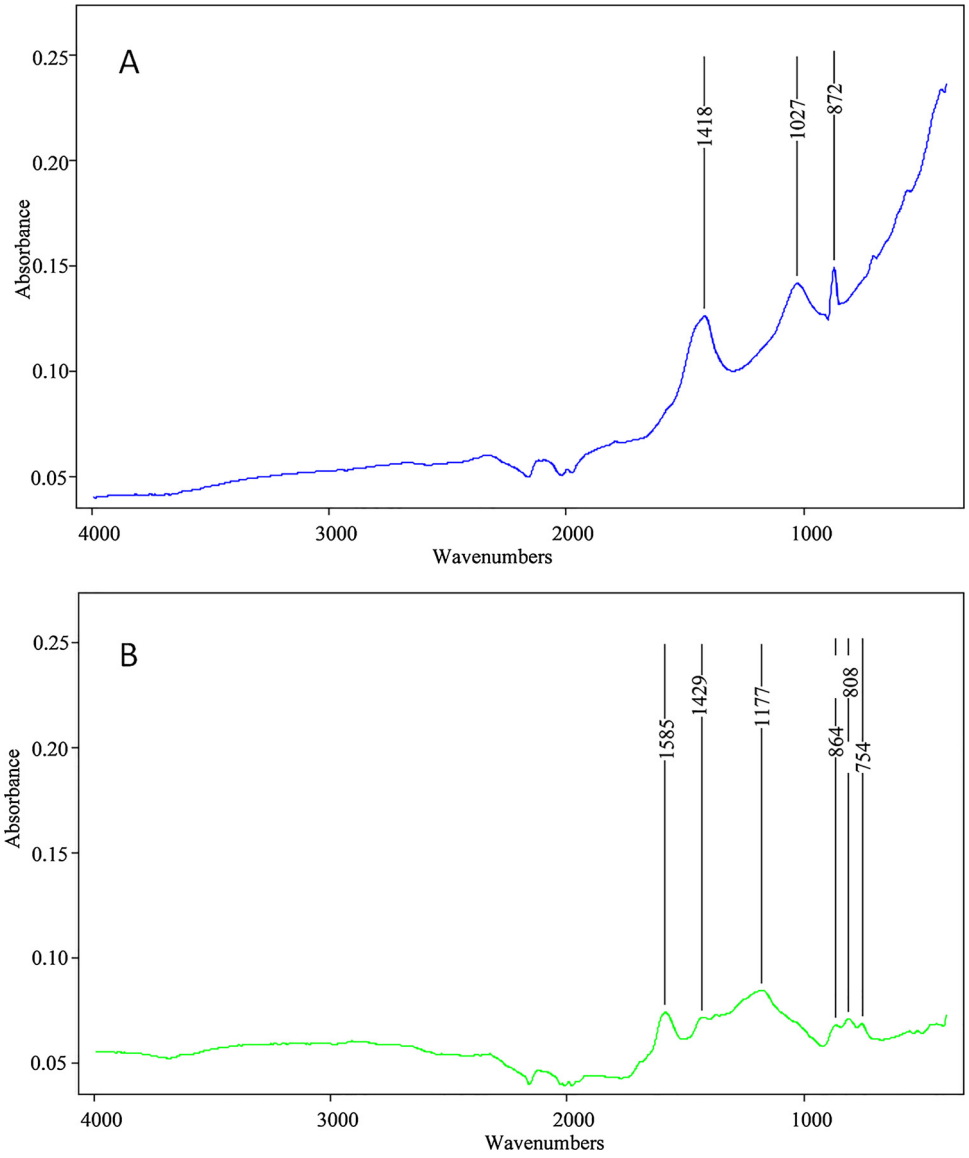

Fig. 5. FTIR spectra of (A) commercial biochar (CB), and (B) pinewood biochar (PB).

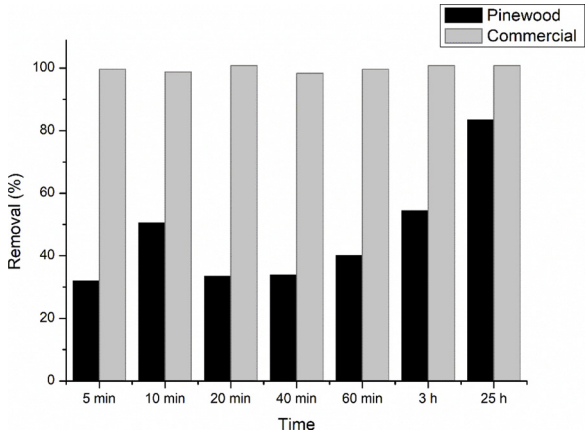

Fig. 6. Cr(III) removal using commercial and laboratory-made pinewood biochar as a function of contact time.

to investigate the sorption isotherms of Cr(III) adsorption (see Section 2.6.2). The Langmuir isotherm model assumes that adsorbate molecules occupy only one active site on adsorbent surface. It also assumes that maximum adsorption happens in monolayer form, which means that molecules of adsorbate are adsorbed only on the free surface of adsorbent and there is no interaction between adsorbed molecules [44]. On the other hand, the Freundlich model assumes that adsorption happens on a heterogeneous adsorbent surface by multilayer adsorption. The isotherms derived from the Langmuir and Freundlich models for sorption of Cr(III) on CB are shown in Figs. 7 (A) and (B) respectively.

The parameters obtained from the Langmuir and Freundlich models are listed in Table 5. The values of the correlation coefficients (R^2) for the Langmuir model was 0.98 ($p = 0.056$) and for the Freundlich model was 0.99 ($p = 0.008$). According to Table 5, it can be said that the linear fits using the two equations were good for explaining the adsorption, but the fit with Freundlich isotherm model was relatively better. This suggests that biochar surface has some heterogeneity and sorption happens in multilayer. The n value ($n = 2.7$) indicates that adsorption of Cr(III) on biochar for this study is a physical process which is in agreement with other literatures [45,46].

The effect of adsorbent dosage was also evaluated, and the results for the Cr(III) uptake using various amounts of CB (0.5, 2 and 5 g/L) are shown in Fig. 8 (A).

The equilibrium Cr(III) uptake capacity (q_e) was found to decrease

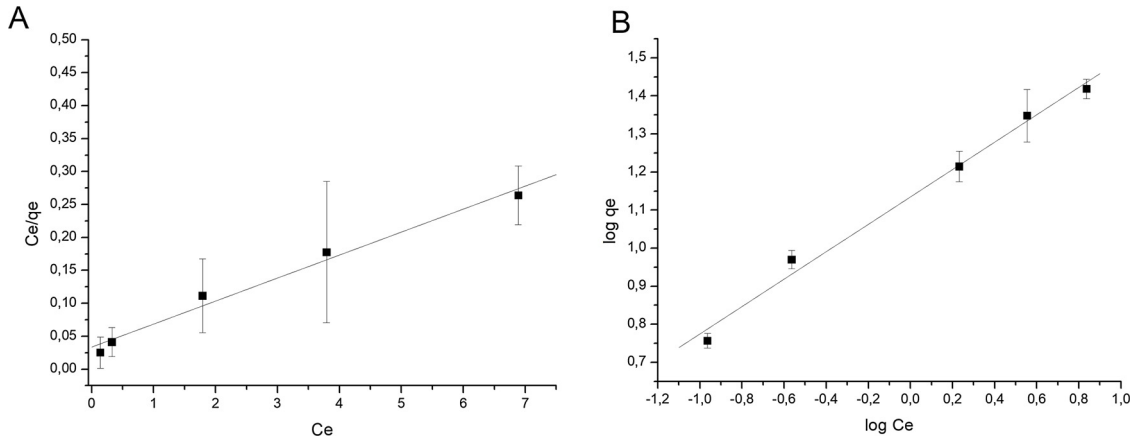

Fig. 7. A) Langmuir and B) Freundlich model for adsorption of Cr(III) onto CB (solution volume = 125 mL, adsorbent dose = 0.0625 g, initial Cr(III) concentration = 1 – 20 mg/L, contact time = 50 min, T = 25 °C. Error bars represent the standard deviation of the two replicates and straight lines represent linear trendlines.

Table 5
Langmuir and Freundlich parameters for Cr(III) adsorption on CB.

Model	Langmuir			Freundlich		
Parameters	q_m(mg/g)	b_L(L/mg)	R^2	K_f(mg/g) (mg/L)^n	1/n	R^2
Values	28.65	1.04	0.98	13.64	0.36	0.99

(4.31 to 0.6 mg/g) with an increase in the dosage of the adsorbent. On the other hand, removal rate of Cr(III) increased (from 71.77% to 100%) with the increase of adsorbent dose ($p = 0.004$). This can be explained by the hypothesis that increased adsorbent dose provided increased number of available bonding sites for adsorption, which in turn reduced the adsorption capacity per bonding site [19].

Accordingly, the effect of initial chromium concentration was assessed, and Cr(III) adsorption with varying Cr(III) concentration is presented in Fig. 8(B). It is evident that the equilibrium adsorption capacity of Cr(III) on CB increased from 0.19 to 3.9 mg/g with the increase of initial Cr(III) concentration ($p = 0.003$). This indicates that initial ion concentration plays an important role to overcome mass transfer resistance of metal ions between solid and liquid phase. The change in equilibrium adsorption capacity with contact time was also studied at given different initial concentrations ranging from 1 to 20 mg/L. Results are shown in Fig. 9.

Cr(III) adsorption was rapid for the first 50 min, and continued at a slower rate afterwards till it reached equilibrium ($p = 0.004 - 0.011$ at different initial concentration). Equilibrium adsorption capacity increased with the increase of initial Cr(III) concentration.

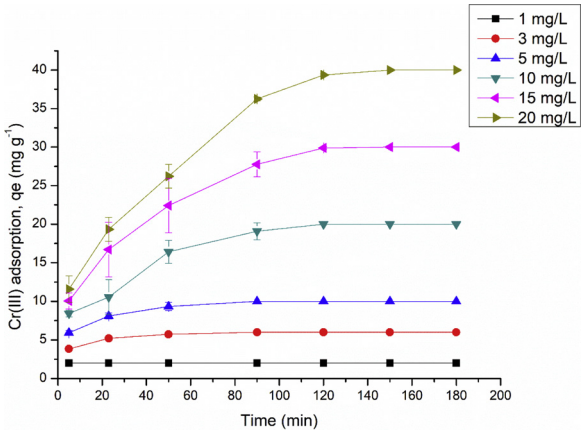

Fig. 9. Effect of initial Cr(III) concentration and contact time on Cr(III) adsorption.

3.4. Kinetic model of adsorption of trivalent chromium by CB

Different kinetic models can be employed to investigate the rate-control mechanism of Cr(III) adsorption on CB. In this study, pseudo-first order and pseudo-second order were evaluated. The linear form of pseudo-first order kinetic equation is

$$\ln(q_e - q_t) = \ln q_e - k_1 t \quad (5)$$

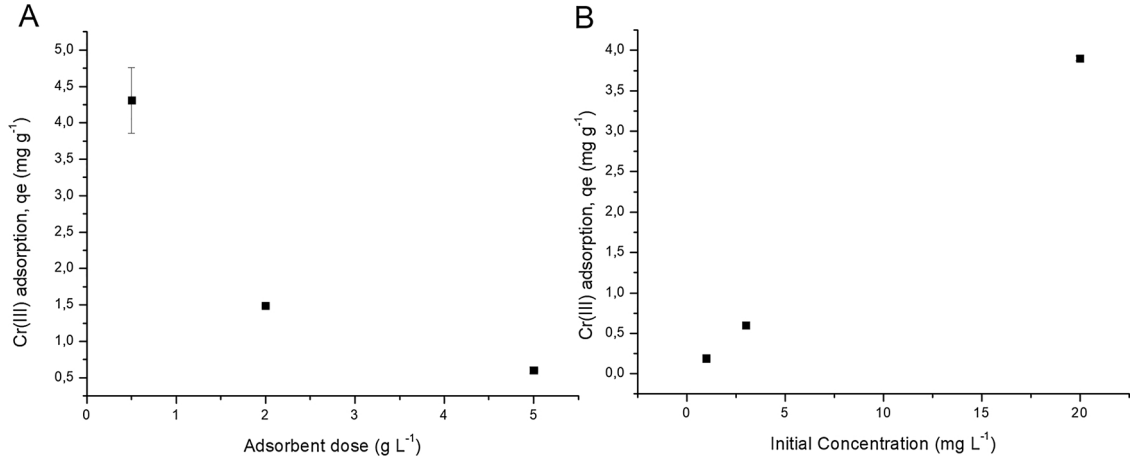

Fig. 8. Effect of A) adsorbent dose and B) initial concentration on the removal of Cr(III). Error bars represent the standard deviation of the two replicates.

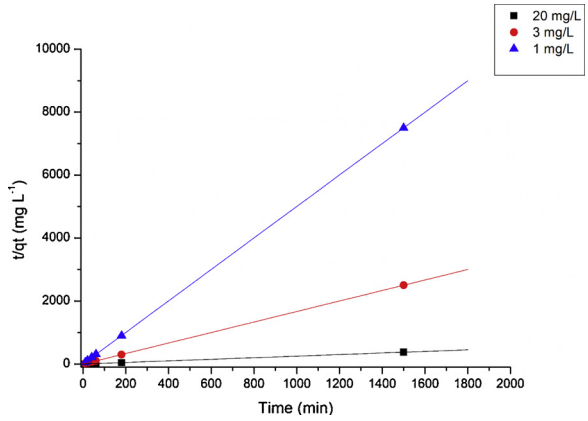

Fig. 10. Pseudo-second order kinetic for adsorption of Cr(III) on CB. Straight lines represent linear trendlines.

The linear form of pseudo-second order kinetic equation is:

$$\frac{t}{q_t} = \frac{1}{k_2 q_e^2} + \frac{t}{q_e} \quad (6)$$

Here, q_e is the amount of Cr(III) adsorbed onto the adsorbent at equilibrium (mg/g), q_t is the amount of Cr(III) adsorbed at any time t (mg/g), and k_1 (min^{-1}) and k_2 are the rate constant of the pseudo-first order and pseudo-second order kinetic adsorption respectively which can be calculated from the slope of the linear plot of $\ln(q_e - q_t)$ and t/q_t vs. t. Fig. 10 represents the fit of pseudo-second order kinetics models to the adsorption of Cr(III) by CB.

The calculated value of k_1, k_2, q_e and their corresponding correlation coefficient values (R^2) are presented in Table 6. R-squared describes the proportion of the variation in the dependent variable explained by the independent variables whereas adjusted R-squared explains the statistic based on the number of independent variables in the model. For the best estimate of the linearity, multiple regression analysis have been conducted and adjusted R^2 values have been reported here.

The regression coefficients for the models show that pseudo-second order kinetic model fitted best with adsorption data. When pseudo-first order kinetic equation was applied to describe Cr(III) adsorption, the equilibrium adsorption capacity (q_e) of CB were calculated to be 0.11 mg/g for 20 mg/L initial Cr(III) concentration and 0.033 mg/g for 3 mg/L initial Cr(III) concentration which were significantly lower than the experimental values of 3.90 mg/g and 0.60 mg/g respectively. Therefore, the pseudo-first order model is not applicable for Cr(III) adsorption on CB. Hence, the kinetic adsorption data were further employed to pseudo-second order kinetic model and it was found that this model predicted the values of equilibrium adsorption capacity as 4 mg/g and 0.6 mg/g for 20 mg/L and 3 mg/L initial Cr(III) concentration respectively which almost accurately match with the experimentally acquired values. Therefore, it could be stated that chemisorption might be the rate-limiting step of Cr(III) adsorption on CB. It can also be shown that the values of k_2 decreased with the increase of initial Cr(III) concentration. This was because when initial concentration increases it takes longer time to reach equilibrium, hence the rate constant decreases.

Table 6
Pseudo-first order and pseudo-second order kinetic parameters for Cr(III) adsorption on CB.

C_0	Experimental	Pseudo-first order			Pseudo-second order		
(mg/L)	Calculated				Calculated		
	q_e (mg/g)	k_1 (min^{-1})	q_e (mg/g)	R^2	k_2(g mg^{-1} min^{-1})	q_e (mg/g)	R^2
20	3.90	−0.002	0.11	0.152	0.155	4	0.99
3	0.60	−0.002	0.033	0.2197	10.59	0.6	0.99
1	0.19	N/A	N/A	N/A	3.52	0.2	0.99

3.5. Application of CB as pretreatment for algal cultivation

Having verified that CB outperformed PB in terms of Cr(III) adsorption in synthetic waters, its adsorption capabilities were tested on real tannery wastewater, to assess its possible application as a pretreatment for algae cultivation. In this case, the tannery wastewater sample showed different characteristics compared to the previous one: TWW-2 were found particularly polluted, with higher content of nutrients and metals compared to TWW-1, as reported in Table 2 and 3.

Generally, it appeared that different metals were adsorbed from the tannery wastewater by the CB, compared to PB (see Section 3.1): Al, As, Ni, S, Na, Si were partially removed by the application of CB (10 g L^{-1} for 30 min), as well as Fe and Ca, which was removed as in the case of PB. A slight increase of K and Mg was observed, but also a reduction of P, which was not observed previously with PB. No significant differences were instead found for the other metals analysed. Concerning chromium, a removal from 2.14 mg L^{-1} to 1.2 mg L^{-1} was observed, accounting for 44 % reduction of the initial TWW content. This result is lower than that expected based on previous adsorption experiments carried out in synthetic medium, which is certainly due to the complexity of the wastewater used. In fact, part of the COD was removed by the application of biochar, suggesting competition of organic matter to the biochar adsorption capabilities.

On the other hand, the application of biochar on TWW-2 showed similar results on the cultivation of *C. protothecoides*, as reported in Fig. 11. It should be noticed that the higher pollution level of the TWW-2 caused a strong reduction of the growth capabilities of microalgae in the raw wastewater with respect to that obtained in TWW-1, with a growth rate of about 0.23 ± 0.001 d^{-1}, and cell death after 3 days. On the opposite, the application of biochar pretreatment showed an increase of the growth rate up to 0.52 ± 0.06 d^{-1} ($p = 0.024$), suggesting that the application of biochar was beneficial even in highly polluted waters.

Nutrients removal was affected by the different microalgae growth in the two cases, as reported in Supplementary Materials (Figure S2). In particular, COD removal did not change as a consequence of biochar pretreatment, and was equal to 64 ± 1% in both cases. On the other hand, N and P removal improved from 14 % to 34 % ($p = 0.079$) and from 73 % to 88 % ($p = 0.046$), respectively, thanks to biochar pretreatment. It should be noted that the N concentration in TWW-2 was

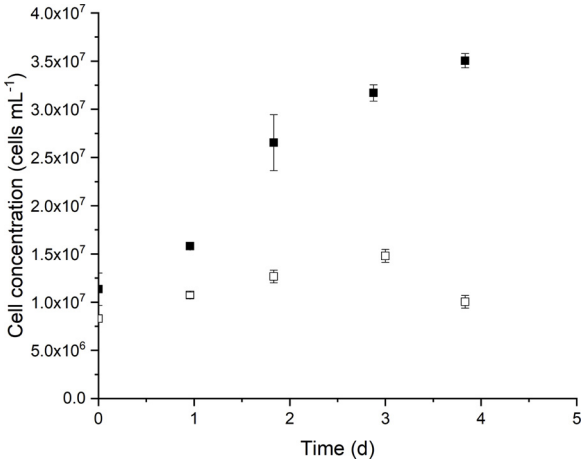

Fig. 11. Growth of *Chlorella protothecoides* in tannery wastewaters (TWW-2) with (black dots) and without (open dots) biochar pre-treatment. Error bars represent standard deviation of two biological replicates.

slightly higher than that of TWW-1. In this case, the beneficial effect of the biochar filtration pre-treatment was even more evident, due to the significantly higher pollution level of TWW-2, which strongly hindered biomass growth. The removal of nitrogen is also interesting as it is stored in the biomass, and not lost in the atmosphere as in the case of conventional nitrification/denitrification processes, showing the potential of microalgae in a waste-to-product perspective.

In summary, the results of this study show that a combined biochar-microalgae process for tannery wastewater treatment might be promising in view of an industrial bioremediation approach, by increasing algal growth while also reducing the amount of heavy metals in the biomass. The quality of the influent tannery wastewaters, as well as the characteristics of the biochar, can have a strong impact on the overall performances, so that further investigation is necessary to optimize the process. The complexity of the tannery wastewater composition should also be considered, as, if the biochar is not specific enough for metal removal, some competition for adsorption site may occur, thus lowering the metals remediation.

4. Conclusions

This work aimed at assessing whether the combination of a biochar filtration step followed by microalgal cultivation could result in a promising technology for treating industrial wastewaters from tanneries. These wastewaters have a complex composition, which may cause inhibition phenomena in microorganisms. In our experiments, microalgal-bacteria consortia were found to be able to grow and partially remove nutrients from such a stream, however growth was slower compared to those reported in standard media. On the other hand, the application of a biochar filtration step on the raw wastewaters resulted in improved growth (by 61 % and 126 % for two different sets of experiments) and nutrient removal for the microalgal species tested. In addition, it was found that, if the target of biochar adsorption is trivalent chromium, the biochar production process is the key for an efficient removal of this metal. In fact, a commercial biochar produced by slow pyrolysis of mixed feedstock at 500 °C allowed achieving an almost total removal of chromium III from synthetic water, significantly higher than that obtained with the biochar produced in the lab by slow pyrolysis of pinewood at 400 °C. Ultimately, the pollution level of the tannery wastewater influences the performances of both the biochar adsorption and the microalgal cultivation steps. Nonetheless, biochar pretreatment always resulted in improved microalgal growth and nutrients removal performances, highlighting the potential of the combined treatment for tannery wastewater bioremediation. Economic feasibility of such adsorption process widely depends on the regeneration/re-use of the spent adsorbent. A comprehensive desorption study would be an interesting scope for future work.

Funding

This research did not receive any specific grant from funding agencies in the public, commercial, or not-for-profit sectors.

Declaration of Competing Interest

The authors declare that they have no known competing financial interests or personal relationships that could have appeared to influence the work reported in this paper.

Acknowledgements

Authors would like to thank Prof. Alberto Bertucco for valuable discussion, Leonardo Costa and Martina Pastore for helping in preliminary experiments, and Medio Chiampo S.P.A. for providing wastewaters.

Appendix A. Supplementary data

Supplementary material related to this article can be found, in the online version, at doi:https://doi.org/10.1016/j.jwpe.2020.101431.

References

[1] C. Zhao, W. Chen, Research Article A Review for Tannery Wastewater Treatment: Some Thoughts Under Stricter Discharge Requirements, (2019), pp. 26102–26111.
[2] J. Tolfo da Fontoura, S. Rotermund, A.L. Araujo, N. Ramirez, M. Rubleske, M. Farenzena, M. Gutterres, Tannery wastewater treatment with Scenedesmus sp, IULTCS Congr. (2015) 1–10.
[3] M. Ballén-Segura, L. Hernández Rodríguez, D. Parra Ospina, A. Vega Bolaños, K. Pérez, Using Scenedesmus sp. for the phycoremediation of tannery wastewater uso de Scenedesmus sp. Para la ficorremediación de aguas residuales de curtiembres, Tecciencia. 12 (2016) 69–75, https://doi.org/10.18180/tecciencia.2016.21.11.
[4] A. Cassano, J. Adzet, R. Molinari, M. Buonomenna, J. Roig, E. Drioli, Membrane treatment by nanofiltration of exhausted vegetable tannin liquors from the leather industry, Water Res. 37 (2003) 2426–2434, https://doi.org/10.1016/S0043-1354(03)00016-2.
[5] C. Di Iaconi, Biological treatment and ozone oxidation: Integration or coupling? Bioresour. Technol. 106 (2012) 63–68, https://doi.org/10.1016/J.BIORTECH.2011.12.007.
[6] S.D. Alexandratos, Ion-Exchange Resins: A Retrospective from Industrial and Engineering Chemistry Research, Ind. Eng. Chem. Res. 48 (2009) 388–398, https://doi.org/10.1021/ie801242v.
[7] G. Dotro, B. Jefferson, M. Jones, P. Vale, E. Cartmell, T. Stephenson, A review of the impact and potential of intermittent aeration on continuous flow nitrifying activated sludge, Environ. Technol. 32 (2011) 1685–1697, https://doi.org/10.1080/09593330.2011.597783.
[8] F. Shen, X. Chen, P. Gao, G. Chen, Electrochemical removal of fluoride ions from industrial wastewater, Chem. Eng. Sci. 58 (2003) 987–993, https://doi.org/10.1016/S0009-2509(02)00639-5.
[9] S. Longo, B.M. d'Antoni, M. Bongards, A. Chaparro, A. Cronrath, F. Fatone, J.M. Lema, M. Mauricio-Iglesias, A. Soares, A. Hospido, Monitoring and diagnosis of energy consumption in wastewater treatment plants. A state of the art and proposals for improvement, Appl. Energy 179 (2016) 1251–1268, https://doi.org/10.1016/j.apenergy.2016.07.043.
[10] M. Nagi, M. He, D. Li, T. Gebreluel, B. Cheng, C. Wang, Utilization of Tannery Wastewater for Biofuel Production : New Insights on Microalgae Growth and Biomass Production, (2020), pp. 1–14, https://doi.org/10.1038/s41598-019-57120-4.
[11] U.N. Rai, S. Dwivedi, R.D. Tripathi, O.P. Shukla, N.K. Singh, Algal biomass: an economical method for removal of chromium from tannery effluent, Bull. Environ. Contam. Toxicol. 75 (2005) 297–303, https://doi.org/10.1007/s00128-005-0752-6.
[12] S. Balaji, T. Kalaivani, C. Rajasekaran, M. Shalini, S. Vinodhini, S.S. Priyadharshini, A.G. Vidya, Removal of heavy metals from tannery effluents of Ambur industrial area, Tamilnadu by Arthrospira (Spirulina) platensis, Environ. Monit. Assess. 187 (2015) 325, https://doi.org/10.1007/s10661-015-4440-7.
[13] K.V. Ajayan, M. Selvaraju, P. Unnikannan, P. Sruthi, Phycoremediation of tannery wastewater using microalgae Scenedesmus species, Int. J. Phytoremediation 17 (2015) 907–916, https://doi.org/10.1080/15226514.2014.989313.
[14] C. Das, K. Naseera, A. Ram, R.M. Meena, N. Ramaiah, Bioremediation of tannery wastewater by a salt-tolerant strain of Chlorella vulgaris, J. Appl. Phycol. 29 (2017) 235–243, https://doi.org/10.1007/s10811-016-0910-8.
[15] Y. Dai, N. Zhang, C. Xing, Q. Cui, Q. Sun, The adsorption, regeneration and engineering applications of biochar for removal organic pollutants : a review, Chemosphere 223 (2019) 12–27, https://doi.org/10.1016/j.chemosphere.2019.01.161.
[16] S.M. Shaheen, N.K. Niazi, N.E.E. Hassan, I. Bibi, H. Wang, D.C.W. Tsang, Y.S. Ok, N. Bolan, J. Rinklebe, Wood-based Biochar for the Removal of Potentially Toxic Elements in Water and Wastewater : a Critical Review, 6608, (2019), https://doi.org/10.1080/09506608.2018.1473096.
[17] T.M. Abdel-Fattah, M.E. Mahmoud, S.B. Ahmed, M.D. Huff, J.W. Lee, S. Kumar, Biochar from woody biomass for removing metal contaminants and carbon sequestration, J. Ind. Eng. Chem. 22 (2015) 103–109, https://doi.org/10.1016/j.jiec.2014.06.030.
[18] N. Bordoloi, R. Goswami, M. Kumar, R. Kataki, Biosorption of Co (II) from aqueous solution using algal biochar: kinetics and isotherm studies, Bioresour. Technol. 244 (2017) 1465–1469, https://doi.org/10.1016/j.biortech.2017.05.139.
[19] P. Regmi, J.L. Garcia Moscoso, S. Kumar, X. Cao, J. Mao, G. Schafran, Removal of copper and cadmium from aqueous solution using switchgrass biochar produced via hydrothermal carbonization process, J. Environ. Manage. 109 (2012) 61–69, https://doi.org/10.1016/j.jenvman.2012.04.047.
[20] H. Zheng, W. Guo, S. Li, Y. Chen, Q. Wu, X. Feng, R. Yin, S.H. Ho, N. Ren, J.S. Chang, Adsorption of p-nitrophenols (PNP) on microalgal biochar: analysis of high adsorption capacity and mechanism, Bioresour. Technol. 244 (2017) 1456–1464, https://doi.org/10.1016/j.biortech.2017.05.025.
[21] E. Agra, D. Kalderis, E. Diamadopoulos, Arsenic and Chromium Removal from Water Using Biochars Derived from Rice Husk, Organic Solid Wastes and Sewage Sludge 133 (2014), pp. 309–314, https://doi.org/10.1016/j.jenvman.2013.12.007.
[22] J. Shang, J. Pi, M. Zong, Y. Wang, W. Li, Q. Liao, Journal of the Taiwan Institute of

Chemical Engineers Chromium removal using magnetic biochar derived from herb-residue, J. Taiwan Inst. Chem. Eng. 68 (2016) 289–294, https://doi.org/10.1016/j.jtice.2016.09.012.
[23] S. Zhu, X. Huang, D. Wang, L. Wang, F. Ma, Enhanced hexavalent chromium removal performance and stabilization by magnetic iron nanoparticles assisted biochar in aqueous solution : mechanisms and application potential, Chemosphere 207 (2018) 50–59, https://doi.org/10.1016/j.chemosphere.2018.05.046.
[24] Z. Peng, H. Zhao, H. Lyu, L. Wang, H. Huang, Q. Nan, J. Tang, UV Modification of Biochar for Enhanced Hexavalent Chromium Removal From Aqueous Solution, Environmental Science and Pollution Research, 2018, pp. 10808–10819.
[25] J. Yu, C. Jiang, Q. Guan, P. Ning, J. Gu, Q. Chen, J. Zhang, R. Miao, Enhanced removal of Cr (VI) from aqueous solution by supported ZnO nanoparticles on biochar derived from waste water hyacinth, Chemosphere 195 (2018) 632–640, https://doi.org/10.1016/j.chemosphere.2017.12.128.
[26] F. Ahmad, A.U. Khan, A. Yasar, The potential of chlorella vulgaris for wastewater treatment and biodiesel production, Pakistan J. Bot. 45 (2013) 461–465.
[27] E.A. Ramos Tercero, E. Sforza, M. Morandini, A. Bertucco, Cultivation of Chlorella prototheocoides with urban wastewater in continuous photobioreactor: biomass productivity and nutrient removal, Appl. Biochem. Biotechnol. 172 (2014) 1470–1485, https://doi.org/10.1007/s12010-013-0629-9.
[28] E. Sforza, M. Pastore, A. Spagni, A. Bertucco, Microalgal-bacteria gas exchange in wastewater: how mixotrophy may reduce the oxygen supply for bacteria, Environ. Sci. Pollut. Res. (2018) In press.
[29] M.D. Huff, S. Kumar, J.W. Lee, Comparative analysis of pinewood, peanut shell, and bamboo biomass derived biochars produced via hydrothermal conversion and pyrolysis, J. Environ. Manage. 146 (2014) 303–308, https://doi.org/10.1016/j.jenvman.2014.07.016.
[30] Z.H. Yang, S. Xiong, B. Wang, Q. Li, W.C. Yang, Cr(III) adsorption by sugarcane pulp residue and biochar, J. Cent. South Univ. 20 (2013) 1319–1325, https://doi.org/10.1007/s11771-013-1618-4.
[31] P. Temperatures, L. Zhou, D. Xu, Y. Li, Q. Pan, J. Wang, L. Xue, Phosphorus and Nitrogen Adsorption Capacities of Biochars Derived from Feedstocks at Di ff erent, (n.d.) 1–16.
[32] M. Zhang, B. Gao, Y. Yao, Y. Xue, M. Inyang, Synthesis of porous MgO-biochar nanocomposites for removal of phosphate and nitrate from aqueous solutions, Chem. Eng. J. 210 (2012) 26–32, https://doi.org/10.1016/j.cej.2012.08.052.
[33] A.K.- Kozłowska, R. Włodarczyk, K. Wystalska, Biochar Compared With Activated Carbon for Landfill Leachate Treatment 42 (2019).
[34] E. Sforza, R. Cipriani, T. Morosinotto, A. Bertucco, G.M. Giacometti, Excess CO2 supply inhibits mixotrophic growth of Chlorella prototheocoides and Nannochloropsis salina, Bioresour. Technol. 104 (2012) 523–529, https://doi.org/10.1016/j.biortech.2011.10.025.
[35] H.-W. Kim, S. Park, B.E. Rittmann, Multi-component kinetics for the growth of the cyanobacterium Synechocystis sp, PCC6803, Environ. Eng. Res. 20 (2015) 347–355, https://doi.org/10.4491/eer.2015.033.
[36] N. Powell, A. Shilton, Y. Chisti, S. Pratt, Towards a luxury uptake process via microalgae – defining the polyphosphate dynamics, Water Res. 43 (2009) 4207–4213, https://doi.org/10.1016/j.watres.2009.06.011.
[37] T. Chen, Z. Zhou, S. Xu, H. Wang, W. Lu, Adsorption behavior comparison of trivalent and hexavalent chromium on biochar derived from municipal sludge, Bioresour. Technol. 190 (2015) 388–394, https://doi.org/10.1016/j.biortech.2015.04.115.
[38] H. Li, X. Dong, E.B. da Silva, L.M. de Oliveira, Y. Chen, L.Q. Ma, Mechanisms of metal sorption by biochars: biochar characteristics and modifications, Chemosphere 178 (2017) 466–478, https://doi.org/10.1016/j.chemosphere.2017.03.072.
[39] H. Li, X. Dong, E.B. da Silva, L.M. de Oliveira, Y. Chen, L.Q. Ma, Mechanisms of metal sorption by biochars: biochar characteristics and modifications, Chemosphere 178 (2017) 466–478, https://doi.org/10.1016/j.chemosphere.2017.03.072.
[40] J.W. Lee, M. Kidder, B.R. Evans, S. Paik, A.C. Buchanan, C.T. Garten, R.C. Brown, Characterization of biochars produced from cornstovers for soil amendment, Environ. Sci. Technol. 44 (2010) 7970–7974, https://doi.org/10.1021/es101337x.
[41] M. Ahmad, S. Soo, A. Upamali, M. Vithanage, M. Zhang, J. Sik, S. Lee, Y. Sik, Bioresource Technology Trichloroethylene adsorption by pine needle biochars produced at various pyrolysis temperatures, Bioresour. Technol. 143 (2013) 615–622, https://doi.org/10.1016/j.biortech.2013.06.033.
[42] L. Qian, W. Zhang, J. Yan, L. Han, W. Gao, R. Liu, M. Chen, Effective removal of heavy metal by biochar colloids under different pyrolysis temperatures, Bioresour. Technol. 206 (2016) 217–224, https://doi.org/10.1016/j.biortech.2016.01.065.
[43] J. Pan, J. Jiang, R. Xu, Adsorption of Cr(III) from acidic solutions by crop straw derived biochars, J. Environ. Sci. (China). 25 (2013) 1957–1965, https://doi.org/10.1016/S1001-0742(12)60305-2.
[44] Langmuir, The constitution and fundamental properties of Solids and liquids. Part I. Solids, J. Am. Chem. Soc. 38 (1916) 2221–2295.
[45] G. McKay, M.S. Otterburn, A.G. Sweeney, The removal of colour from effluent using various adsorbents—III. Silica: Rate processes, Water Res. 14 (1980) 15–20.
[46] A. Ozer, H.B. Pirinççi, The adsorption of Cd(II) ions on sulphuric acid-treated wheat bran, J. Hazard. Mater. 137 (2006) 849–855.

CHAPTER 5

CONCLUSIONS AND RECOMMENDATIONS

The dissertation aims to serve as a valuable resource for future researchers in this field to identify opportunities and challenges associated with biochar's application in heavy metal removal and to develop innovative and sustainable solutions for water treatment and management.

As discussed in Chapter 2, numerous studies have demonstrated the impressive potential of biochar as a cost-effective and sustainable solution for water remediation. The review acknowledges that although biochar has significant potential as a metal adsorbent, there are several gaps and limitations in the existing literature. For example, there has been limited research conducted on the disposal options for Pb(II)-loaded biochar, regeneration of biochar, and the use of column flow setups. Moreover, most studies have focused on single-metal solutions, which may not accurately reflect real-world scenarios. To address these gaps and limitations, future research should conduct a comprehensive analysis of toxic Pb(II) leaching from biochar to identify the most feasible management solution for spent biochar. Furthermore, there is a need for more studies to establish design criteria for scaling up the system and gain a comprehensive understanding of the mechanisms underlying Pb(II) sorption behavior. In summary, the review highlights both the opportunities and engineering challenges of using biochar as a metal adsorbent and serves as an essential resource for researchers working in this area.

In Chapter 3, the adsorption study has successfully demonstrated the potential of biochar as a cost-effective adsorbent for removing Pb(II) from contaminated drinking water through a fixed bed continuous flow process. The focus on commercially available biochar and its use in a flow-through system is a unique approach that sheds light on the effectiveness of biochar in

addressing the issue of lead contamination. Additionally, the study emphasizes the potential of locally produced biochar from clean biomass sources as a sustainable and low-cost option for removing Pb(II) from water. Based on the findings of this study, it is recommended that further research be conducted to optimize the biochar production process and investigate the use of different types of biomass sources. Moreover, efforts should be made to develop a practical and scalable point-of-use water filter using biochar as an adsorbent, which can be deployed in regions where access to clean drinking water is limited.

In Chapter 4, in collaboration with the University of Padova, Italy team, the use of biochar as a pretreatment measure for the bioremediation of tannery wastewater was investigated. The application of biochar obtained from two different sources (laboratory made Pinewood biochar and commercial biochar) in the wastewater to remove Cr(III) led to a significant increase in microalgae growth rates (61% - 126%) and it was concluded that biochar production parameter effects the Cr removal efficiency which is in agreement of the findings of Chapter 2 and Chapter 3. This knowledge can be further elaborated for practical application.

In conclusion, the dissertation provides valuable insights into the potential of biochar as a sustainable and cost-effective solution for heavy metal removal from contaminated water. The study's findings underscore the need for further research to address the engineering challenges associated with scaling up the system and standardizing the market for biochar as an adsorbent. The dissertation's contribution to the field of water treatment and management is significant, and the findings will help guide future research in this area.

APPENDICES

APPENDIX A: EPA P3 PROPOSAL

Abstract Opportunity Number: EPA-G2017-P3-Q4 – Water

Funding Opportunity Number and Research Area: P3 Awards: A National Student Design Competition for Sustainability Focusing on People, Prosperity and the Planet; Funding Opportunity Number: EPA-G2017-P3-Q4 – Water

Project Title: Low-cost Household Biochar Water Filter for Lead Removal

Principal Investigator (P.I.):

Sandeep Kumar, skumar@odu.edu Associate Professor, Department of Civil & Environmental Engineering, Old Dominion University. www.odu.edu/directory/people/s/skumar

Student Team:

Name	*Background*	*Status*	*Role*
Ms. Pushpita Kumkum	BS & MS in Civil Engineering	PhD student Civil & Environmental Engineering	Student's Team Lead
Mr. Aaron Lyons	BS Civil Engineering	BS Student (Junior)	Team Member
Ms. Kim Bethea	BS Civil Engineering	BS Student (Junior)	Team Member
Mr. Jose Tendilla Jr.	BS Civil Engineering	BS Student (Junior)	Team Member
Ms. Haley Morgan	BS Civil Engineering	BS Student (Sophomore)	Team Member
Mr. Aaron Cox	BS Civil Engineering	BS Student (Junior)	Team Member
Mr. Jacob Landis	BS in Civil Engineering	Industry Consultant	Consultant
Mr. Timothy Evard	BS in Civil Engineering	Industry Consultant	Consultant
Ms. Angela Barnes	BS in Biology	MS Student Research Administration	Project Advisor
Mr. Caleb Talbot	BS Applied Science MS Environmental Engineering	PhD Student Civil & Environmental Engineering	Project Advisor

Institution: Old Dominion University, 5115 Hampton Road Blvd. Norfolk, VA

Student Represented Departments and Institution: Department of Civil & Environmental Engineering, and Biology

Project Period and Location: August 15, 2017 to August 14, 2018, *Awardee Institution:* Old Dominion University Research Foundation, Norfolk, VA; *Performing Institution:* Old Dominion University, Norfolk, VA

Proposed EPA Project Cost: $15,000

Total Project Amount: $15,000

Project Summary:

- **Objective:** Heavy metal contamination in drinking water is a growing concern due to its severe health effect in human. Conventional processes like use of activated carbon for the adsorption of metals i. e., lead has always been an expensive method which has precluded its ubiquitous use. We propose to design and develop a low-cost household water filter using biochar to introduce a user-friendly cost effective system for removing lead from drinking water. There are several intellectual merits (based on our several prior published studies) of the proposed filter. First, the proposed filter reduces the cost and makes it a more effective approach since biochar is significantly cheaper and has higher cation exchange capacity (CEC) than activated carbon in lead removal. Second, the proposed filter is an easy-to-use system that works in residential faucet water flow and requires no professional help for the installation. Third, the proposed filter is effective in natural water condition and does not require any pH adjustment.

- **Description:** Biochar can be a cost effective substitute to activated carbon in lead adsorption because of its porous structure, irregular surface, high surface to volume ratio and presence of oxygenated functional group. We propose to design a household water filter that uses biochar as an adsorbent for removing lead from drinking water. The proposed filter integrates the conventional filter and adsorption potential of biochar in order to create a system that can eliminate lead from supplied water. It will significantly decrease the cost for abatement of lead pollution. In addition, the proposed filter uses only biochar (a renewable material) for filtration and production of biochar is a relatively simple process. . Furthermore, this project will provide a good opportunity for educating the public, especially school students in local community. We plan to attend and present our results in the regional science fairs. We specifically target annual Tidewater Science & Engineering Fair, which welcomes all the K-12 students from in the Hampton Roads area.

- **Results:** The expected deliverables of the proposed filter consists of three stages. In the stage one, theoretical investigation will be performed on the proposed filter. The research will focus on breakthrough point calculation, material selection, product design, and efficiency evaluation. In the stage two, the research team will build a prototype of the filter to evaluate the practical lead removal performance of the proposed concept. The third stage is to demonstrate the potentiality of the prototype filter for successful elimination from lead contaminated drinking water.

Contribution to Pollution Prevention or Control: The proposed project practically put an end to the dependence on activated carbon and therefore reduces the

cost and difficulty in removing lead to ensure safe drinking water. Being a renewable material, the proposed biochar filter will produce minimum pollution to the environment.

Supplemental Keywords: human health, toxics, pollution prevention, drinking water treatment technologies, cost-benefit.

Low-cost Household Biochar Water Filter for Lead Removal

Section 1: Proposed Research

Opportunity Number: EPA-G2017-P3-Q4 – Water

The proposed project is directly related to the EPA/P3 objectives of ensuring long-term sustainability including the prevention and/or control of the man-made or man-induced alteration of the chemical, physical, biological, and radiological integrity of water.

Challenge Definition:

According to United Nations, "The human right to water entitles everyone to sufficient, safe, acceptable, physically accessible and affordable water for personal and domestic uses."("General Comment No 15," n.d.). It is the responsibility of the government to ensure its people have access to safe, sufficient, and affordable water. There is increasing concern over health effects of toxic compounds released into the natural environment. Drinking water becomes contaminated due to levels of toxins or suspended solids. The Clean Water Act and the Safe Drinking Water Act are two pioneering pieces of legislation regulating the discharge of pollutants into the waters and set the water quality standards for all contaminants in surface water in United States. However; even with strict regulations in place, mishaps persist.

As an example, in Flint, Michigan a crisis effected safe drinking water. Lead piping was outlawed thirty years ago, but it is estimated that almost ten million pipes remain in use today (Wines, M., & Schwartz, J., 2016). When the states switched the source of water supply from Lake Huron to the Flint River in 2014 (Ganim, & Tran, 2016), the river water tested 19 times more corrosive than lake water according to a study by Virginia Tech. Toxic lead began leaching into the city's water supply causing a national health crisis. According to the Centers for Disease Control (CDC) and Prevention ("Lead", 2016a), there are half a million children with blood level concentrations of lead ranging from one to five micrograms per deciliter. This range in toxin concentration requires public health intervention enforced by the CDC. According to the World Health Organization, high lead levels in the blood are especially harmful to children and pregnant women, and can cause learning disabilities, behavioral problems, and mental retardation. For adults, blood lead levels less than 5 μg/dL decreases kidney function ("Lead", 2016b); for pregnant women high levels of lead in the circulatory system reduces fetal growth. Medical treatment may reduce the amount of lead in the blood but cannot reverse the damage (Pilsner et al., 2009). This intensifies the need for prevention and a sustainable system that can effectively remove lead from tap water after reaching the homes of citizens. Various methods are used to remove metal from water and wastewater, i.e., chemical precipitation, ion-exchange, adsorption, membrane filtration, electrochemical treatment technologies, etc. (Fu, & Wang, Q. 2011). Adsorption is the most efficient for metal removal (Liu, & Zhang, 2009) and activated carbon has been used widely in many applications as an effective adsorbent but high production cost (Salam, Reiad, & ElShafei, 2011) created the necessity of a low-cost alternative like biochar. **The goal is to design a filter that can effectively**

remove lead from tap water using biochar and make it safe for drinking towards the people of the household.

Research Description:

The major challenge of using biochar as a cost competitive method is to assess what quantity of lead a given amount of biochar can adsorb before supersaturation in a continuous flow packed-bed system. Adsorption of a substance involves its accumulation at the interface between two phases. Breakthrough; the point at which all adsorption sites are occupied-adsorbate and adsorbent are in equilibrium, of a given amount of biochar data can be used to design a household water filter for drinking water free of lead contamination. This P3 award team proposes to design a biochar filter for removal of lead from tap water using the principle of adsorption based on the schematics shown in Figure 1.1 for real applications.
This project will follow the below goals:

Goal 1: Theoretical investigation will be performed on the proposed filter. The research will focus on breakthrough point calculation, material selection, and efficiency evaluation

Goal 2: The research team will build a prototype of biochar filter to evaluate the practical lead removal potential of the proposed concept.

Goal 3: The research team will demonstrate the efficiency of the filter of eliminating lead from supplied household water

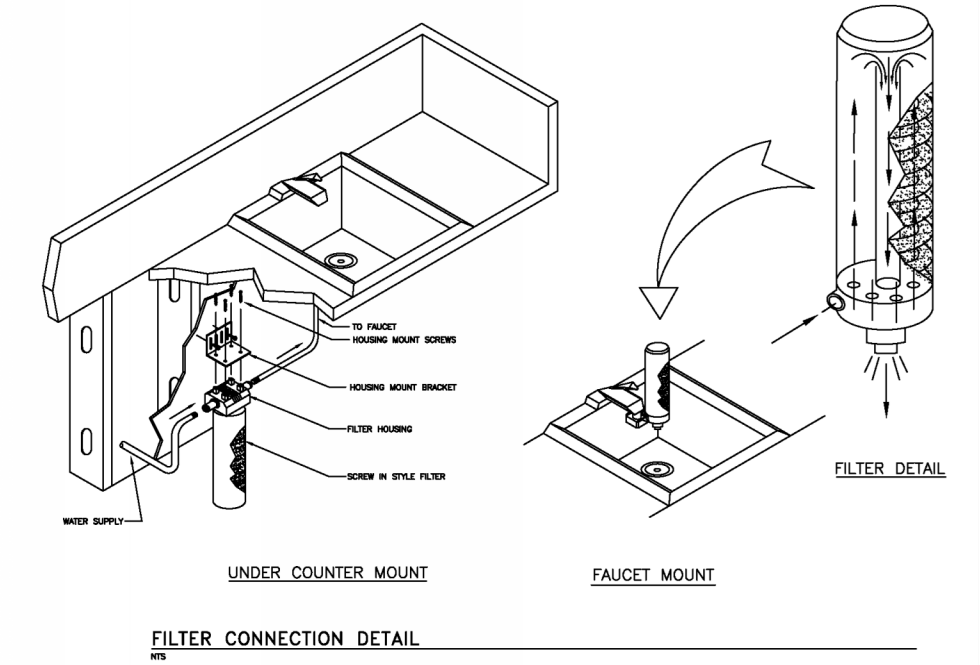

Figure 1.1 Proposed Concept for the Biochar filter

This filter is designed for ease of use for any person that may need it. To meet this goal the schematic (Figure 1.1) demonstrates how the product is envisioned: simple

installation of filter, mounting onto the faucet, and replacement of the filter cartridge as needed. Under the counter filters can also be produced for those that are not in need of immediate use; a product designed for longevity rather than providing potable water in emergency situations. Materials will be inexpensive to ensure convenience for those in need and are available for shipment to areas of crisis. Plastics manufacturers can be utilized for mass production and use of char, as opposed to GAC, will also reduce cost. To guarantee operational design, additional testing and refinement is necessary to secure an appropriate factor of safety.

As shown in figure 1.2, there are three stages in this project to engage intended end users. Additionally, this filter can be used in different types of residential areas.

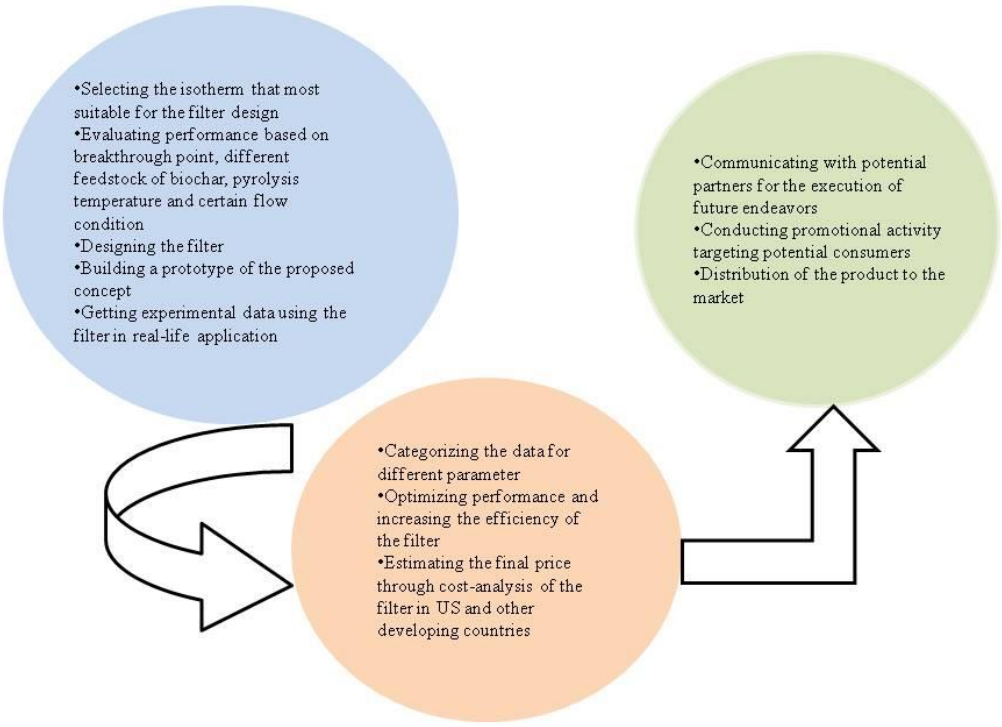

Figure 1.2. Road Map for the Proposed Concept.

Research Background:

The project is backed up with years of research data on the use of biochar for metals removal from water which are published by the PI in following publications:

1. T.M. Abdel-Fattah, M.E. Mahmoud, S.B. Ahmed, M.D. Huff, J.W. Lee, **S. Kumar**, Biochar from Woody Biomass for Removing Metal Contaminants and Carbon Sequestration, *Journal of Industrial and Engineering Chemistry* 25, 103-109, (**2015**).
2. Mohamed E. Mahmoud, Gehan M. Nabil, Nabila M. El-Mallah, Heba I. Bassiouny **Sandeep Kumar** and Tarek M. Abdel-Fattah, Kinetics, Isotherm, and Thermodynamic Studies of the Adsorption of Reactive Red 195 Dye from Water by Modified Switchgrass Biochar Adsorbent" *Journal of Industrial and*

Engineering Chemistry (**2016**) Volume 37, 25 May 2016, Pages 156–167. doi:10.1016/j.jiec.2016.03.020

3. Regmi P., Garcia M., **Kumar S.,** Cao X., Mao J., Schafran G., Removal of Copper and Cadmium from Aqueous Solution using Switchgrass Biochar Produced via Hydrothermal Carbonization Process. *Journal of Environmental Management;* (**2012**), 10, 61-69.
4. **Kumar, S.**; Loganathan, V.A.; Gupta R.B.; Barnett, M. An Assessment of U(VI) removal from groundwater using biochar produced from hydrothermal carbonization, *Journal of Environmental Management*; (**2011**), 92, 2504-2512.

The idea of designing a biochar filters for lead removal stems from recent needs and developing a marketable products spinning off from several proven lab-scale studies by the PI. An interdisciplinary student team with interest in water and sustainable design has worked for nearly 1 year in PIs laboratory to conceptualize this project idea to take it for an everyday use by developing a marketable product.

Biochar, which results from thermal degradation of organic materials such as crop residue, forest residue, wood, manure, and other materials, is a carbon rich material that is porous with oxygen functional groups and aromatic surfaces. Because of its high surface-to-volume ratio, cation exchange capacity (CEC), and strong affinity for non-polar substances such as PAHs, dioxins, furans, and other compounds, biochar can be a potential sorbent for metals, organic pollutants, and pesticides. Recently, biochar has attracted much attention due to its potential application in environmental management. It is also a byproduct from upcoming biorefineries, which are expanding following the government's drive toward biofuels. In view of the growing biofuels industry, it is important to add value to the byproduct (biochar) collected at the end of the bioenergy cycle in part to make biofuels more cost competitive.

The processing conditions and type of biofuel being produced generally determine the composition, properties, and yield of biochar. Slow/fast pyrolysis or hydrothermal carbonization (HTC) are usually used for producing biofuels and biochar from lignocellulosic biomass. These processes are usually conducted in the temperature range of 250-400ºC. The HTC process is comparatively low emission and a hazardous waste free process because it uses water as the sole reaction medium under pressure and heat. The HTC process has ability to utilize mixed biomass feedstock without prior pretreatment or drying gives it an edge in terms of energy savings over other thermochemical processes where prior drying is required. Pyrolysis/HTC produced biochar can be subsequently activated with the use of alkali (KOH/NaOH) solution to increase its BET surface area or surface properties to improve its CEC. The PI possess all necessary facility for producing and activating biochar in his laboratory. Table 1 shows elemental composition of biochar produced in the PI lab.

Table 1: Composition of Switchgrass and Biochar Used in the Study

Elements	C (wt%)	Ash	Ca ($mg \cdot kg^{-1}$)	K	Mg	P	Fe	Mn	Na	Pb
Switchgrass	44.6	1.3	2105	4082	4514	941	115	48	701	1
HTC Biochar	70.5	3.2	2029	665	2215	481	258	53	395	<0.1

Compared to switchgrass, HTC biochar had a much higher carbon percentage and a comparatively lower inorganic content.

The BET surface area of HTC biochar, activated HTC Biochar, and powder activated carbon (PAC) were examined as part of the study to help assess what effect surface area may have contributed to differences in metal removal. The effect of KOH activation can be seen in the increase of BET surface area of the Activated HTCB biochar (5.01 g/m^2) showing an increase of 2.4x over the non-activated biochar (2.11 g/m^2) (Table 4). The BET surface area of PAC (726 g/m^2) was more than two orders of magnitude greater than both of these adsorbents.

Table 2: BET Surface Area of HTC Biochar Activated HTCB and PAC.

	HTC Biochar	Activated HTCB	PAC
BET surface area	2.11 m^2/g	5.01 m^2/g	726 m^2/g

The adsorption of positively charged lead, copper and cadmium ions mostly occurrs via attraction to negatively charged surface groups or through the formation of direct surface complexes to biochar. Figure 1.3 shows the FTIR spectra of HTC biochar, activated HTCB, and PAC in the near IR region (wave number: 4000–400 cm^{-1}). The spectra suggest the presence of several oxygen functional groups in both HTC biochar and activated HTCB biochar whereas the spectra of PAC clearly indicate the absence of such functional groups.

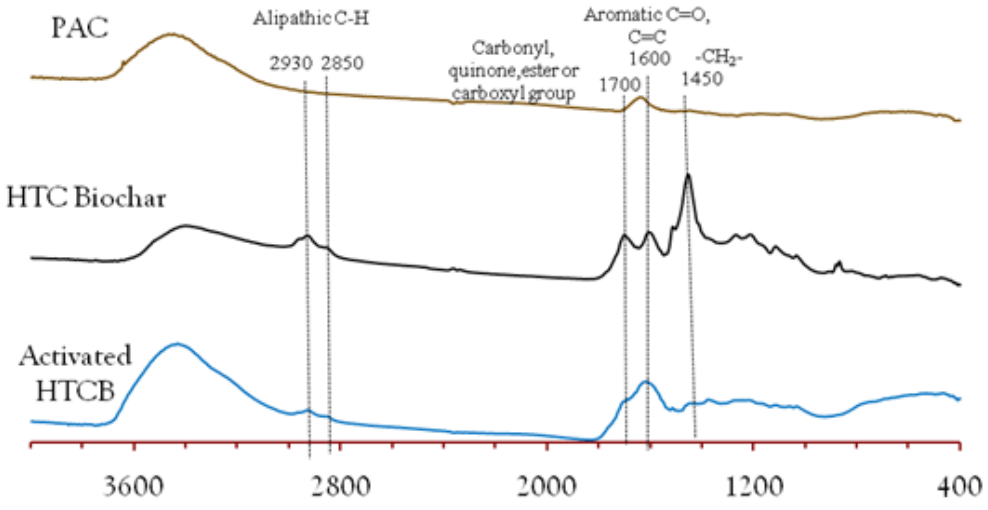

Figure 1.3: FTIR Spectrum comparing powder activated carbon (PAC), HTC biochar, and activated biochar (HTCB).

Results (outputs/outcomes), Evaluation and Demonstration

Preliminary Study: A focused study by the PI had shown the efficacy of removing lead from water through means of biochar. The results were presented at the 22nd Annual Environment Virginia Symposium, Lexington, VA on April 5-7, 2011 titled Biochar: A Renewable Material for Removing Contaminants from Water. The parameters from this past experiment are as follows:

- 40 mg/L lead (as lead nitrate)
- 3.0 mL/min flow rate through column
- 50 mL biochar volume (Sampling after 48 hours exhibited 0 mg/L of lead penetration)
- Total lead adsorption = 3 mL/min X 40 mg/L X 1L/1000mL X 48 h X 60 min/ 48 h = 345.6 mg/L

Results showed the potential efficacy of lead adsorption in a continuous packed bed flow setup but does not specify when breakthrough will occur. The intention of conducting this experiment is to achieve breakthrough. To accomplish a conclusion, the point at which the adsorbent is no longer accepting any adsorbate must be reached. This will be essential to use this adsorbent in a filter design that can be used as a product by different customers.

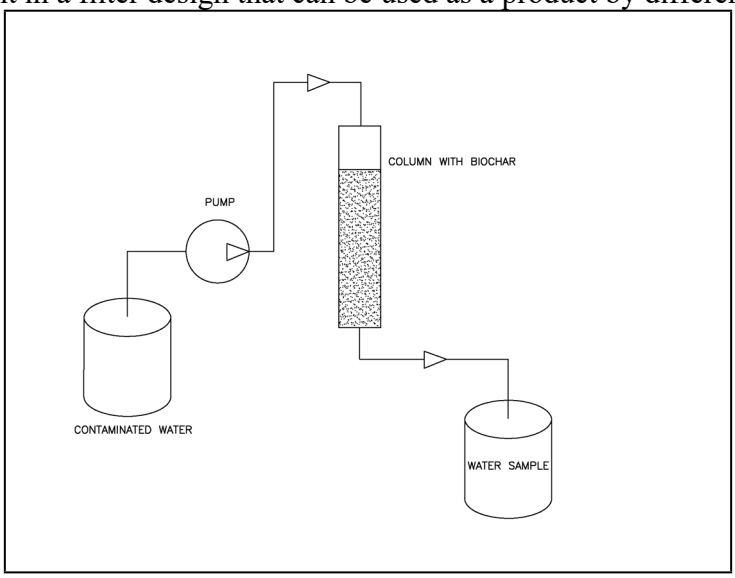

Figure 1.3. Experimental set-up

The procedure for mixing the stock solution was done according to the Standard Methods for Examination of Water and Wastewater 22nd edition. The biochar for this project was prepared from woodchips by slow pyrolysis process which was conducted at 400 degrees Celsius at a reaction time of 30 minutes. 500 mg/l lead solution was prepared from 20 g/l stock solution, diluting with (1:1) HNO_3 which lowered the pH of the solution to less than 2, this is a standard procedure for preserving the sample during metal analysis. Sample was collected every 0.5 h

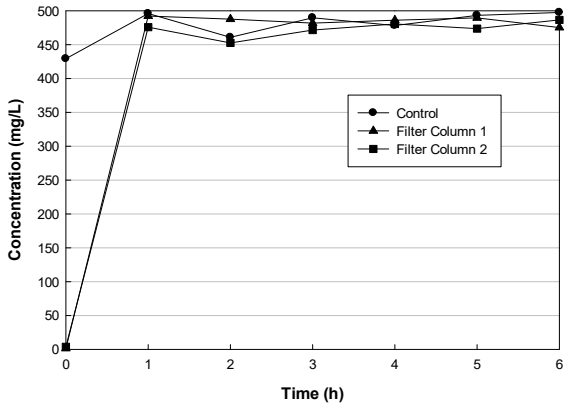

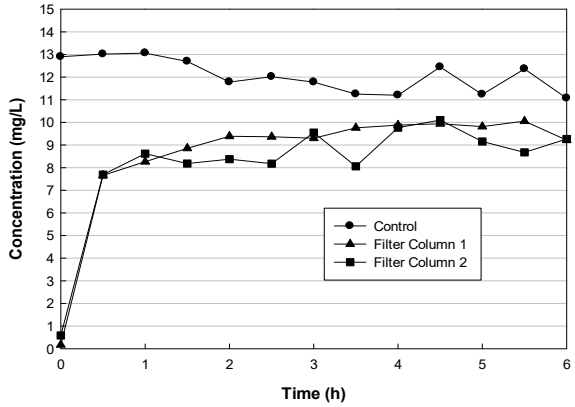

(a) (b)

Figure 1.4. (a) Concentration of Lead vs Time (initial lead concentration = 500 mg/l) (b) Concentration of Lead vs Time (initial lead concentration = 15 mg/l)

The pH of the lead solution was adjusted back to pH ~ 7 using 1M NaOH before running through the columns and at about pH 5, the solution started creating a precipitation of Pb(OH)2 which results in some discrepancy in the concentration. To avoid this discrepancy, the lead solution was prepared the same day of the next experiment. The results in figure 1.4 (a) show the concentrations of lead expressed different aspects of the filter columns containing biochar and the control (which did not contain any biochar). Total run time was 6hrs and sampling interval was 1 hr. In this case, sample was collected at the very first hour (t = 0 h) so that the breakthrough point can be investigated. For t_0 hr the concentration of lead was found near zero for the duplicates, for the control it was close to the initial concentration. The samples showed relatively consistent concentration of lead throughout the rest of the experiment for control and for the filter columns as well. This figure shows the biochar columns became saturated in the first hour and lost the potential of removing lead. In support of this hypothesis, the next experiment was conducted using a lower concentration of lead (15 mg/l) and decreasing the sampling interval to 30mins to observe the change of concentration more accurately. The figure 1.4 (b) also shows that for this t_0 hr the concentration of lead was found close to zero for the duplicates even at this low concentration where as for the control it was close to the initial concentration. The samples showed relatively consistent concentration

of lead throughout the rest of the experiment for control and for the filter columns as well. Presumably it can be said that the biochar columns got saturated at the very first hour and lost the potential of removing lead anymore. This data concur with the data from previous studies where no lead concentration was detected in the filtered water at the first hour. The idea is to progress this experiment further to find out the breakthrough point accurately. The data will be used to identify the most suitable adsorption isotherm (among Langmuir and Freundlich) applicable for the design of the proposed filter.

To turn this into an effective and marketable product, some improvements need to be made. Modifications to the experimental design would create more concise results in future testing. There are indications that not all of the biochar was effectively utilized in the experimentation. In using a downward drip method through the packed biochar, there was likely a specific flow channel that would result in contact time for only some of the biochar, leaving some particles untouched. By implementing an upward flow system as opposed to downward, this would completely saturate all the biochar packed in the column. This will allow the same amount of biochar to adsorb more lead giving results for a superior filter design.

The most effective filter design is one in which all of the resources are used efficiently; an achievement that will be gained in future testing. The type of material used in this experiment was Alder wood. Future testing would include analysis of different sources of organic material to produce a char that is more effective. The procedure of pyrolysis can also have an effect on the composition of the biochar. Producing biochars at different temperatures and lengths of time is also something to consider.

It is essential to consider the availability and life cycle costs of the materials used in a business scenario. In other words, how does our use of this natural resource ultimately impact our environment? There is potential in finding a source of organic matter and even biochar itself from the byproduct of other processes such as from logging and forest clearing operations. Wood processing mills have sawdust and woodchips as a byproduct of their operation that could be utilized. Bio-refineries utilize processes such as hydrothermal liquefaction; pyrolysis (used for bio-oil and syngas), as gasification to convert lignocellulosic biomass into biofuels. These organizations produce biochar as a direct byproduct which is sold to reduce their production costs. In potential business practice of this study, it is critically important to remain as a green as possible which means exhausting options like sources of feedstock or char before anything else.

A pressurized system would be implemented to test with a higher flow rate to observe how the results withstand a larger scale. The current experiment flow rate is six milliliters per second while the average home faucet is at a much higher rate of 133 millimeters per second. Continued testing is necessary to support the validity of this experiment, providing credibility when communicating with potential partners for the execution of future endeavors.

This project depends on the clarification of essential factors. A biochar supplier with the ability to mass produce a supply to meet the needs of this production. A cost analysis for the quantity needed would be performed to determine which company would be most viable to use. The biochar filter would initially be marketed to the citizens of

Flint Michigan and other areas that are affected by lead in drinking water. Also, there is a potential to be marketed to developing countries with subpar infrastructure.

Section 2: Relationship of Challenge to Sustainability (People, Prosperity and the Planet)

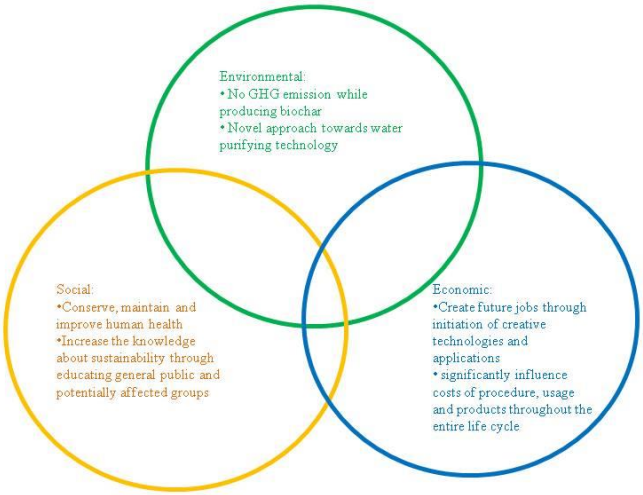

Figure 1.5. Schematic of relation between environment, social, and economics.

People:

Sandeep Kumar (PI): Dr. Kumar earned his PhD degree in chemical engineering from Auburn University in 2010. He possesses more than twenty years of professional experience in industry, R&D, and academic research in the area of carbon black, nuclear fuels, and biofuels with a focus in new process development, process engineering and project management. Dr. Kumar started his professional career in 1994 as a process engineer and was a certified project management professional (PMP®) between year 2007-2011. For the last five years, Dr. Kumar has been actively engaged with biofuel/bioproduct startup companies. Recently, he played a lead role in designing and commissioning a pilot-scale hydrothermal extractor customized for the extraction of tobacco biomass sugar at the Tyton BioEnergy facility located in Danville, VA. http://www.godanriver.com/work_it_sova/news/bioscience-company-re-imagining-tobacco-for-new-age-with-machine/article_e808e8b6-5812-11e5-8bf8-07820208e5e7.html
Dr. Kumar is a NSF CAREER award recipient and has two granted patents along with several publications in the proposed research area.

The interdisciplinary students' team proposed here will have opportunity work of hands experience in design of experiments, conducting experiments in laboratory, analyses related to water quality, products design, demonstration, interaction with local community, business development, and many outreach activities. The impact of this

project is directly on people living in areas which has seen lead contaminations in water as well as sudden surge of contaminants due to some failures.

Prosperity:

The project aims to develop a low-cost, user friendly technology that efficiently removes lead from potable water and ensures the right for pure, clean drinking water for developed and developing countries all over the world. Lead poses severe health defects in human biological system which makes it essential to certify that the supplied water is completely lead-free. Among the bio-sorption methods of metal removal, lead activated carbon is a costly technique making it difficult for ordinary citizens to afford. Biochar an economical easy-to-use system. When successful, the proposed technology has potential to be transformative and will meet the need for a sustainable method to ensure safe drinking water. Furthermore, the accomplishment of this project will have a major impact on the water treatment sector of developing countries.

Planet:

Impact of the proposed project will be: i) reducing the energy requirement ii) an efficient procedure for biochar production, iii) production of biochar from various feedstocks, iv) water purification using biochar with minimal resources required, v) enrichment of the literature of lead removal using adsorption principal of biochar, vi) training of graduate and undergraduate students to enhance environment literacy, vii) reduction in greenhouse gas emission through the development of biofuels.

Section 3: Project Management

Regarding to the goals, four people are in the research plan, there are several tasks in the Figure 1.6. for Phase I and II:

Task 1: Low pressure testing with existing setup
Task 2: Experimental apparatus setup
Task 3: Prototype design and testing prototype
Task 4: Creating a business plan
Task 5: Writing proposal for Phase II funding and final report of Phase !

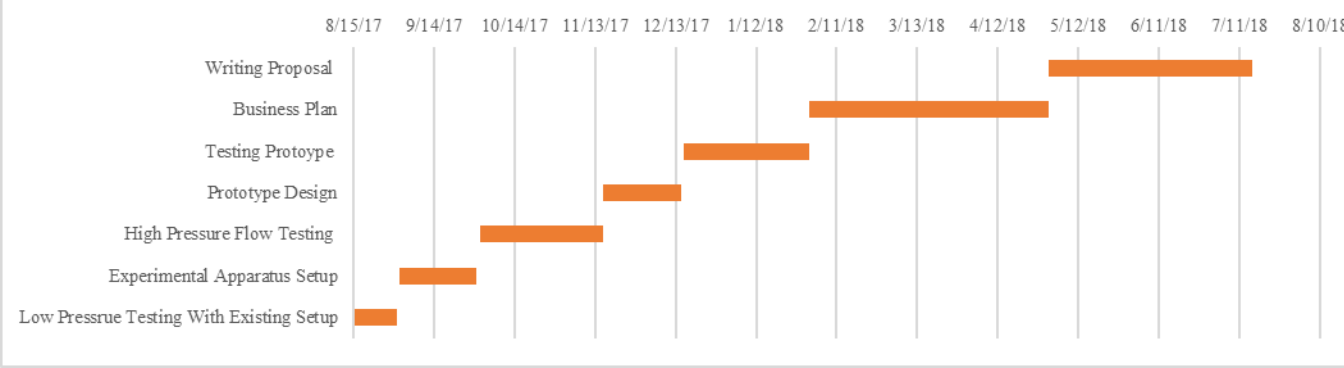

Figure 1.6. Proposed timeline.

Table 2 shows the all student team responsibilties. Student team leader, Pushpita Kumku, has several work experience in developing methodology, running experimental projects and investigations of the system behavior. Jacob Landis has experiences on system design and experiments.

Timothy Evard and Angela Barnes are undergraduate students with background in civil and environmental engineering and Biology. They have expertise in soil, water, and environmental evaluation.

People	2017					2018						
	Aug	Sep	Oct	Nov	Dec	Jan	Feb	Mar	Apr	May	Jun	Jul
Pushpita	T1	T1	T2	T2	T3	T3	T4	T4	T5	T5	Report	
Jacob		T1	T2	T2	T3	T3	T4	T4	T5	T5		
Timothy			T2	T2			T4	T4	T5	T5		
Angela							T4	T4	T5	T5		

Table 1. Student team responsibilities

Facilities and Resources:

The Biomass Laboratory (BRL) at ODU directed by Dr. Sandeep Kumar is at Kaufman Hall (Civil and Environmental Engineering) and occupy a laboratory space of approximately 3000 square feet equipped with fume hoods and small equipment. The laboratory houses high temperature and high pressure equipment for conducting the supercritical water based research for biofuels applications. Students will have access to gas chromatograph (TCD & FID), high temperature (500°C) and high pressure (5000 psi) batch reactor (Parr Reactor), ICS-5000 ion chromatography system, calorimeter (Parr Instruments), and BET surface area and pore volume analyzer (Quantachrome NOVA 2200e), Labconco freeze dryer, rotary vacuum evaporator, UV-Vis Spectrophotometer (Varian), Total carbon/nitrogen (TOC/NOC) analyzer (Shimadzu), Particle size analyzer (Coulter Multisizer), Zeta potential (Coulter Delsa 440SX), atomic absorption spectrophotometer, and many small conventional analytical instruments.

Regarding the team specialists, facilities from the labs, and also primary data from the other researcher which is proposed in this proposal, this team are so motivated to set up the system at Old Dominion University.

Section 4: Educational and Interdisciplinary Aspects of Research

This research is an excellent efficient system. It will have a large impact on communities, because people will be able to use the filter in their residences without needing any special expertise. The students' team will follow the experience in sustainable process improvement. The practical experience the team will gain with this system will make it

easier to take development to the next level, which is establishing a small business and commercializing the system. In this description, students as a team can be educated.

Educational:

The research effort outlined above provides a context to communicate the principles of sustainability, green processes, and necessity of integrated approaches to complex water treatment problems to the students. The students' team will get hands-on experience in sustainable process development, the importance of innovation through research and development, demonstration of sustainable projects, and see the opportunity of developing small business.

This study is designed to conduct a number of integrated educational and outreach activities, all of which communicate the necessity of integrated approaches to complex water treatment technology and environmental engineering issues. As a senior faculty, the PI sets the long-term education and outreach goal. The successful implementation of P3 Award will motivate students for innovation in addressing environmental concerns.

Interdisciplinary Team:

The PI has a chemical engineering background and has more than fifteen years of professional experience in industry and R&D. The students team comprise of students from Environmental Engineering, a senior with Civil Engineering and Biology background. The proposed interdisciplinary research provides the opportunity to use PI's reaction engineering and project management skills to environmental engineering areas which is crucial for the development of biochar filter with minimal environmental impacts. The technical challenges proposed here involve the knowledge /contributions from several other disciplines such as chemistry, environmental engineering, mechanical engineering and biology.

Human Subjects Research Statement (HSRS)

This is to declare that “the proposed research does not involve human subjects”.

References

1. Fu, F., & Wang, Q. (2011). Removal of heavy metal ions from wastewaters: a review. *Journal of environmental management*, *92*(3), 407-418.
2. Ganim, S., & Tran, L. (2016, January 13). How tap water became toxic in Flint, Michigan. *CNN*. Retrieved October, 2016, from http://www.cnn.com/2016/01/11/health/toxic-tap-water-flint-michigan/
3. General Comments No 15 « Rights to Water and Sanitation. (n.d.). Retrieved January, 2017, from http://www.righttowater.info/progress-so-far/general-comments-2/
4. Lead (2016a, September 07). Retrieved October, 2016, from https://www.cdc.gov/nceh/lead/
5. Lead. (2016b, December 6). Retrieved October, 2016, from https://www.niehs.nih.gov/health/topics/agents/lead/
6. Liu, Z., & Zhang, F. (2009). Removal of lead from water using biochars prepared from hydrothermal liquefaction of biomass. *Journal of Hazardous Materials, 167*(1–3), 933-939. doi:http://dx.doi.org/10.1016/j.jhazmat.2009.01.085
7. Pilsner, R., Hu, H., Ettinger, A., Sanchez, B., Wright, R., Cantonwine, D., ... & Hernández-Avila, M. (2009). Influence of prenatal lead exposure on genomic methylation of cord blood DNA. *Epidemiology*, *20*(6), S84.Salam, O. E. A., Reiad, N. A., & ElShafei, M. M. (2011). A study of the removal characteristics of heavy metals from wastewater by low-cost adsorbents. *Journal of Advanced Research*, *2*(4), 297-303.
8. Wines, M., & Schwartz, J. (2016, February 9). Unsafe Lead Levels in Tap Water Not Limited to Flint. *Holes in Safety Net let Contaminants in Water*. Retrieved from https://www.nytimes.com/2016/02/09/us/regulatory-gaps-leave-unsafe-lead-levels-in-water-nationwide.html?_r=0Yu, X., Ying, G., & Kookana, R. S. (2009). Reduced plant uptake of pesticides with biochar additions to soil. *Chemosphere, 76*(5), 665-671.
9. T.M. Abdel-Fattah, M.E. Mahmoud, S.B. Ahmed, M.D. Huff, J.W. Lee, **S. Kumar**, Biochar from Woody Biomass for Removing Metal Contaminants and Carbon Sequestration, *Journal of Industrial and Engineering Chemistry* 25, 103-109, (**2015**).
10. Mohamed E. Mahmoud, Gehan M. Nabil, Nabila M. El-Mallah, Heba I. Bassiouny **Sandeep Kumar** and Tarek M. Abdel-Fattah, Kinetics, Isotherm, and Thermodynamic Studies of the Adsorption of Reactive Red 195 Dye from Water by Modified Switchgrass Biochar Adsorbent" *Journal of Industrial and Engineering Chemistry* (**2016**) Volume 37, 25 May 2016, Pages 156–167. doi:10.1016/j.jiec.2016.03.020
11. Regmi P., Garcia M., **Kumar S.,** Cao X., Mao J., Schafran G., Removal of Copper and Cadmium from Aqueous Solution using Switchgrass Biochar Produced via Hydrothermal Carbonization Process. *Journal of Environmental Management;* (**2012**), 10, 61-69.
12. **Kumar, S.**; Loganathan, V.A.; Gupta R.B.; Barnett, M. An Assessment of U(VI) removal from groundwater using biochar produced from hydrothermal carbonization, *Journal of Environmental Management*; (**2011**), 92, 2504-2512.

Pushpita Kumkum, EIT

US Citizen

pushpitakumkum04@gmail.com
https://www.linkedin.com/in/pushpita-kumkum/
Odessa, FL
+1-330-329-0757

Key Qualifications

- 7+ years of research and industry experience in environmental engineering, water quality management and water and wastewater treatment principle.
- Participated in several outreach activities to educate stakeholders on environmentally responsible practices, covering topics such as water treatment, water conservation, and sustainable solutions for removing heavy metals (specifically Lead) from water.
- Experienced in water quality monitoring through sample collection and laboratory analysis for research and consulting projects.
- Skilled in technical writing with experience in preparing proposals, technical memorandum and scientific reports for grant applications
- Contributing author to AWWA M20 Manual update playing a key role in enhancing chapters through collaboration with industry experts and demonstrating expertise in water treatment principle and mechanism.
- **Analytical equipment tools:** Atomic Absoprtion Spectrophotometer (AAS), Ion Chromatograph (IC), Gas Chromatography/ Mass spectrometry (GC/MS), Total Organic Halogen Analayzer (TOX), UV/Vis Spectrophotometer, Elemental Analyzer, BET Surface Area Analyzer, Thermogravimetric Analyzer (TGA), Fourier-Transform Infrared Spectrophotometer (FTIR), Centrifuge.

Education

- **Ph.D. Candidate** in Civil and Environmental Engineering
  Old Dominion University, Norfolk, VA, USA — *Expected graduation: Spring 2024*
- **MS** in Civil Engineering (Environmental Focus)
  The University of Akron, Akron, OH, USA — *May 2013*
- **BS** in Civil Engineering
  Bangladesh University of Engineering and Technology, Dhaka, Bangladesh — *Oct 2009*

Experience

- **Civil Engineer II/III - Water** — Nov 2021 – Present
  Civil and Environmental Engineer - Black and Veatch — *Tampa, FL*
  - Contribute as a team member to the integrated program management for water provider agencies, involving CIP (scope, schedule and cost) data updates, verification of designs, and coordination with project owners.
  - Assist on a variety of projects, including pilot plant operations, chemical system master planning, sewer line and liner installations inspections, water treatment plant upgrades, water supply alternatives and permitting matrices.
  - Support the planning and design of municipal water and wastewater facilities, including distribution, treatment, and conveyance/collection systems
  - Analyzing data and drafting project report containing plans, design specification, timeline and schedules.

- **Research Scientist** May 2021 – Aug 2021
  Research Scientist Intern - National Science Foundation *Remote*
  - Performed research to characterize dynamics of biocrusts and their effects on hydrologic processes of infiltration and evaporation.
  - Conducted literature reviews and summarized research findings to presented in conferences.

- **Water and Wastewater Treatment** Aug 2017 – Present
  Teaching/ Research Assistant - Biomass Research Lab at Old Dominion University *Norfolk, VA*
  - Designing and developing a novel, sustainable technology that includes reactor design and efficiency test to remove lead (Pb) from drinking water (funded by USEPA).
  - Evaluating the application of biochar as an engineered solution to remove microplastics, heavy metals (lead, chromium, copper), ammonia, chloride and other contaminants for treating landfill leachate and stormwater.
  - Investigating the increase of microalgal growth in tannery wastewater by pretreatment with biochar.
  - Mentored and led a team of 6 undergraduate students to prepare the winning proposal (Grant No. SU839266) for a USEPA design competition known as "P3 : People, Prosperity and Planet" which involved design and development of a low cost household biochar filter for lead removal.
  - Analyzing data and drafting project report containing plans, design specification, timeline and schedules.

- **Water Quality Monitoring** May 2011 – May 2013
  Research Assistant at The University of Akron *Akron, OH*
  - Analyzed fate and transport of pharmaceuticals during drinking water treatment (funded by NSF).
  - Evaluated transformation of anthropogenic contaminants into organic DBPs.
  - Monitored drinking water source quality for 3 cities (Akron, Barberton, Ravenna) in terms of excess nutrient or other contaminants.

Journal Publications (selected)

- Pushpita Kumkum, David R. Bridenstine, Nana Osei B. Ackerson, Thomas A. Ternes, Michael J. Plewa, Susan D. Richardson , Stephen E. Duirk."Iodinated Pharmaceuticals as Precursors to Total Organic Halogen Formation in the Presence of Chlorinated Oxidants and Natural Organic Matter" — Poster Presentation in 245th ACS National Meeting and Exposition, April 2013, New Orleans, LA.
- Pushpita Kumkum and Sandeep Kumar. "Evaluation of Pb(II) removal potential of biochar in a fixed-bed continuous flow adsorption system", Journal of Health and Pollution" (2020)
- Eleonora Sforza, Pushpita Kumkum, Elena Barbera, Sandeep Kumar. "Bioremediation of industrial effluents: How a biochar pretreatment may increase the microalgal growth in tannery wastewater", Journal of Water Process Engineering (2020)

Affiliation and Membership

• Water Environment Federation (WEF) • ODU Environmental Engineering Student Association (EESA)
• American Society of Civil Engineers (ASCE)

Key Projects

- **Long-term 54 MGD Facilities Plan** 2023 - Present
  Client: GRU Murphree WTP *Gainesville, FL*
  - Assist in data analysis by reviewing documents, finding data gaps, Disinfection Unit analysis and other process areas evaluation (challenges and issues), life-cycle cost analysis, and workshop presentation preparation.

- **CIP Data Updates** 2021 - Present
  Client: Tampa Bay Water *Clearwater, FL*
  - Assist Integrated Program Manager in updating the scopes, cost estimates and schedules for CIP projects. Assist in data collection by reviewing documents, finding data gaps, and developing new project Statement of Work (SOW), project schedule/Gantt chart in MS Project and cost estimates and specification update.

- **Master Water Plan Program Management** 2023 - Present
  Client: Tampa Bay Water *Clearwater, FL*
  - Assist in the program management support for water supply source selection and feasibility study for detailed analysis of selected source and treatment alternatives.

- **Wastewater Pipeline Sliplining** 2021 - Present
  Client: Hillsborough County *Tampa, FL*
  - Review shop drawing. Assist condition assessment by reviewing CCTV inspection and provide recommendation for rehabilitation of the defective collection main and laterals. Inspection of liner installation/site work. Assist preparing GIS maps by providing information/data

- **Regional Water Quality Study - Pilot Plant Operation** 2021 - 2022
  Client: Tampa Bay Water *Land O' Lakes, FL*
  - Performed pilot plant operation to investigate the comparative efficiency of Ion Exchange and GAC system. Prepared and collected sample for laboratory analysis, identified issues and provided solutions to troubleshoot for successful operation of the pilot. Collected field data and reported to the client.

- **Chemical Systems Master Plan** 2021 - 2022
  Client: Tampa Bay Water *Clearwater, FL*
  - Attend all project progress meetings and prepare meeting minutes. Prepare invoice progress reports. Assist developing a database for existing chemical systems and updating chemical standard documents including materials and sizing, installation methods and specifications. Assist preparing presentation for workshops and draft Technical Memorandum (TM). Review and address client comments for the submission of final TM

- **Bithlo Park Water Supply Alternatives Evaluation** 2022
  Client: Orange County *Orlando, FL*
  - Review of historical information available, identify data gaps to assist evaluating water supply alternatives. Assist the team with water demand calculation, pipe sizing, cost estimate and TM preparation.

- **Regional Surface WTP (SWTP) Expansion** 2023 - Present
  Client: Tampa Bay Water *Tampa, FL*
  - Assist in owner's advisor activity, meeting coordination, risk management, grant funding application support.

- **South Hillsborough County Supply Expansion 26-mile Pipeline** 2023 - Present
  Client: South Hillsborough County *Hillsborough, Florida*
  - Assisted in emergency interconnection pipe routing study, pre-bid meeting route review preparation, stakeholder register, risk register, BODR comment review and coordination.

- **Regional Surface WTP (SWTP) Contract and Performance Audit** 2023 - Present
  Client: Tampa Bay Water *Tampa, FL*
  - Assist in collected data review, plant performance evaluation, plant inspection coordination and contract language review.

- **Wastewater Master Plan Update** 2021 - 2022
  Client: Sarasota County *Sarasota, Florida*
  - Compiled information collected from technical experts to perform regulatory review. Reviewed existing regulation and coordinated to capture potential changes to develop a comprehensive updated master plan.

- **Water Reclamation Facility (WRF) Master Plan** 2023
  Client: City of Clearwater *Clearwater, FL*
  - Assisted with the existing system evaluation task by conducting detailed field visits to each WRF which included assessing the physical condition assessment and interviewing with City staffs

- **As-Needed System Engineering – Pasco Growth POC Capacity Support** 2023
  Client: Tampa Bay Water *Tampa, FL*
  - Assisted in peaking factor analysis and demand projection, TM preparation.

- **Medard Reservoir Toe-drain Replacement** 2021
  Client: South West Florida Water MNanagement District (SWFWMD) *Plant City, FL*
  - Inspection of the construction work and report to the client.

- **Desal Intake Connection Phase II** 2021
  Client: Tampa Bay Water *Tampa, FL*
  - Assisted in permitting proceedings by coordination with state/county agencies (FDEP, SWFWMD). Assisted preparing risk register.

- **Venice WTP RO Upgrades- Existing Pipeline Evaluations** 2023
  Client: City of Venice *Venice, FL*
  - Assisted in pipe velocity calculation, demand projection review, permitting and TM preparation.

- **Water Study Cost Benefit Analysis** 2023
  Client: City of North Port *City of North Port, FL*
  - Assisted with the data analysis and workshop presentation

- **Laurel Lakes WTP** 2023
  Client: Laurel Lakes, LLC *Polk County, FL*
  - Assisted in Basis of Design Report (BODR) by preparing groundwater sampling plan.